Biological Activities of Chemical Constituents from the Roots of *Clausena excavata* Burm. f. and Their Semi-Synthetic Analogs

Thanatcha Samsee

A Thesis Submitted in Partial Fulfillment of Requirements for
degree of Master of Science in Chemistry
April 2025

ฤทธิ์ทางชีวภาพของสารองค์ประกอบทางเคมีจากรากของสันโสก (*Clausena excavata* Burm. f.) และสารอนุพันธ์กึ่งสังเคราะห์

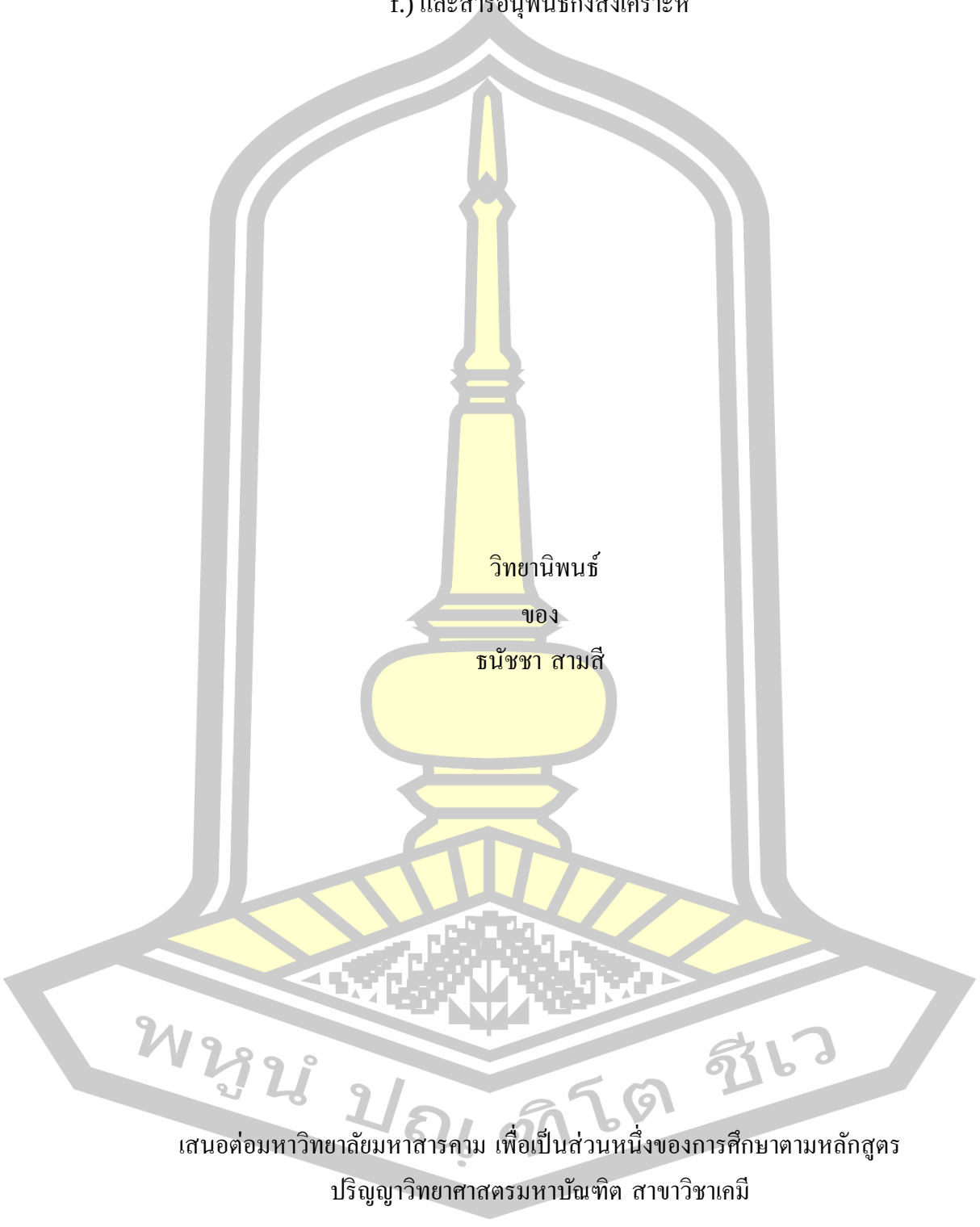

วิทยานิพนธ์

ของ

ธนัชชา สามสี

เสนอต่อมหาวิทยาลัยมหาสารคาม เพื่อเป็นส่วนหนึ่งของการศึกษาตามหลักสูตร

ปริญญาวิทยาศาสตรมหาบัณฑิต สาขาวิชาเคมี

เมษายน 2568

Biological Activities of Chemical Constituents from the Roots of *Clausena excavata* Burm. f. and Their Semi-Synthetic Analogs

Thanatcha Samsee

A Thesis Submitted in Partial Fulfillment of Requirements

for Master of Science (Chemistry)

April 2025

The examining committee has unanimously approved this Thesis, submitted by Miss Thanatcha Samsee , as a partial fulfillment of the requirements for the Master of Science Chemistry at Mahasarakham University

Examining Committee

.....Chairman
(Assoc. Prof. Panawan Moosophon , Ph.D.)

.....Advisor
(Assoc. Prof. Prapairat Seephonkai , Ph.D.)

.....Committee
(Assoc. Prof. Chatthai Kaewtong , Ph.D.)

.....Committee
(Asst. Prof. Pakin Noppawan , Ph.D.)

Mahasarakham University has granted approval to accept this Thesis as a partial fulfillment of the requirements for the Master of Science Chemistry

.....	.....
(Prof. Pairot Pramual , Ph.D.)	(Prof. Anongrit Kangrang , Ph.D.)
Dean of The Faculty of Science	Acting Dean of Graduate School

TITLE Biological Activities of Chemical Constituents from the Roots of *Clausena excavata* Burm. f. and Their Semi-Synthetic Analogs

AUTHOR Thanatcha Samsee

ADVISORS Associate Professor Prapairat Seephonkai , Ph.D.

DEGREE Master of Science **MAJOR** Chemistry

UNIVERSITY Mahasarakham University **YEAR** 2025

ABSTRACT

Phytochemical investigation of a crude methanol extract of roots of *Clausena excavata* resulted in the isolation of dentatin (32), clausarin (33), nordentatin (34), xanthyletin (35), clausine K (43), heptaphylline (46), 7-methoxymukonal (77), kinocoumarin (80), and citrusarin A (115), Semi-synthetic analogs of 80, 33 and 34, compounds 80a, 33a-33d, and 34b-34d, were obtained for biological assays. Compounds 32-34, 80, 33a and 80a showed antimalarial activity against with EC_{50} values of >7.66, 0.58, 5.62, 1.10, 1.97 and 3.25 µM, respectively. The isolated compounds 46 and 80, and the synthetic analogs 33b, 33c, 34b and 34c, displayed stronger α-glucosidase inhibitory activity (IC_{50} = 32.89-92.55 µM) than acarbose (IC_{50} 391.47 µM). For nitric oxide (NO) inhibition in macrophage cells, 33 displayed the strongest activity (IC_{50} = 27.95 µM), followed by 33d with IC_{50} = 33.62 µM and 34 with IC_{50} = 35.41 µM. These activities were 7.9-6.2 folds stronger than the positive control, diclofenac (IC_{50} = 222.42 µM). The synthetic compounds 33b and 34b were further evaluated for their cytotoxicity against A549 cells due to their observed toxicity toward RAW 264.7 cells in the NO inhibitory activity assay. The results revealed that these two compounds were cytotoxic against A549 cells, with 33b being more effective (IC_{50} = 11.71 µM) than cisplatin (IC_{50} = 21.56 µM), while the activity of 34b (IC_{50} = 22.39 µM) was comparable to that of cisplatin.

Keyword : Clausena excavata Pyranocoumarins Carbazole alkaloids Anti-malarial activity α-Glucosidase inhibitory activity NO inhibitory activity

ACKNOWLEDGEMENTS

I would like to thank Center of Excellence for Innovation in Chemistry (PERCH-CIC), Ministry of Higher Education Science, Research and Innovation, for financial support. I would like to thank the Postgraduate Scholarship that supports my research. The Department of Chemistry, Faculty of Science, Mahasarakham University (MSU), are acknowledged.

I am grateful to Professor Rapatbhorn Patrapuvich, Tachin Khulmanee and their group for teaching me how to test for malaria effects at Drug Research Unit for Malaria (DRUM), Faculty of Tropical Medicine, Mahidol University.

Most importantly, I would like to gratefully acknowledge Assoc. Prof. Dr. Prapairat Seephonkai my supervisor, who gave me guidance, support and encouragement throughout my study.

Finally, I would like to thank my family and friends for their support, care and encouragement throughout my studies.

Thanatcha Samsee

TABLE OF CONTENTS

Page

LIST OF FIGURE

Page

LIST OF ABBREVIATIONS

AIDS	Acquired immunodeficiency syndrome
MOLT-3	Acute lymphoblastic leukemia
A. fumigatus	*Aspergillus fumigatus*
MCF7	Breast cancer
Ealcd.	Calculated
^{13}C	13-Carbon
C. tropicalis	*Candida tropicalis*
C	Carbon
CO_2	Carbon dioxide
CEM-SS	*Cellosaurus* cell lines
PERCH-CIC	Center of excellence for innovation in chemistry
C. excavata	*Clausena excavata* Burm. f.
COSY	Correlation spectroscopy
J	Coupling constant
CC	Column chromatography
°C	Degree celsius
DNA	Deoxyribonucleic acid
$CDCl_3$	Deuterated chloroform
DMSO-d_6	Deuterated dimethylsulphoxide
CD_3OD	Deuterated methanol
DMDO	Dimethyldioxirane

MTT	3-(4, 5-dimethylthiazol-2-yl)-2,5-diphenyltetrazolium bromide
d	Doublet (spectral multiplicity)
dd	Doublet of doublet (spectral multiplicity)
DMEM	Dulbecco's modified eagle's medium
EBV-EA	Epstein-Barr virus early antigen
EtOAc	Ethyl acetate
Fr.	Fraction
g	Gram
HeLa	Henrietta Lacks
Hz	Hertz
HMBC	Heteronuclear multiple bond correlation
HMQC	Heteronuclear multiple quantum coherence
HRESIMS	High-Resolution Electrospray Ionization Mass Spectrometry
h	Hour
HUCCA-1	Human cholangiocarcinoma
HepG2	Human hepatocellular liver carcinoma cancer
HIV-1	Human immunodeficiency virus
A549	Human lung cancer
H_2	Hydrogen
IC_{50}	50% Inhibitory concentration
CH_3I	Iodomethane

LPS	Lipopolysaccharide
L	liter
EC_{50}	50% Maximal effective concentration
MS	Mass spectroscopy
RAW 264.7	Macrophage-like cells
MHZ	Megahertz
MeOH	Methanol
m	meter
m-CPBA	meta-chloroperoxybenzoic acid
µg	Microgram
µM	Micromolar
Mg	Miligram
mM	Milimolar
mL	Milliliter
MIC	Minimum inhibitory concentration
min	Minute
M. circinelloides	*Mucor circinelloides*
m	Multiplet (spectral multiplicity)
nM	Nanometer
NO	Nitric oxide
NT	Not test
NMR	Nuclear magnetic resonance
NMR	Nuclear Magnetic Resonance

NOESY	Nuclear over hauser effect spectroscopy
TPA	12-*O*-tetradecanoylphorbol-13-acetate
KB	Oral cavity cancer
Pd	Palladium
ppm	Parts per million
H_3SO_4	Phosphoric acid
P. falciparum	*Plasmodium falciparum*
PTI	Potential therapeutic index
K_2CO_3	Potassium carbonate
^1H	1-Proton
q	Quartet (spectral multiplicity)
rt.	Room Temperature
s	Singlet (spectral multiplicity)
Na_2CO_3	Sodium Carbonate
H_2SO_4	Sulfuric acid
NCI-H187	Small cell lung cancer
TLC	Thin-layer chromatography
t	Triplet (spectral multiplicity)
UK	United Kingdom
USA	United States of America

CHAPTER 1

INTRODUCTION

1.1. Background

Thailand has one of the highest biodiversity in Southeast Asia because Thailand is located in the tropics and next to the sea. The weather condition is suitable for plant growth. In Thailand, there is 2,187 plant species out of 10,000 species was reported in 2018. This number is up to 18% of the plant that can be used as medicinal plant by local people (Phumthum et al., 2018).

Medicinal plants have been used by indigenous physicians since pre-Hispanic times and are part of the traditional knowledge of humanity (Heinrich et al., 1998). The use of medicinal plants derives from having secondary metabolites with pharmacological properties, and some are an important source of components for antitumor, antiviral, antiepileptic, antibiotic, antiinflammation, antinociceptive, among others (Alonso-Castro et al., 2011).

The genus *Clausena*, is a local medicinal plant in South East Asia for the treatment belongs to the cold, malaria, abdominal pain, dermatopathy and snakebite (Wu & Furukawa, 1982). Rutaceae family, contains about 14 species of evergreen trees. *Clausena excavata* Burm. f. of in Thailand, it is a locally name “San Soak”, “Hat-sa-khun-tad (Huang et al., 1997). Pharmacologically, many secondary metabolites, including alkaloids and coumarins, have been tested for their biological

activities, such as anticancer, immunomodulatory, anti-human immunodeficiency virus, antioxidant, antibacterial, insecticidal, antifungal, antinociceptive, antimalarial, and antiplatelet effects in this plant.

Therefore, in this study, natural product compounds isolated from the root of *C. excavata* and their semi-synthetic compounds from *C. excavata* collected in northeastern Thailand, were selected to evaluate for chemical investigation of the MeOH and their biological activities were studied. In addition, semi-synthetic compounds of the natural product compounds isolated from *C. excavata* were prepared and evaluated for their biological activity.

1.2. Research objective

This research aims to phytochemical investigate the root of *C. excavata* and to evaluate the biological activities of the isolated compounds and their semi-synthetic analogs from *C. excavata*.

1.3. Expected result

The expected results of this research are information of phytochemicals produced in the root of *C. excavata* and the biological activity of these isolated natural product compounds and the semi-synthetic analogs.

1.4. Scope of research

Scope of research are; (1) phytochemical investigation of the root of *C. excavata* and (2) evaluation of biological activities of the isolated compounds from

the root of *C. excavata* and the semi-synthetic analogs which include antimalarial activity against *Plasmodium falciparum* (K1) , α-glucosidase and nitric oxide inhibitory activities, and cytotoxicity against A459 cell lines.

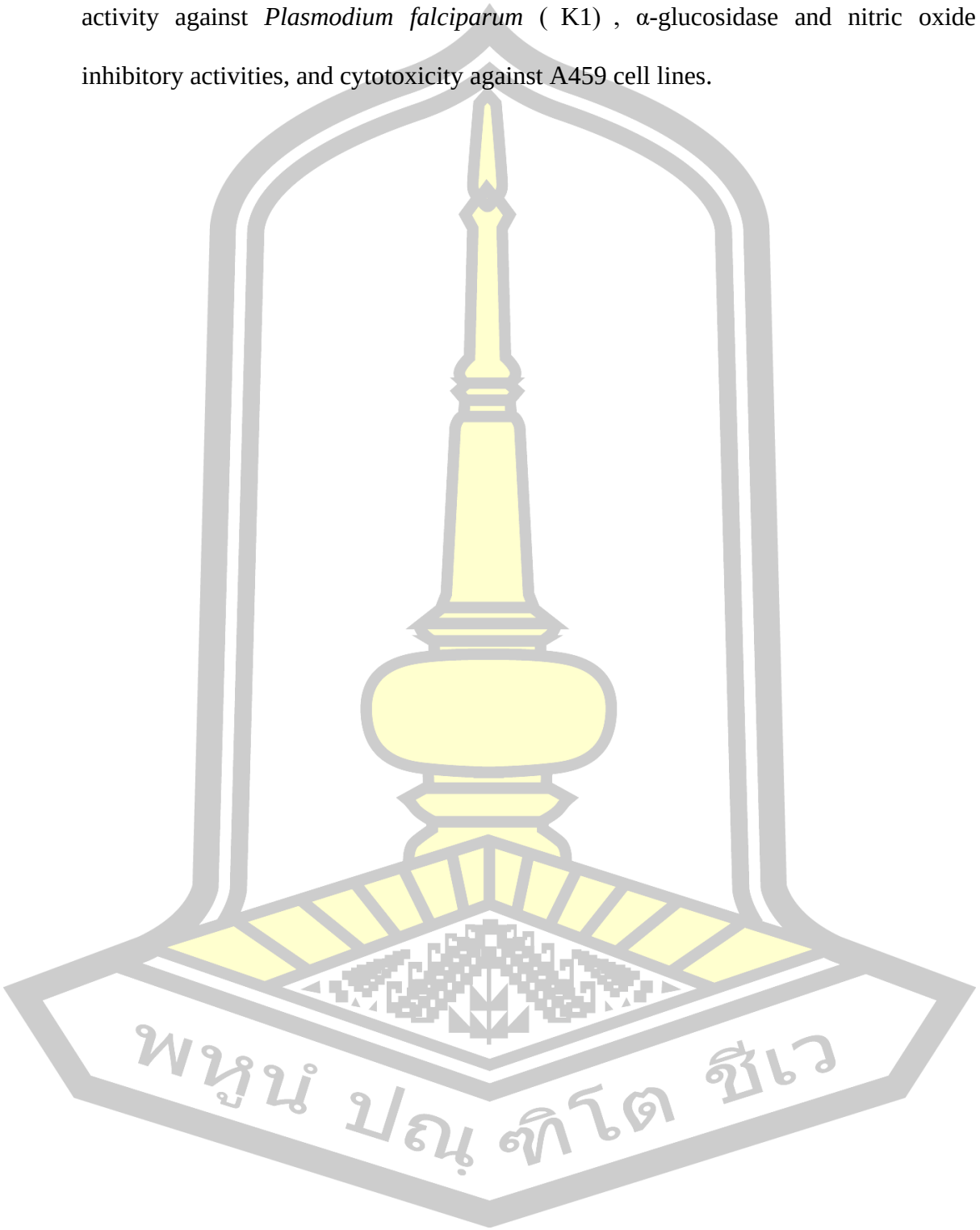

CHAPTER 2

LITERATURES REVIEW

2.1. *Clausena excavata*

Clausena excavata Burm. f. (family Rutaceae), is an evergreen wild shrub or a small slender tree, which can grow up to 4 meters tall in height (Wiart, 2006). It bears small yellowish flowers with green berries which turn translucent pink upon ripening (**Figure 1**). This medicinal plant was used in Thai folk medicine for treatment of cold, malaria, acquired immunodeficiency syndrome, dermatopathy, abdominal pain, snake-bite and as a detoxification agent (Wu et al., 1994). It is a rich source of pyranocoumarins, many of which display interesting biological and pharmacological activities (Seephonkai et al., 2023) (Sunthitikawinsakul et al., 2003) (N. Kongkathip & Kongkathip, 2009) (Peng, Zheng, et al., 2013)(Lim et al., 2019). Besides coumarins, carbazole alkaloids have also been reported from *C. excavata* (Sunthitikawinsakul et al., 2003)(Wu et al., 1996)(Chakthong et al., 2016). Carbazole alkaloids isolated from *Clausena* species were shown to have a myriad of biological activities, including inhibition of Lipopolysaccharide-induced nitric oxide (NO) production in mouse macrophage RAW 264.7 cells, neuroprotective effect (Tan et al., 2022) and α-glucosidase inhibitory activity (Liu et al., 2021).

(**A**) (**B**) (**C**)

Figure 1. leaf (**A**), stem (**B**) and fruit (**C**)
https://www.nparks.gov.sg/florafaunaweb/flora/3/6/3675#,
https://identify.plantnet.org/es/prosea/observations/1016320338

There are numbers of reports of chemical constituents from *Clausena excavata*. Here is a summary of compounds isolated from different parts of *C. excavata* found in ScienceDirect and PubMed database since 2000.

2.2. Isolated compounds from the aerial part of *C. excavata*

Five new tetranortriterpenoids, (11*β*)-21,23-dihydro-11, 21-dihydroxy-23-ox oobacunone (=21,23-dihydro-21-hydroxy-23-oxozapoterin) (**1**), (11*β*)-21,23-dihydro-11,23-dihydroxy-21-oxoobacunone (=21,23-dihydro-23-hydroxy-21-oxozapoterin) (**2**), (1*α*,11*β*)-1,2,21,23-tetrahydro-1,11,23-trihydroxy-21-oxoobacunone (=21,23-dihydro-23-hydroxy-21-oxoclausenarin) (**3**), (1*α*,11*β*)-23-ethoxy-1,2,21,23-tetrahydro -1,11-dihydroxy-21-oxoobacunone (=23-ethoxy-21,23-dihydro-21-oxo clausenarin) (**4**), and (11*β*)-1,2,21,23-tetrahydro-11,23-dihydroxy-21-oxoobacunoic acid) (**5**), together with a known zapoterin (=(11*β*)-11-hydroxyobacunone) (**6**) (**Figure 2**), were isolated from the aerial part of *C. excavata* (He et al., 2002).

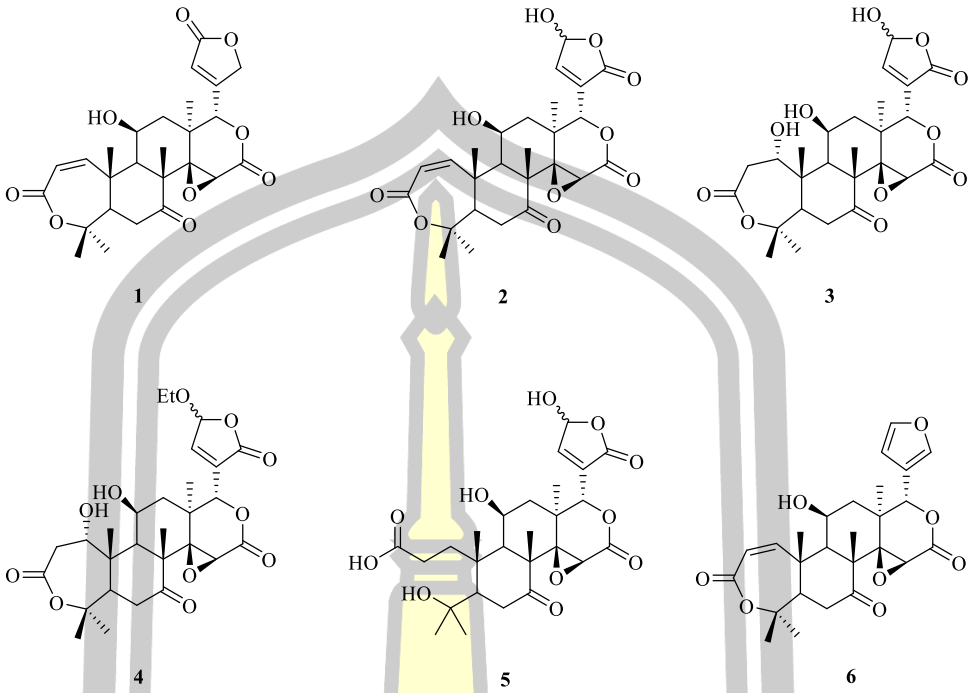

Figure 2. Structures of compounds **1**–**6**.

2.3. Isolated compounds from the leaf of *C. excavata*

Ten new furanone-coumarins, clauslactone A (**7**), clauslactone B (**8**), clauslactone C (**9**), clauslactone D (**10**), clauslactone E (**11**), clauslactone F (**12**), clauslactone G (**13**), clauslactone H (**14**), clauslactone I (**15**) and clauslactone J (**16**), together with a known carbazole, clauszoline M (**17**), and a coumarin, umbelliferone (**18**) (**Figure 3**), were isolated from the leaf of *C. excavata* (Ito et al., 2000). Nine furanone-coumarins (**7**–**12** and **14**–**16**) were found to exhibit inhibitory activity against 12-*O*-tetradecanoylphorbol-13-acetate-induced Epstein-Barr virus early antigen activation in Raji cells.

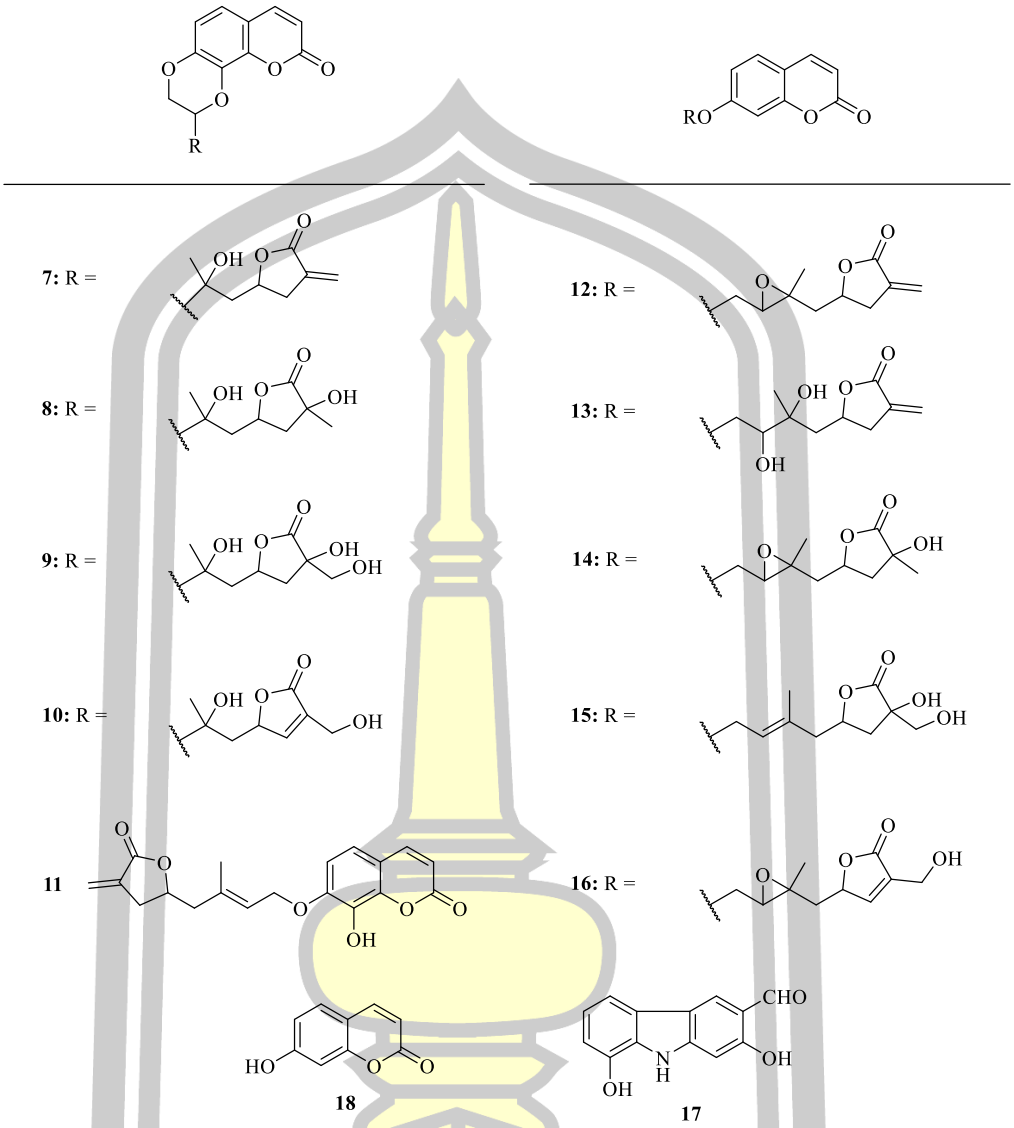

Figure 3. Structures of compounds **7**–**18**.

Four new furanone-coumarins, clauslactone N (**19**), clauslactone O (**20**), clauslactone P (**21**), and clauslactone Q (**22**) (**Figure 4**), were isolated from the leaf and twig of *C. excavata* (Takemura et al., 2002).

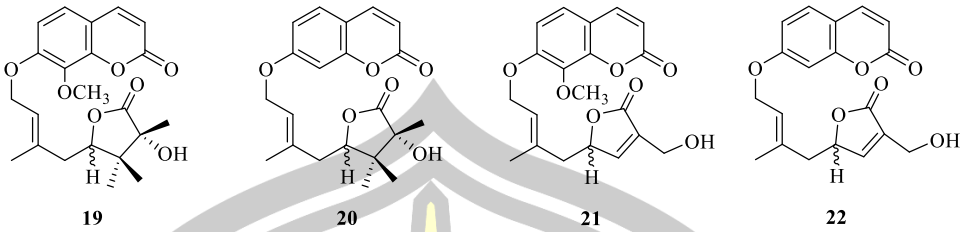

Figure 4. Structures of compounds **19**–**22**.

Three new coumarins, clauslactone R (**23**), clauslactone S (**24**), clauslactone T (**25**), together with fourteen known coumarins, 5-geranyloxy-7-hydroxycoumarin (**26**), clauslactone M (**27**), anisocoumarin J (**28**), excavatin E (**29**), excavatin G (**30**), clausenidin (**31**), dentatin (**32**), clausarin (**33**), nordentatin (**34**), xanthyletin (**35**), xanthoxyletin (**36**), murrayacoumarin C (**37**) (**Figure 5**), clauslactone B (**8**) and umbelliferone (**18**), (**Figure 3**) and eleven carbazole alkaloids, 3-formylcarbazole (**38**), 2-methoxy-3-formylcarbazole (**39**), 2-hydroxy-3-formyl-7-methoxycarbazole (**40**), clausine C (**41**) clausine E (**42**) clausine K (**43**) clausine L (**44**) mukonal (**45**) heptaphylline (**46**), 2,7-dihydroxy-3-formyl-1-(3'-methyl-2'-butenyl)carbazole (**47**), and heptazoline (**48**) (**Figure 5**), were isolated from the leaf and stem of *C. excavata* (Xin et al., 2008). Compounds **42** and **47** were exhibit moderate topoisomerase II inhibitory effects at the concentration of 50 µM.

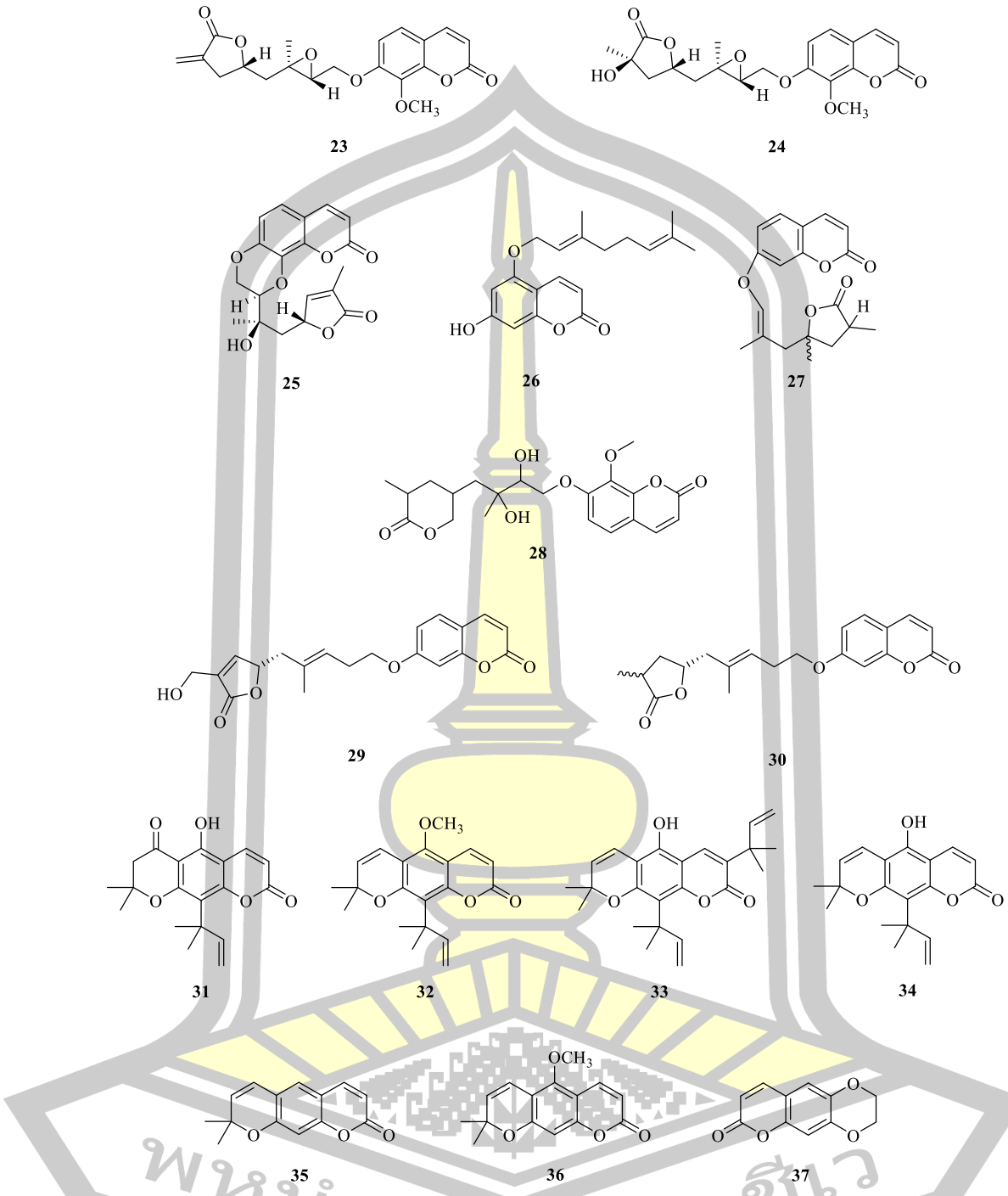

Figure 5. Structures of compounds **23**–**48**.

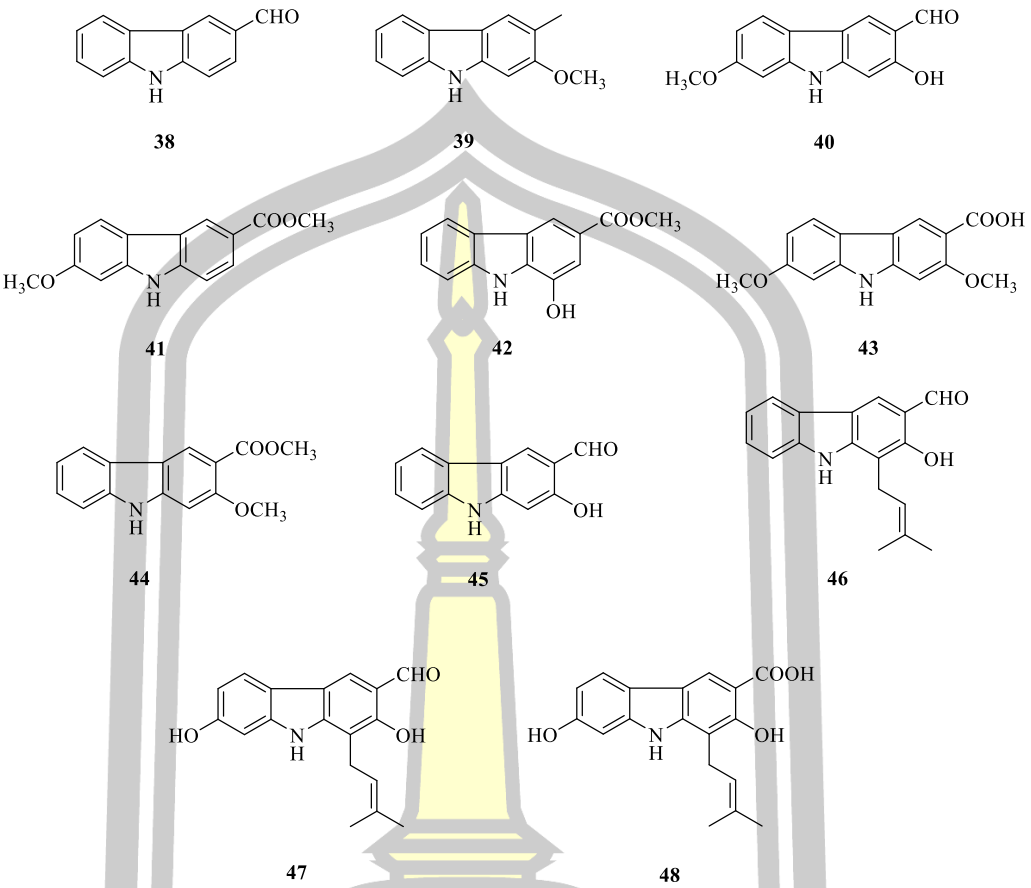

Figure 5 (continue)**.** Structures of compounds **23**–**48**.

A new γ-lactone coumarin, excavarin A (**49**), together with clauslactone D (**50**) (**Figure 6**), were isolated from the leaf of *C. excavata* (Kumar et al., 2012). Compound **49** was found antifungal activity to be stronger than that of the standard antibiotic nystatin against the clinically important pathogens, *Aspergillus fumigatus*, *Candida tropicalis* and *Mucor circinelloides* with MIC of 0.625, 0.039 and 0.078 mg/mL, respectively.

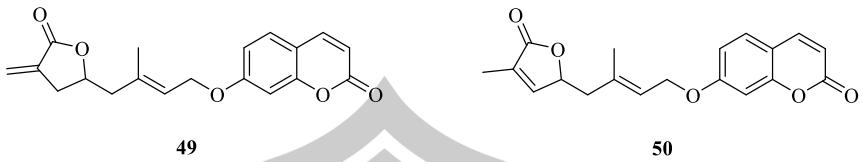

49 50

Figure 6. Structures of compounds **49** and **50**.

2.4. Isolated compounds from the stem of *C. excavata*

A new carbazole alkaloid, clausine TY (**51**), together with two known carbazole alkaloids, clausine H (**52**), and clausine B (**53**) (**Figure 7**), were isolated from the stem bark of *C. excavata* (Taufiq-Yap et al., 2007). Compound **51** showed significant cytotoxicity against *Cellosaurus* cell lines with IC_{50} value of 8.2 µg/mL.

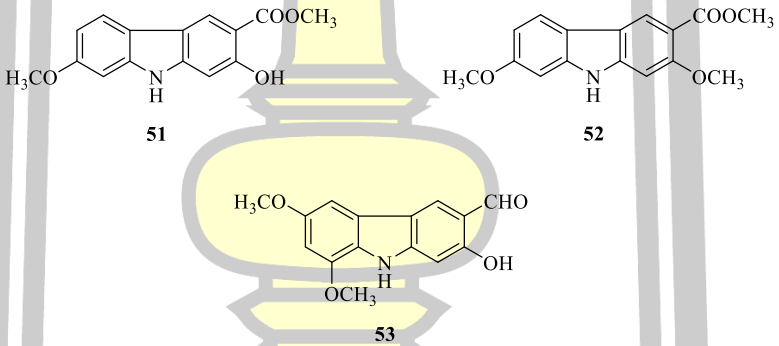

51 52 53

Figure 7. Structures of compounds **51**–**53**.

A new carbazole alkaloid, sansoakamine (**54**), together with eleven known compounds, mukonine (**55**) , lansine (**56**), methyl-carbazole-3-carboxylate (**57**), murrayanine (**58**), mukonidine (**59**), *O*-methylmukonal (**60**), clauszoline I (**61**), *O*-demethylmurrayanine (**62**), methyl-1,6-dihydroxy-9*H*-carbazole-3-carboxylate (**63**), clausine Z (**64**) (**Figure 8**), and 3-formylcarbazole (**38**) (**Figure 5**), were isolated from the stem bark of *C. excavata* (Sripisut & Laphookhieo, 2010). Compound **60**

showed moderate anti-malarial activity against *P. falciparum* with a MIC value of 6.74 µg/mL.

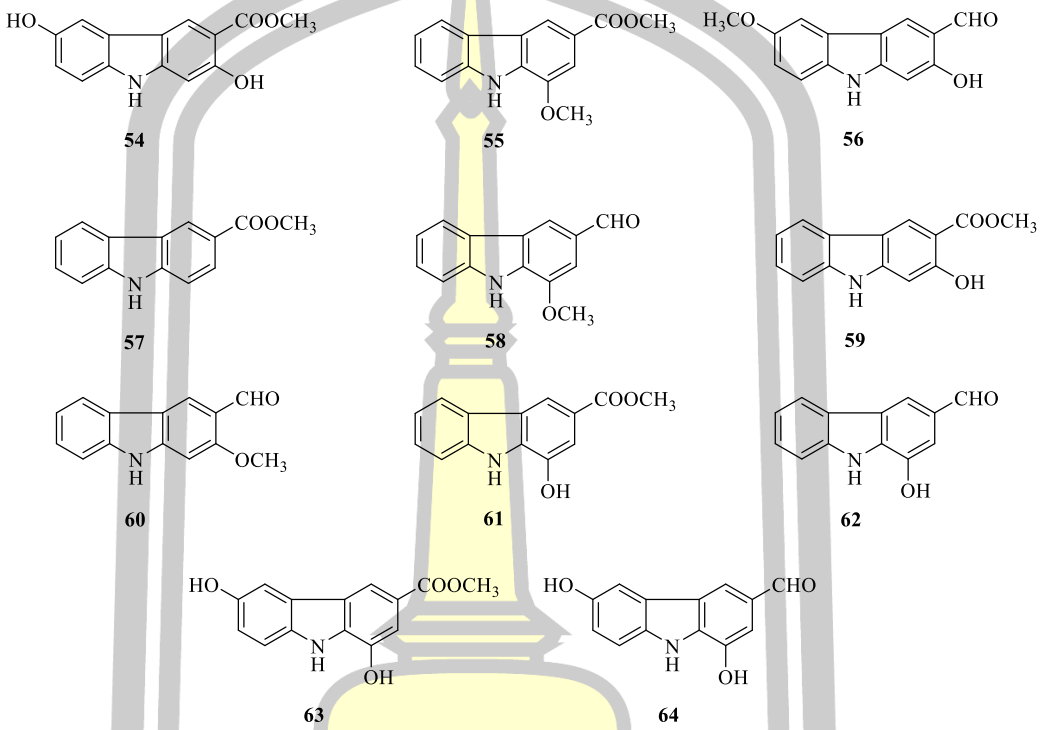

Figure 8. Structures of compounds **54**–**64**.

A new carbazole alkaloid, excavatine A (**65**), and two new alkaloids, excavatine B (**66**), and excavatine C (**67**) (**Figure 9**), were isolated from the stem and leaf of *C. excavata* (Peng et al., 2013). Compound **65** exhibited cytotoxicity against human lung cancer and Henrietta Lacks cell lines with the IC_{50} values of 5.25 and 1.91 µg/mL, respectively.

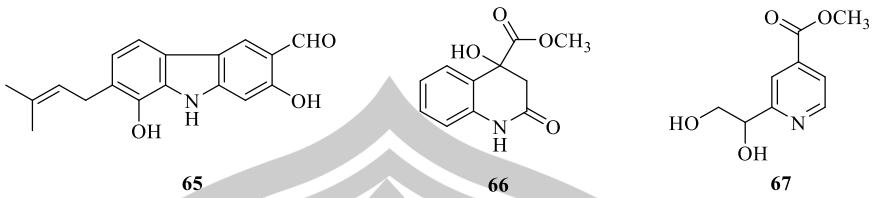

65 **66** **67**

Figure 9. Structures of compounds **65**–**67**.

A carbazole-pyranocoumarin conjugate, carbazomarin B (**68**), and two carbazole alkaloids, 6-methoxymukonidine (**69**) and 2-hydroxy-3-methoxycarbazole (**70**) together with twenty-seven known compounds, murrayafoline A (**71**), girinimbine (**72**), *O*-methylclausenolide (**73**) (**Figure 10**) , xanthoxylatin (**74**), dictamine (**75**), 7-methoxymethylcarbazole-3-carboxylate (**76**), 7-methoxy mukonal (**77**), hortiamide (**78**), 3-formyl-2,7-dimethoxycarbazole (**79**), kinocoumarin (**80**), 7-hydroxy-8-(1,1-dimethylallyl) citrusarin (**81**), isomukonidine (**82**), valencic acid (**83**), and clausenarin (**84**) (**Figure 10**) , clausine H (**52**) (**Figure 7**) , dentatin (**32**), nordentatin (**34**), 3-formylcarbazole (**38**), clausine K (**43**), clausine L (**44**), mukonal (**45**), heptaphylline (**46**) (**Figure 5**), mukonine (**55**), lansine (**56**), murrayanine (**58**), mukonidine (**59**), *O*-methylmukonal (**60**) (**Figure 8**), were isolated from the stem of *C. excavat*a (Chakthong et al., 2016). Compound **69** showed moderate cytotoxicity to human cholangiocarcinoma, acute lymphoblastic leukemia and human hepatocellular liver carcinoma cancer cell lines with IC_{50} values of 15.09–28.50 µg/mL. Compounds **34** and **46** were found to show moderate cytotoxic activity against HepG2 cell line with IC_{50} values of 11.33 and 12.33, respectively. Compound **43** exhibited strong cytotoxicity with IC_{50} value of 1.05 µg/mL, better than a standard drug (etoposide, IC_{50} 13.40 µg/mL).

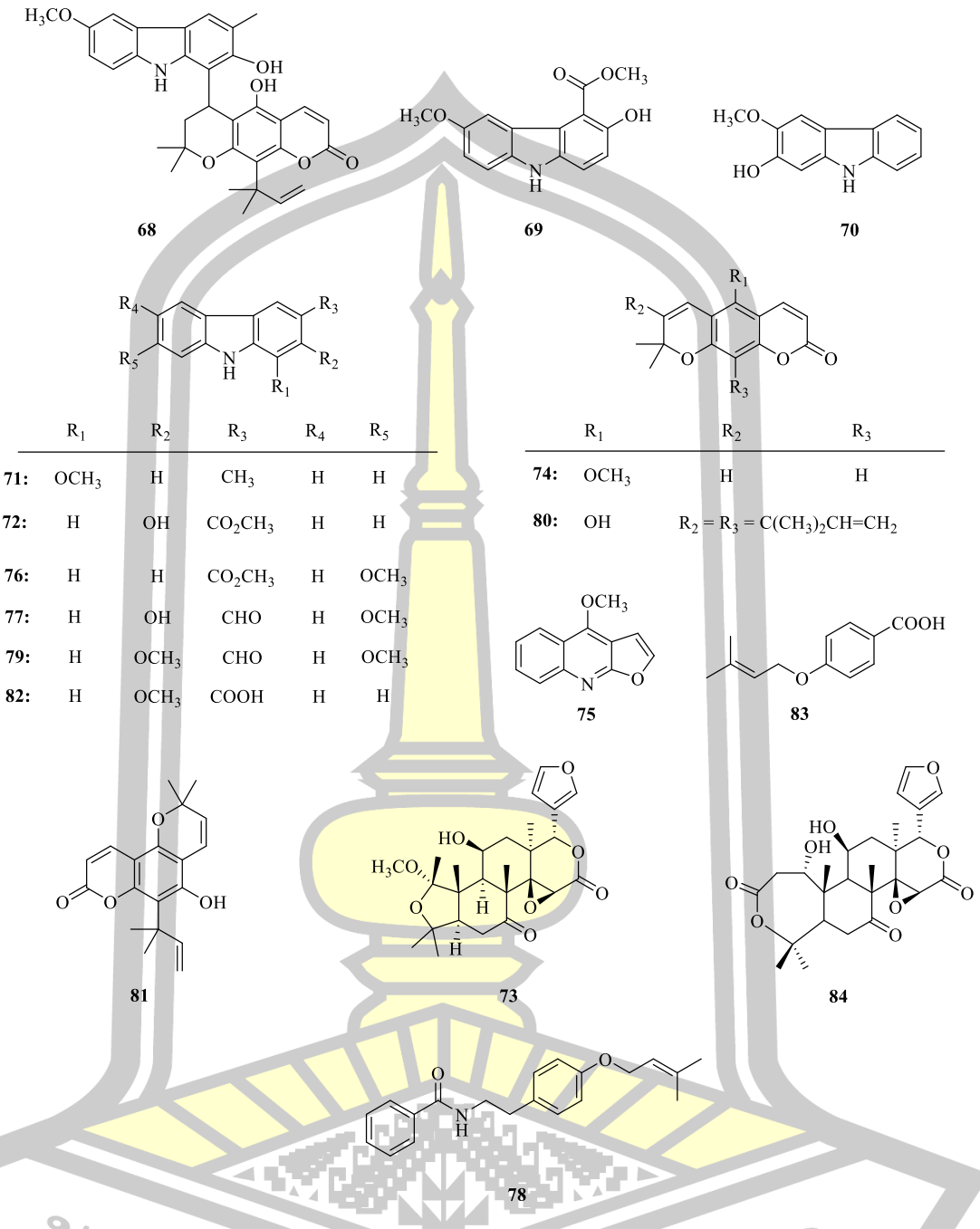

Figure 10. Structures of compounds **68**–**84**.

A limonoid, clausenarin (**84**), a sterol, stigmasterol (**85**), a depside, atranorin (**86**) and a xanthone, lichexanthone (**87**) (**Figure 11**) , Three carbazole alkaloids, clausine H (**52**) (**Figure 7**), heptaphylline (**46**), heptazoline (**48**) (**Figure 5**) together with four prenylated coumarins, clausenidin (**31**), dentatin (**32**), nordentatin (**34**), and

xanthoxyletin (**36**) (**Figure 5**), were isolated from the stem of *C. excavata* (Lim et al., 2019). Compounds **86** and **87** were the first report on the isolation from the genus *Clausena*.

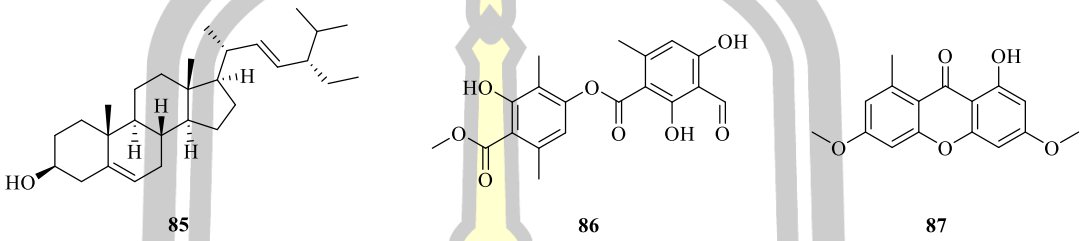

85 **86** **87**

Figure 11. Structures of compounds **85**–**87**.

Five pyranocoumarins, clausenidin (**31**), dentatin (**32**), clausarin (**33**), nordentatin (**34**) (**Figure 5**) and kinocoumarin (**80**) (**Figure 10**) , together with a coumarin, 8-hydroxy-3″,4″-dihydrocapnolactone-2',3'-diol (**88**) (**Figure 12**) , were isolated from the root of *C. excavata* (Seephonkai et al., 2023). Compounds **33** and **80** exhibited potent antiplasmodial activities with EC_{50} values of 0.58 and 1.10 µM, respectively, while **31**, **32**, **34 and 88** had EC_{50} values of 7.15, 7.66, 5.62 and 13.2 µM, respectively.

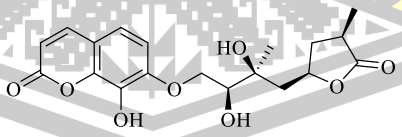

Figure 12. Structure of compound **88**.

2.5. Isolated compounds from the root of *C. excavata*

Three carbazole derivatives, clauszoline J (**89**) (**Figure 13**), *O*-methylmukonal (**60**) (**Figure 8**) , 3-formyl-2,7-dimethoxycarbazole (**79**) (**Figure 10**) , and a pyranocoumarin, clausenidin (**31**) (**Figure 5**), were isolated from the rhizome and root of *C. excavata* (Kongkathip et al., 2005). Compounds **60 79 89** and **31** displayed anti-human immunodeficiency virus-1 activity in a syncytial assay with EC_{50} values of 5.3, 12.0, 29.1 and 34.2 μM, respectively, and thus exhibited potential therapeutic index values of 7.0, 56.7, 8.0 and 1.6 respectively.

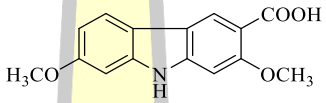

Figure 13. Structure of compound **89**.

Four natural pyranocoumarins, clausenidin (**31**), clausarin (**33**), nordentatin (**34**), and xanthoxyletin (**36**) (**Figure 5**), together with compounds **31**, **33**, **34**, and **36**, were designed and synthesized to give seventeen pyranocoumarin analogues, 10-(1,1-dimethylpropyl)-5-hydroxy-8,8-dimethyl-7,8-dihydropyrano[3,2-γ]chromen-2,6-dione (**90**), 5-hydroxy-8,8-dimethyl-10-(1-methyl-1-oxiranylethyl)-7,8-dihydr pyrano[3,2-γ]chromen-2,6-dione (**91**), 10-(1,1-dimethylallyl)-5-methoxy-8,8-dimethyl-7,8-dihydropyrano[3,2-γ]chromen-2,6-dione (**92**), 10-(1,1-dimethylpropyl) -5-methoxy-8,8-dimethyl-7,8-dihydropyrano[3,2-γ]chromen-2,6-dion (**93**), 5-methoxy-8,8-dimethyl-10-(1-methyl-1-oxiranylethyl)-7,8-dihydro-pyrano[3,2-γ] chromen-2,6-dione (**94**), 10-(1,1-dimethylpropyl)-5-hydroxy-8,8-dimethyl-7,8-dihydro-6*H*-pyrano[3,2-γ]chromen-2-one (**95**), 10-(1,1-dimethylallyl)-5-methoxy-8,8-

dimethyl-8*H*-pyrano[3,2-γ]chromen-2-one (**96**), 10-(1,1-dimethylpropyl)-5-methoxy-8,8-dimethyl-7,8-dihydro-6*H*-pyrano[3,2-γ]chromen-2-one (**97**), 4-(1,1-dimethylallyl)-9-methoxy-2,2-dimethyl-1α,9β-dihydro-*2H*-1,3,5-trioxacyclopropa[α] anthracen-6-one (**98**), 9-methoxy-2,2-dimethyl-4-(1-methyl-1-oxiranylethyl)-1α,9β-dihydro-2*H*-1,3,5trioxacyclopropa[α]anthracen-6-one (**99**), 3,10-bis-(1,1-dimethyl propyl)-5-hydroxy-8,8-dimethyl-7,8-dihydro-6*H*-pyrano[3,2-γ] chromen-2-one (**100**), 3,10-bis-(1,1-dimethylallyl)-5-methoxy-8,8-dimethyl-8*H*-pyrano[3,2-γ]chromen-2- one (**101**), 3,10-bis-(1,1-dimethylpropyl)-5-methoxy-8,8-dimethyl-7,8-dihydro-6*H*-pyrano[3,2-γ]chromen-2-one (**102**), 4,7-bis-(1,1-dimethylallyl)-9-methoxy-2,2-dimethyl-1α,9β-dihydro-2*H*-1,3,5-trioxacyclopropa[α]anthracen-6-one (**103**), 9-methoxy-2,2-dimethyl-4,7-bis-(1-methyl-1-oxiranylethyl)-1α,9β-dihydro-2*H*-1,3,5-trioxacyclopropa[α]anthracen-6-one (**104**), 5-methoxy-8,8-dimethyl-7,8-dihydro-6*H*-pyrano[3,2-γ] chromen-2-one (**105**) and 9-methoxy-2,2-dimethyl-1α,9β-dihydro-2*H*-1,3,5-trioxacyclopropa[α]anthracen-6-one (**106**), were isolated from the root of *C. excavata* (Su et al., 2009) (**Figure 14**). Compounds **31**, **33**, **90**, **92**, **93**, **95**, **96**, **97**, **98**, **102** and **103** showed anti-hepatitis B virus with EC_{50} values of 1.88, 6.38, 1.14, 11.25, 5.35, 1.34, 1.64, 1.63, 5.50, 6.60 and 4.56 μM respectively. **33**, **34**, **95**, **99** and **102** showed cytotoxic activity against four human cancer cell lines (A549, MCF7, KB, and nasopharynx) with EC_{50} values of 8.70, 17.32, 9.63, 9.96, 2.98, 7.96, 1.61, 1.59, 8.84, 16.34, 9.25, 9.11, 12.21, 17.73, 8.21, 7.73, 11.78, 11.42, 6.50 and 6.12 μg/mL respectively.

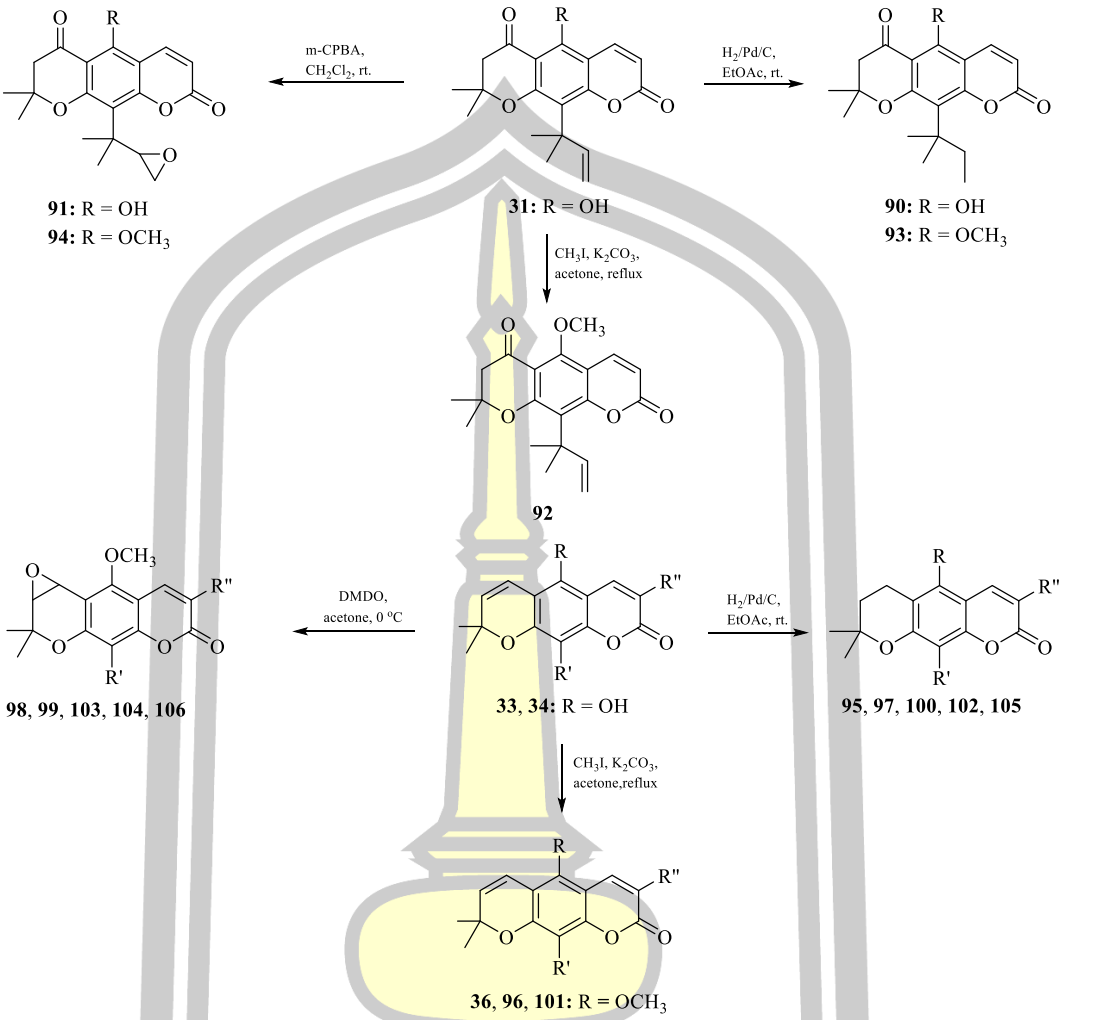

	R	R′	R″
34:	OH		H
95:	OH		H
96:	OCH_3		H
97:	OCH_3		H
98:	OCH_3		H

	R	R′	R″
99:	OCH_3		H
33:	OH		
100:	OH		
101:	OCH_3		
102:	OCH_3		

	R	R′	R″
103:	OCH_3		
104:	OCH_3		
36:	OCH_3	H	H
105:	OCH_3	H	H
106:	OCH_3	H	H

Figure 14. Structures of compounds **90**–**106**.

Six coumarins, clausine D (**107**), clausine F (**108**), scopoletin (**109**) , binorponcitrin (**110**) (**Figure 15**), clausenidin (**31**), dentatin (**32**), nordentatin (**34**), xanthoxyletin (**36**) (**Figure 5**) and twelve alkaloids, 2-hydroxy-3-3-formyl-2,7-dimethoxycarbazole (**111**) and murrayacine (**112**) (**Figure 15**), clausine H (**52**) (**Figure 7**), clauszoline I (**61**) (**Figure 8**), clauszoline J (**89**) (**Figure 13**), heptaphylline (**46**) 2-hydroxy-3-formyl-7-methoxycarbazole (**40**), (**Figure 5**), murrayanine (**58**) (**Figure 8**), murrayafoline A (**71**) and dictamine (**75**) (**Figure 13**), were isolated from the root of *C. excavata* (Sripisut et al., 2012). Compounds **34**, **58** and **112** exhibited highest cytotoxicity against oral cavity cancer, breast cancer and small cell lung cancer cell lines with IC_{50} values of 5.95 3.76 and 5.65 µg/mL, respectively.

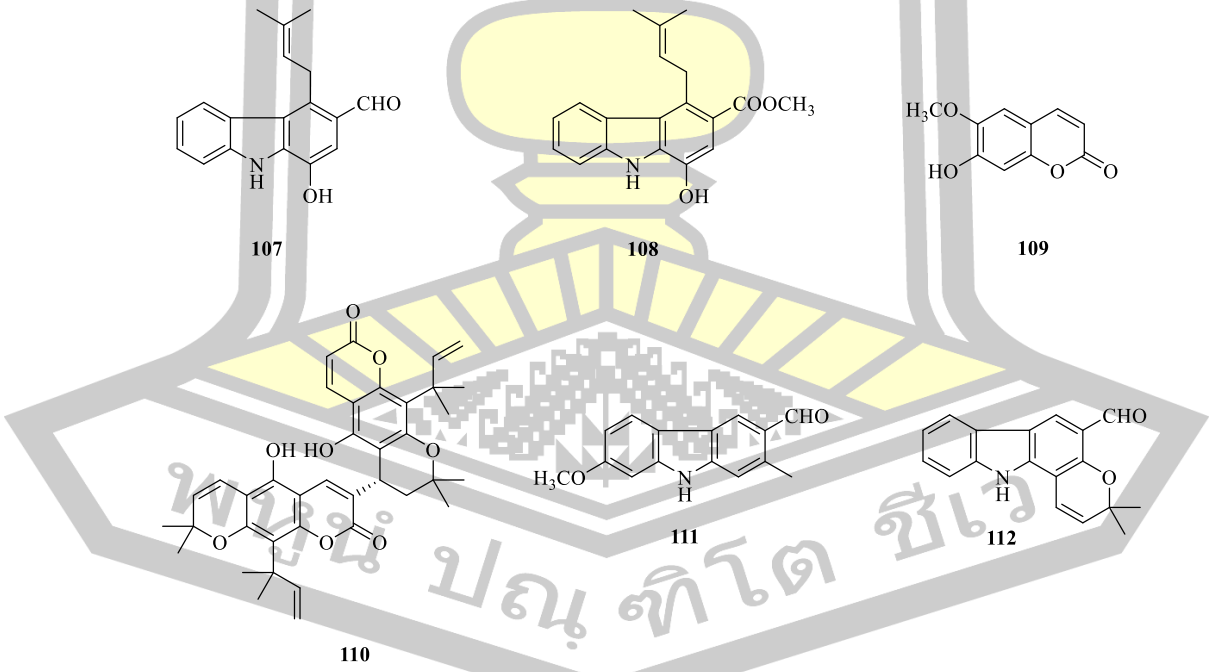

Figure 15. Structures of compounds **107**–**112**.

Two new coumarins, clauexcavatins A (**113**) and clauexcavatins B (**114**) together with seven known coumarin, citrusarin A (**115**), clausenidin methyl ether (**116**) (**Figure 16**), clausenidin (**31**), dentatin (**32**), clausarin (**33**), nordentatin (**34**), and xanthyletin (**35**) (**Figure 5**), were isolated from the root of *C. excavata* (Peng et al., 2013).

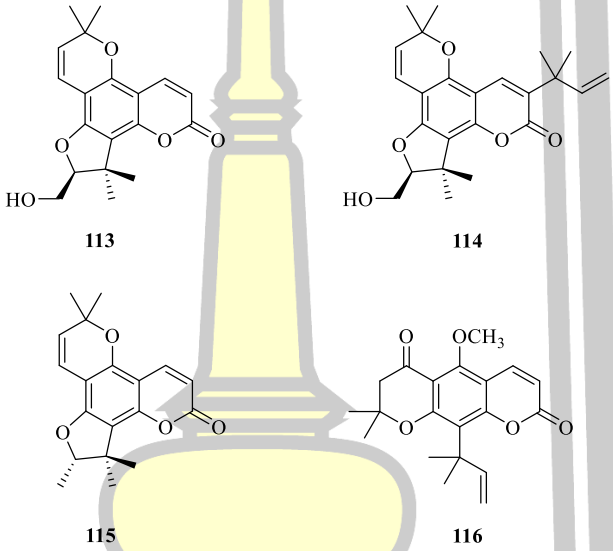

Figure 16. Structures of compounds **113**–**116**.

A new pyrano coumarin, excavatin A (**117**) (**Figure 17**), together with two known compounds nordentatin (**34**) (**Figure 5**) and binorpocitrin (**110**), were isolated from the root of *C. excavate* (Thant et al., 2019). Compounds **117**, **34** and **110** showed antioxidant activity with IC_{50} values 0.286, 0.02, 0.278 mM. Compound **34** exhibited inhibition activity against maltase and sucrase with IC_{50} values 5.45 and 43.57 mM. However, compounds **110** and **117** displayed inhibition on yeast α-glucosidase with IC_{50} values 5.58 and 1.92 mM, respectively.

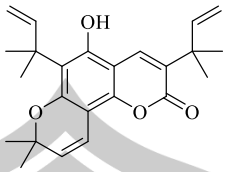

Figure 17. Structure of compound **117**.

Two known compounds, dentatin (**32**) and heptaphylline (**46**) were isolated from the root of *C. excavata* (**Figure 5**) (Thant et al., 2019). Compounds **32** and **46** exhibited highest inhibitory on maltase enzymes with IC_{50} values 6.75 and 11.46 µM (positive control, acarbose (IC_{50}, 2.35 µM)).

A new carbazole pyranocoumarin conjugate, carbazomarin C (**118**) (**Figure 28**), together with a known carbazole alkaloid, mukonine (**55**) (**Figure 8**), and a pyranocoumarin, xanthoxyletin (**36**) (**Figure 5**), were isolated from the root of *C. excavata* (Aminah et al., 2019). Compounds **36** and **118** displayed exhibited inhibition activity against yeast α-glucosidase with IC_{50} values 4.81 and 0.22 mM. Compounds **36** and **118** have stronger inhibition activity than the standard, acarbose (IC_{50} value 4.89 mM).

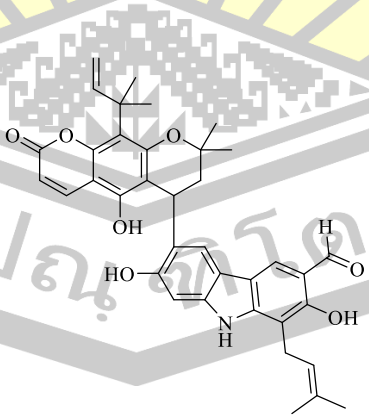

Figure 18. Structure of compound **118**.

A carbazole alkaloid, 7-hydroxy heptaphylline (2,7-dihydroxy-3-formyl-1-(3'-methyl-2'-butenyl) carbazole) (**119**), was isolated from the root *C. excavata* (**Figure 19**)(Thant et al., 2020). Compound **119** was evaluated by 3-(4,5-dimethylthiazol-2-yl)-2,5-diphenyltetrazolium bromide assay against on HeLa cancer cells. This compound exhibited moderate inhibition activity with IC_{50} 41.4 µg/mL.

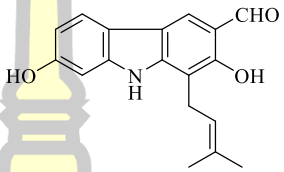

Figure 19. Structure of compound **119**.

CHAPTER 3

MATERIAL AND METHOD

3.1. General experimental procedure

All the chemicals and reagents for the synthesis were purchased from Sigma Aldrich (St. Louis, MO, USA). ^{1}H and ^{13}C NMR spectra were recorded at ambient temperature on a Bruker Ascend-400 (Bruker BioSpin, Rheinstetten, Germany) with deuterated solvents; deuterated chloroform ($CDCl_3$) (δ_H 7.26/δ_C 77.0 ppm), deuterated methanol (CD_3OD) (δ_H 3.31/δ_C 49.0 ppm), and deuterated dimethyl sulfoxide (DMSO-d_6) (δ_H 2.50/δ_C 39.5 ppm). High resolution electrospray ionization mass spectrometry (HRESIMS) spectra were measured using a Bruker micrOTOF mass spectrometer (Bruker Daltonik, Bremen, Germany) and Agilent TOF/Q-TOF mass spectrometer (Agilent Technologies, CA, USA). UV absorbance values were recorded by UV/Vis spectrophotometer microplate reader (FLUOstar® Omega, BMG LABTECH, Ortenberg, Germany, and SPECTROstar Nano, BMG LABTECH, Ortenberg, Germany). A Merck (Darmstadt, Germany) silica gel 60 and Sephadex LH-20 (Sigma Aldrich, St. Louis, MO, USA). Pre-coated silica gel 60 F_{254} on aluminium sheets (Merck, Darmstadt, Germany) were used for analytical thin-layer chromatography (TLC).

3.2. Plant material

The root of *Clausena excavata* (**Figure 20**) was collected from Walai Rukhavej Botanical Research Institute (WRBRI), Mahasarakham University, Na Dun District, Maha sarakham Province, Thailand, on 8 February, 2022. The plant material

was collected and identified by K. Wongpakam, WRBRI. A voucher specimen (Wongpakam 19-16) was deposited at WRBRI, Mahasarakham University.

Figure 20. The root of *C. excavata*

3.3. Extraction

Roots of *C. excavata* were collected from Walairukhavej Botanical Research Institute (WRBRI), Na Dun District, Maha Sarakham Province, Thailand, in July 27, 2018. The plant material was identified by K. Wongpakam, and a voucher specimen (Wongpakam 19-16) was deposited at WRBRI, Mahasarakham University, Khanwarawichai District, Maha Sarakham Province, Thailand.

3.4. Isolation of the crude MeOH extract

Small pieces of the air-dried roots of *C. excavata* (300 g) were refluxed in MeOH (5 L, 4.5 h, twice). The mixture was filtered and the MeOH solution was evaporated under reduced pressure to obtain a dark brown gum (40.0 g), which was applied on a silica gel column (400 g), and eluted with gradient mixtures of hexane–EtOAc (80:20, 60:40, 40:60, 20:80), hexane–EtOAc–AcOH (20:80:5), and then EtOAc–CH_3COOH (100:5), to obtain fourteen fractions Fr.A–N.

Fr.A (596 mg) was applied over a silica gel column (54 g), and eluted with gradient mixtures of hexane–EtOAc (80:20, 60:40, 40:60, 20:80, 0:100), to give eight subfractions Sfr. A1–8. Sfr.A3–5 were combined (138 mg) and a combined fraction was applied on a silica gel column (13 g), and eluted with gradient mixtures of hexane–EtOAc (80:20, 60:40, 40:60, 20:80, 0:100), and then with EtOAc–MeOH (80:20, 60:40, 40:60, 50:50) to afford **46** (25.3 mg) and **115** (7.1 mg). Sfr.A7 (242 mg) was applied over a silica gel column (25 g), and eluted with gradient mixtures of hexane–EtOAc (80:20, 60:40, 40:60, 20:80, 0:100) to yield **33** (180.3 mg).

Fr.B (2.31 g) was purified by a silica gel column (230 g) CC, and eluted with gradient mixtures of hexane–EtOAc (80:20, 60:40, 40:60, 20:80, 0:100), to obtain five subfractions Sfr.B1–5. Sfr.B1 (237 mg) was applied on a silica gel column (24 g), and eluted with gradient mixtures of hexane–EtOAc (80:20, 60:40, 40:60, 20:80) to give **33** (144.2 mg).

Fr.C (668 mg) was applied over a silica gel (65 g), and eluted with gradient mixtures of hexane–EtOAc (80:20, 60:40, 40:60, 20:80, 0:100), to get five subfractions Sfr.C1–5. Sfr.C2 (352 mg) was washed by stirring in hexane and then crystallized in hexane to afford **32** (320.0 mg).

Fr.D (205 mg) was purified by silica gel column (20 g) CC, and eluted with gradient mixtures of hexane–EtOAc (80:20, 60:40, 40:60, 20:80, 0:100), to give ten subfractions Sfr.D1–10. Sfr.D4 (64 mg) was applied on a silica gel column (10 g),

and eluted with gradient mixtures of hexane–EtOAc (80:20, 60:40, 40:60, 20:80, 0:100) to obtain a collected subfraction which was further purified over a Sephadex LH-20 column, and eluted with MeOH to yield **80** (12.7 mg).

Fr.E (368 mg) was applied over a silica gel column (36 g), and eluted with gradient mixtures of hexane–EtOAc (80:20, 60:40, 40:60, 20:80, 0:100), to obtain nine subfractions Sfr.E1–9. Sfr.E2 (89 mg) was applied on a silica gel column (10 g), and eluted with gradient mixtures of hexane–EtOAc (80:20, 60:40, 40:60, 20:80, 0:100), to provide two main subfractions Sfr.E2a and E2b. Each of Sfr.E2a (21 mg) and Sfr.E2b (9 mg) were separately purified by a Sephadex LH-20 column CC, and eluted with MeOH to afford **35** (3.2 mg) and **77** (0.8 mg). Sfr.E4 (278 mg) was purified over silica gel column (20 g), and eluted with gradient mixtures of hexane–EtOAc (80:20, 60:40, 40:60, 20:80, 0:100), to give **34** (20.0 mg).

Fr.F (1.53 g) was washed by stirring in hexane (3.5 mL, ×2) and then with CH_2Cl_2 (3.5 mL, ×2) to yield **34** (1.07 g).

Fr.G–I were combined (1.15 g) and this combined fraction was applied over a silica gel column (120 g), and eluted with hexane–EtOAc (80:20, 60:40, 40:60, 20:80, 0:100), to get ten subfractions Sfr.G1–10. Sfr.G3 (520 mg) was applied over a silica gel column (50 g), and eluted with gradient mixtures of hexane–EtOAc (60:40, 40:60, 20:80, 0:100), and then EtOAc–MeOH from (90:10, 80:20, 70:30) to afford **34** (318.4

mg). Sfr.G5 (312 mg) was applied on a silica gel column (28 g), and eluted with the same manner of the mobile phase described above to yield **32** (150.4 mg).

Fr.J (247 mg) was purified by silica gel column (25 g) CC, and eluted hexane–EtOAc (60:40, 40:60, 20:80, 0:100), and then EtOAc–MeOH from (90:10, 80:20, 70:30) to give **34** (38.0 mg).

Fr.K (491 mg) was purified over a silica gel column (40 g), and eluted with gradient mixtures of hexane–EtOAc (80:20, 60:40, 40:60, 20:80, 0:100), and then EtOAc–MeOH from (90:10, 80:20, 70:30, 50:50) to give five subfractions Sfr.K1–5. Sfr.K2 (145 mg) was washed by stirring in EtOAc (2 × 1.5 mL) and the residue was purified over a Sephadex LH-20 column, and eluted with MeOH to afford **43** (28.1 mg).

3.5. Semi-synthesis of compounds 33a–33d, 80a and 34b–34d

3.5.1. Compounds **33a** and **80a**

Solutions of **33** (20.4 mg) and **80** (3.6 mg) in acetonitrile (0.5 mL) were mixed with Na_2CO_3 (excess) and stirred for 15 min at room temperature. CH_3I (excess) was then added to the reaction mixtures. The progress of the reactions was monitored by TLC. After the reactions were complete, the mixtures were treated with H_2O (0.5 mL) and extracted with EtOAc (3 × 0.5 mL). The EtOAc layers were dried over anhydrous $MgSO_4$ and then evaporated. The residues were purified by column chromatography over silica gel (2 g for **33a** and 0.4 g for **80a**), using gradient of hexane–EtOAc from 90:10 to 20:80 to afford **33a** and **80a** (**Figure 21**).

3.5.2. Compounds **33b** and **34b**

Solutions **33** (20 mg) and **34** (20 mg) in acetonitrile (0.5 mL) were mixed with Na_2CO_3 (excess) and stirred for 15 min at room temperature. Then, epichlorohydrin (1.0 mL) was added to the reaction mixtures and heated at 45–50 ˚C for 4 h. After cooling to room temperature, 10% H_2SO_4 (0.1 mL) was added dropwise to the mixtures and heated at 85–90 ˚C for 1 h. The progress of the reactions was monitored by TLC. After the reactions were completed, the mixtures were treated with H_2O (0.5 mL) and extracted with EtOAc (3 × 0.5 mL). The EtOAc layers were dried over anhydrous $MgSO_4$ and then evaporated. The residues from the evaporation were purified by column chromatography over silica gel (2 g) and eluted with gradient of hexane–EtOAc from 90:10 to 20:80 to afford **33b** and **34b** (**Figure 22**).

3.5.3. Compounds **33c** and **34c**

Solutions of **33** (20 mg) and **34** (20 mg) in acetonitrile (0.5 mL) were mixed with Na_2CO_3 (excess) and stirred for 15 min at room temperature. Ethyl bromoacetate (1 mL) was then added to the reaction mixtures and were heated at 45–50 ˚C for 2 h. The progress of the reactions was monitored by TLC. After the reaction was completed, the mixtures were treated with H_2O (0.5 mL) and extracted with EtOAc (3 × 0.5 mL). The collected EtOAc layers were dried with anhydrous $MgSO_4$, filtered and evaporated. The residues were purified by column chromatography over silica gel (2 g), using gradient of hexane–EtOAc from 90:10 to 20:80 for each compound to afford **33c** and **34c** (**Figure 22**).

3.5.4. Compounds **33d** and **34d**

Solutions of **33c** and **34c** were added 1-propanol (0.5 mL, 1.0 mL) and 1 M NaOH (0.5 mL, 1.0 mL). The reaction mixtures of **33d** and **34d** were warmed at 45–50 ˚C for 1h and 3h, respectively. The progress of the reactions was monitored by TLC. After the reactions were completed, the mixtures were cooled in ice bath and acidified to pH 5-6 by adding dropwise of 10% H_2SO_4, and stirred for 15 min. The mixtures were evaporated, treated with H_2O (0.5 mL, 1.0 mL) and extracted with EtOAc (3 × 0.5 mL, 3 × 1.0 mL). The collected EtOAc layers were dried over anhydrous $MgSO_4$, filtered and evaporated. The residues were purified by column chromatography over silica gel (2 g for **33d**, and 5.0 g for **34d**), using gradient of hexane–EtOAc from 90:10 to 0:100 and then EtOAc–MeOH from 90:10 to 60:40 to afford **33d** and **34d** (**Figure 22**).

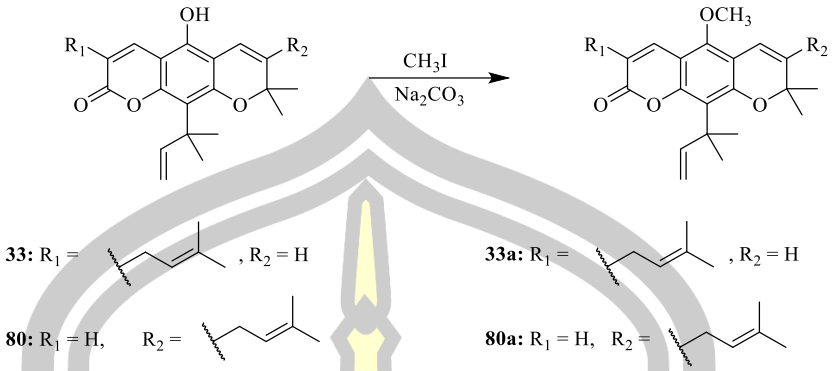

Figure 21. Preparation of compounds **33a** and **80a** by methylation of **33** and **80**.

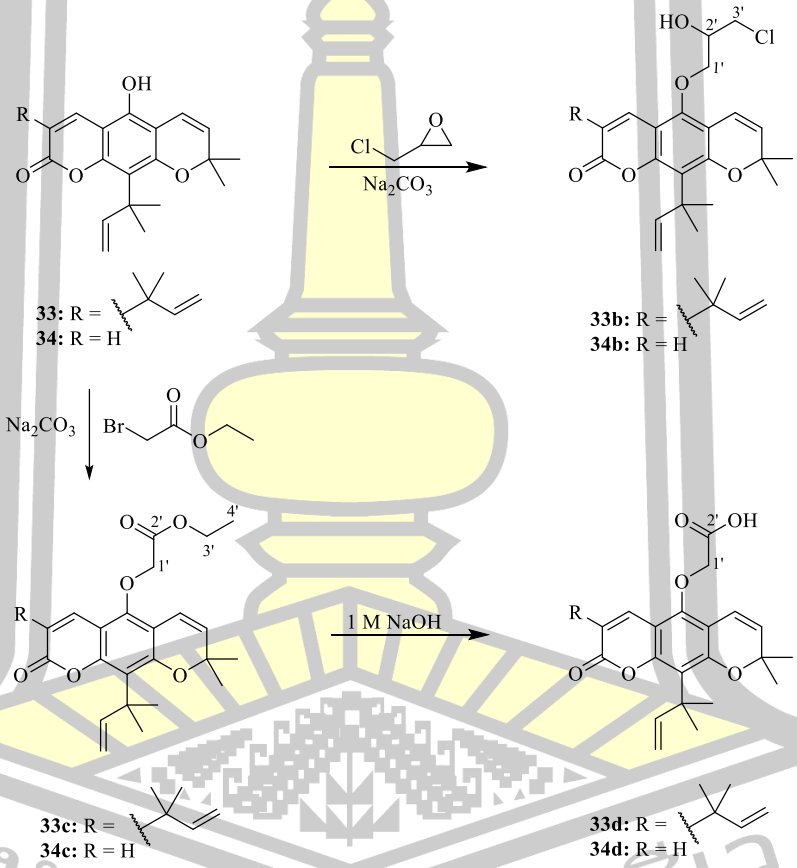

Figure 22. Preparation of compounds **33a–33d** and **34b–34d** from **33** and **34**.

3.6. Structure identification

Structures of the isolated compounds, **32**–**35**, **43**, **46**, **77**, **80** and **115** were elucidated on the basis of spectroscopic data (^{1}H NMR) compared with data reported in literatures. Structures of the semi-synthetic compounds, **33a**–**33d**, **80a** and **34b**–**34d**, were elucidated on the based on their spectroscopic data (^{1}H, ^{13}C NMR and MS spectroscopy) compared with their starting material compounds.

3.7. Antimalarial activity assay

The antiplasmodial activity was tested against a multidrug-resistant *P. falciparum* (K1) reference strain using a standardized fluorescent SYBR Green-based 96-microplate assay (Bennett et al., 2004) (Smilkstein et al., 2004). Parasites were cultured according to a reference procedure (Trager & Jensen, 2005), with slight modifications. Sample solutions were prepared in DMSO and 50 µL were used for the test. For screening, parasites were treated with 5 µg/mL of the samples, 200 nM artesunate (Sigma-Aldrich, Catalog #A3731–100MG) (standard antimalarial drug), or with 0.1% DMSO (control) and then incubated at 37 °C for 72 h under a gas mixture of 5% CO_2, 5% O_2, and 90% N_2. To determine parasite growth inhibition, fluorescence associated with SYBR green-intercalate parasitic DNA of the samples and control was measured at 490 nm excitation and 540 nm emission using the EnVision Multilabel Reader. Parasite growth values were normalized to those for the DMSO solvent control. The results are reported as %inhibition. The assays were carried out in triplicate.

% inhibition = [A (*sample*)-A (*control*)/A (*control*)] x 100

Human blood used in this study was performed under the human use protocol TMEC18-004, approved by the Institute Ethical Review Committee of the Faculty of Tropical Medicine, Mahidol University, Bangkok, Thailand. *P. falciparum* (K1) strain, a chloroquine-and pyrimethamine-resistant strain isolated in Thailand was used (Thaithong & M. Chutmongkonkul, 1983).

3.8. α-Glucosidase inhibitory activity assay

The inhibitory activity toward α-glucosidase was assayed according to the previously described method (Promden et al., 2024). The samples were first dissolved in DMSO to obtain a final concentration of 50 µg/mL 2.5% DMSO in buffer. An aliquot of 10 µL was added to each well of a 96-well microplate. Subsequently, 130 µL of 100 mM phosphate buffer (pH 6.8) was added to each well, followed by addition of 20 µL of α-glucosidase from *Saccharomyces cerevisiae* (0.5 U/mL) (Sigma-Aldrich, St. Louis, MO, USA). The microplate was then incubated at 37 °C for 10 min. The enzymatic reaction was started by adding 50 µL of 2.5 mM *p*-nitrophenyl-*α*-D-glucopyranoside (PNPG) (Sigma-Aldrich, St. Louis, MO, USA) as a substrate. In the control reaction, 10 µL of 2.5% DMSO was used instead of the compounds. The absorbance (A) of the control and samples were measured at 405 nm using a UV/Vis spectrophotometer microplate reader (FLUOstar® Omega, BMG LABTECH, Ortenberg, Germany) and the percentage inhibition was calculated using the equation below:

% inhibition = [A (*sample*)-A (*control*)/A (*control*)] x 100

To determine the IC_{50} values for the active compounds (>50% inhibition at 50 µg/mL), samples were prepared to the final concentrations ranging from 0.5 to 50 µg/mL 2.5% DMSO in buffer, and acarbose (Sigma-Aldrich, St. Louis, MO, USA) was used as a standard inhibitor in the assay. The IC_{50} values were calculated from a graph plotted between % inhibition against their corresponding concentrations.

3.9. NO inhibitory activity assay

Inhibition of NO production was evaluated in LPS (Sigma-Aldrich, St. Louis, MO, USA)-activated murine macrophage RAW 264.7 cells, according to the previously described method with some modifications (Makchuchit & Ruchilak Rattarom, 2017). RAW 264.7 cells were cultured in Dulbecco's Modified Eagle's Medium (DMEM) (Gibco®, Life Technologies Corporation, New York, USA) supplemented with 10% fetal bovine serum (Gibco®, Life Technologies Limited, Paisley, UK) and 1% antibiotic-antimycotic solution (10×10^3 units/mL of penicillin, 10 mg/mL of streptomycin, and 25 µg/mL of amphotericin B (Gibco®, Life Technologies Corporation, New York, USA). The cells were maintained at 37 °C in an incubator with 5% CO_2 and 95% humidity. For the NO inhibitory assay, the RAW 264.7 cells (1×10^6 cells/well) in DMEM were seeded into 96-well plates containing 100 µL of culture medium and incubated for 24 h. Subsequently, the medium was replaced with fresh medium containing 2 µg/mL of LPS, and the test samples were added to each well at a final concentration of 20 µg/mL. DMSO was used in the solvent control wells. After 24 h of incubation, 100 µL of supernatant was transferred to new 96-well plates, and 100 µL of Griess reagent (1% sulfanilamide in 0.1% *N*-(1-naphtyl)ethylenediamine dihydrochloide in 2.5% H_3PO_4 solution) was added to each

well. The absorbance (A) of the samples and the control was measured at 520 nm using a microplate reader (SPECTROstar Nano, BMG LABTECH, Ortenberg, Germany), and the percentage of NO inhibition was determined according to the formula below. Diclofenac sodium (Thermo Scientific, Shanghai, China) was used as a positive control.

$$\% \text{ Inhibition of NO production} = [A\,(\textit{sample})\text{-}A\,(\textit{control})/A\,(\textit{control})] \times 100$$

To evaluate the cytotoxic effect of samples in RAW 264.7 cells in the assay condition, the MTT assay was performed. Briefly, after removing the supernatant from the incubated plate, a 5 mg/mL MTT solution was added to each well, and incubated at 37 °C, in 5% CO_2 for 2 h. Then the medium was removed, and 50 µL of DMSO was added to dissolve the formazan product. The absorbance was measured at 570 nm using a microplate reader (SPECTROstar Nano, BMG LABTECH, Ortenberg, Germany). The percentage of cell survival was considered acceptable if it remained above 70% compared to the control.

3.10. Cytotoxicity assay against human lung cancer A549 cell lines

The cytotoxic activity against A549 cell line was assayed according to the previously described method with some modifications (Alley et al., 1988). Briefly, cell suspensions in the culture medium (100 µL per well) were seeded into 96-well plates and incubated at 37 °C in a humidified 5% CO_2 atmosphere. After 24 h, 100 µL of the culture medium containing the test sample was added to each well, followed by an additional 72 h incubation. After removing half of the medium, 10 µL of 5 mg/mL

MTT (Invitrogen®, Life Technologies Corporation, Oregon, USA) in phosphate buffer saline (Gibco®, Life Technologies Limited, Paisley, UK) was added, and the cells were incubated for 4 h at 37 °C. Then, the medium was removed and DMSO (50 µL per well) was added. The absorbance was measured at 570 nm by a microplate reader (SPECTROstar Nano, BMG LABTECH, Ortenberg, Germany). The absorbance values were used to calculate cell viability relative to the control. All assays were performed in triplicate, and the results were expressed as % cytotoxicity compared to the control group.

CHAPTER 4

RESULTS AND DISCUSSION

4.1. Extraction and TLC of the MeOH extract

Small pieces of the air-dried roots of *C. excavata* (300 g) were refluxed in methanol (5 L, 4.5 h, twice). The mixture was filtered and the methanol solution was evaporated under reduced pressure to obtain a dark brown gum (40.0 g). The crude MeOH extract was analyzed by thin layer chromatography (TLC) for the chemical profile (**Figure 23**).

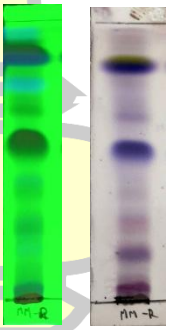

(**A**) (**B**)

Figure 23. TLC chromatogram of the methanol extract when observed under UV light 254 nm (**A**) and then sprayed with p-anisaldehyde sulfuric acid reagent and heated at 100−105 °C for 10 min (**B**).

4.2. Isolation and structure elucidation

Fractionation and purification of the crude methanol extract by column chromatography resulted in the isolation of six pyranocoumarins, *viz.* dentatin (**32**) (Songsiang et al., 2012), clausarin (**33**) (Huang et al., 1997), nordentatin (**34**)

(Songsiang et al., 2012), xanthyletin (**35**) (Cristiane et al., 2009), kinocoumarin (**80**) (Huang et al., 1997), citrusarin A (**115**) (Chan et al., 2010) and three carbazole alkaloids, i. e. clausine K (**43**) (Wu et al., 1996), heptaphylline (**46**) (Ruangrungsi et al., 1990) and 7-methoxymukonal (**77**) (Thongthoom et al., 2010) (**Figure 24**). Structures of these compounds were elucidated by comparison of their ^{1}H NMR spectral data (**Figure A1–7, A14–17**) with those reported in the literature.

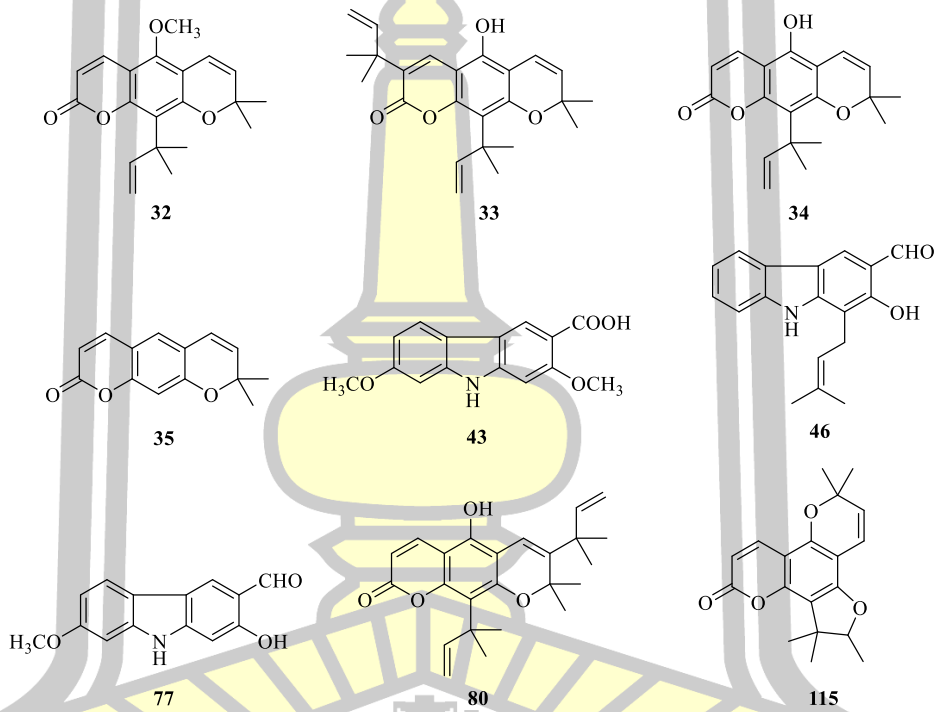

Figure 24. Structures of **32**–**34**, **43**, **46**, **77**, **80** and **115**.

4.2.1. Compound **32** (dentatin)

Compound **32** ($C_{20}H_{22}O_4$), colorless amorphous powder, was identified as dentatin based on spectroscopic data (**Table 1**) compared with those reported in literature (Songsiang et al., 2012). ^{1}H NMR spectrum of **32** in $CDCl_3$ was shown in **Figure A2**.

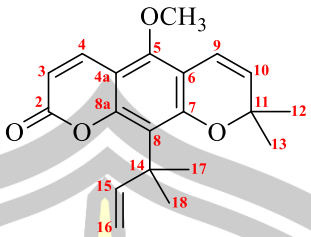

Table 1. ^{1}H (400 MHz) NMR spectroscopic data of **32** in $CDCl_3$.

Position	**32**	**Dentatin**[a]
	δ_H, mult. (*J* in Hz)	δ_H, mult. (*J* in Hz)
2	-	-
3	6.17 (d, 9.6)	6.18 (d, 9.6)
4	7.86 (d, 9.6)	7.86 (d, 9.6)
4a	-	-
5	3.81, s	3.82, s
6	-	-
7	-	-
8	-	-
8a	-	-
9	6.54 (d, 9.9)	6.56 (d, 9.9)
10	5.68 (d, 9.9)	5.69 (d, 9.9)
11	-	-
12	1.63, s	1.66, s
13	1.63, s	1.66, s
14	-	-
15	6.27 (dd, 17.4, 10.6)	6.30 (dd, 17.4, 10.6)
16	4.86 (dd, 17.4,1.1)	4.87 (d, 10.6)
	4.92 (dd, 10.6, 1.1)	4.94 (d, 17.4)
17	1.42, s	1.45, s
18	1.42, s	1.45, s

Calibration of $CDCl_3$ δ_H 7.26 ppm. [a]Songsiang et al., 2012.

4.2.2. Compound **33** (clausarin)

Compound **33** ($C_{24}H_{28}O_4$), colorless amorphous powder, was identified as clausarin based on spectroscopic data (**Table 2**) compared with those reported in literature (Huang et al., 1997). ^{1}H NMR spectrum of **33** in $CDCl_3$ was shown in **Figure A3**.

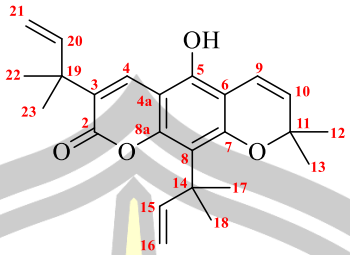

Table 2. ^{1}H (400 MHz) NMR spectroscopic data of **33** in $CDCl_3$.

Position	**33**	**clausarin**[a]
	δ_H, mult. (*J* in Hz)	δ_H, mult. (*J* in Hz)
2	-	-
3	-	-
4	7.95, s	7.85, s
4a	-	-
5	-	-
6	-	-
7	-	-
8	-	-
8a	-	-
9	6.61 (d, 9.9)	6.51 (d,10.0)
10	5.63 (d, 9.9)	5.68 (d, 10.0)
11	-	-
12	1.62, s	1.63, s
13	1.62, s	1.63, s
14	-	-
15	6.27 (dd, 17.4, 10.6)	6.29 (dd, 17.5, 11.0)
16	4.83 (dd, 10.6, 1.1)	4.86 (dd, 11.0, 1.1)
	4.90 (dd, 17.4, 1.1)	4.91 (dd, 17.5, 1.1)
17	1.46, s	1.47, s
18	1.46, s	1.47, s
19	-	-
20	6.17, (dd, 17.4, 10.5)	6.18 (dd, 17.5, 11.0)
21	5.08, (dd, 17.4, 0.9)	5.08 (dd, 11.0, 1.1)
	5.04, (dd, 10.6, 0.9)	5.09 (dd, 17.5, 1.1)
22	1.41, s	1.44, s
23	1.41, s	1.44, s
5-OH	-	5.69, s

Calibration of $CDCl_3$ δ_H 7.26 ppm. [a]Huang et al., 1997.

4.2.3. Compound **34** (nordentatin)

Compound **34** ($C_{19}H_{20}O_4$), colorless amorphous powder, was identified as nordentatin based on spectroscopic data (**Table 3**) compared with those reported in literature (Songsiang et al., 2012). ^{1}H NMR spectrum of **34** in $CDCl_3$ was shown in **Figure A4**.

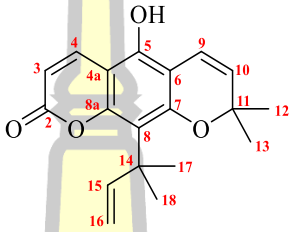

Table 3. ^{1}H (400 MHz) NMR spectroscopic data of **34** in $CDCl_3$.

Position	**34**	**nordentatin**[a]
	δ_H, mult. (*J* in Hz)	δ_H, mult. (*J* in Hz)
2	-	-
3	6.04 (d, 9.6)	6.13 (d, 9.6)
4	8.03 (d, 9.6)	8.04 (d, 9.6)
4a	-	
5	-	-
6	-	-
7	-	-
8	-	-
8a	-	-
9	6.60 (d, 9.9)	6.55 (d, 9.9)
10	5.57 (d, 9.9)	5.67 (d, 9.9)
11	-	
12	1.58, s	1.57, s
13	1.58, s	1.57, s
14	-	-
15	6.23 (dd, 17.4, 10.6)	6.27 (dd, 17.4, 10.6)
16	4.86 (dd, 17.4, 1.1)	4.91 (d, 17.4)
	4.79 (dd, 10.6, 1.1)	4.84 (d, 10.6)
17	1.38, s	1.43, s
18	1.38, s	1.43, s
5-OH	-	6.38, s

Calibration of $CDCl_3$ δ_H 7.26 ppm. [a]Songsiang et al., 2012.

4.2.4. Compound **35** (xanthyletin)

Compound **35** ($C_{14}H_{12}O_3$), colorless amorphous powder, was identified as xanthyletin based on spectroscopic data (**Table 4**) compared with those reported in literature (Cristiane et al., 2009). ^{1}H NMR spectrum of **35** in $CDCl_3$ was shown in **Figure A5**.

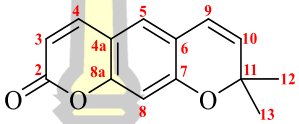

Table 4. ^{1}H (400 MHz) NMR spectroscopic data of **35** in $CDCl_3$.

Position	**35**	**xanthyletin**[a]
	δ_H, mult. (*J* in Hz)	δ_H, mult. (*J* in Hz)
1	-	-
2	-	-
3	6.41 (d, 9.5)	7.60 (d, 9.2)
4	7.79 (d, 9.5)	6.24 (d, 9.2)
4a	-	-
5	6.94, s	6.72, s
6	-	-
7	-	-
8	7.48, s	7.04, s
8a	-	-
9	6.55 (d, 9.9)	6.36 (d, 9.6)
10	5.89 (d, 9.9)	5.71 (d, 9.6)
11	-	-
12	1.68, s	1.43, s
13	1.68, s	1.43, s

Calibration of $CDCl_3$ δ_H 7.26 ppm. [a]Cristiane et al., 2009.

4.2.5. Compound **43** (clausine K)

Compound **43** ($C_{15}H_{13}NO_4$), brownish powder, was identified as clausine K based on spectroscopic data (**Table 4**) compared with those reported in literature (Wu et al., 1996). NMR spectrum (^1H in $CDCl_3$) (^1H, ^{13}C, HSQC, NOSEY, COSY, Dept 135, HMBC in DMSO-d_6) of **43** was shown in **Figure A6–13**.

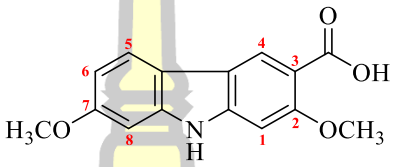

Table 5. ^1H NMR spectroscopic data of **43** in DMSO-d_6.

Position	**43**	**Clausine K**[a]
	δ_H, mult. (*J* in Hz)	δ_H, mult. (*J* in Hz)
1	7.03, s	7.03, s
2-OCH_3	3.89, s	3.89, s
3	-	-
4	8.39, s	8.39, s
5	7.94 (d, 8.4)	7.94 (d, 8.5)
6	6.77 (dd, 8.4, 2.0)	6.77 (dd, 8.5, 2.0)
7-OCH_3	3.83, s	3.83, s
8	6.97 (d, 2.0)	6.97 (d, 2.0)
9	-	-
-NH	11.27, s	11.27, br s

Calibration of DMSO-d_6 δ_H 2.50 ppm. [a]Wu et al. 1996.

4.2.6. Compound **46** (heptaphylline)

Compound **46** ($C_{18}H_{17}NO_2$), yellow needle powder, was identified as heptaphylline based on spectroscopic data (**Table 6**) compared with those reported in literature (Ruangrungsi et al., 1990). ^{1}H NMR spectrum of **46** in $CDCl_3$ was shown in **Figure A14**.

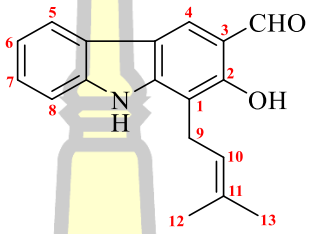

Table 6. ^{1}H (400 MHz) NMR spectroscopic data of **46** in $CDCl_3$

Position	**46**	**heptaphylline**[a]
	δ_H, mult. (*J* in Hz)	δ_H, mult. (*J* in Hz)
1	-	-
2	-	-
3	-	-
4	8.07, s	8.04, s
5	7.83 (d, 7.7)	7.97 (d, 7.6)
6	7.11, m	7.27 (t, 7.6)
7	7.25, (d, 3.8)	7.40 (t, 7.6)
8	7.25, (d, 3.8)	7.40 (d, 7.6)
9	3.48 (d, 6.8)	3.64 (d, 6.8)
10	5.16 (t, 6.8)	5.32 (br t, 6.8)
11	-	-
12	1.62, s	1.77, s
13	1.75, s	1.90, s
2-OH	11.51, s	11.70, s
3-CHO	9.75, s	9.91, s
NH	-	-

Calibration of $CDCl_3$ δ_H 7.26 ppm. [a]Ruangrungsi et al., 1990.

4.2.7. Compound **77** (7-methoxymukonal)

Compound **77** ($C_{14}H_{11}NO_3$), yellow amorphous powder, was identified as 7-methoxymukonal based on spectroscopic data (**Table 7**) compared with these reported in literature (Thongthoom et al., 2010). ^{1}H NMR spectrum of **77** in $CDCl_3$ was shown in **Figure A15**.

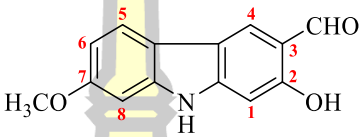

Table 7. ^{1}H (400 MHz) NMR spectroscopic data of **77** in $CDCl_3$.

Position	**77**	**7-methoxymukonal**[a]
	δ_H, mult. (*J* in Hz)	δ_H, mult. (*J* in Hz)
1	-	-
2-OH	11.43, s	11.42, s
3-CHO	9.92, s	9.92, s
4	6.89, s	6.89, s
5	6.86 (d, 8.2)	6.87 (d, 8.2)
6	7.85 (d, 8.2)	7.84 (d, 8.2)
7-OCH_3	3.90, s	3.89, s
8	8.05, s	8.04, s
9-NH	8.13, br	8.15, br

Calibration of $CDCl_3$ δ_H 7.26 ppm. [a]Thongthoom et al., 2010.

4.2.8. Compound **80** (kinocoumarin)

Compound **80** ($C_{24}H_{28}O_4$), colorless amorphous powder, was identified as kinocomarin based on spectroscopic data (**Table 8**) compared with those reported in literature (Huang et al., 1997). ^{1}H NMR spectrum of **80** in $CDCl_3$ was shown in **Figure A16**.

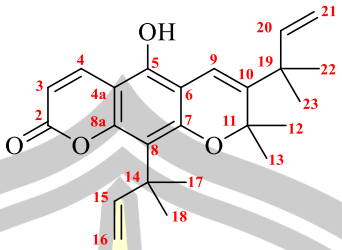

Table 8. ^{1}H (400 MHz) NMR spectroscopic data of **80** in $CDCl_3$.

Position	**80**	**kinocoumarin**[a]
	δ_H, mult. (*J* in Hz)	δ_H, mult. (*J* in Hz)
2	-	-
3	6.14 (d, 9.6)	6.15 (d, 9.7)
4	8.01 (d, 9.6)	8.10 (d, 9.7)
4a	-	-
5	-	6.02, br
6	-	-
7	-	-
8	-	-
8a	-	-
9	6.42, s	6.47, s
10	-	-
11	-	-
12	1.61, s	1.63, s
13	1.61, s	1.63, s
14	-	-
15	5.92 (dd, 17.4, 10.6)	5.92 (dd,17.7, 10.0)
16	4.90 (dd, 17.4, 1.1) 4.84 (dd, 10.6, 1.1)	4.92 (dd, 17.7, 1.0) 4.86 (dd, 10.0, 1.0)
17	1.34, s	1.36, s
18	1.34, s	1.36, s
19	-	-
20	6.28 (dd, 17.4, 10.6)	6.29 (dd, 17.7, 10.0)
21	5.11 (dd, 17.4, 0.7) 5.03 (dd, 10.6, 0.7)	5.10 (dd, 17.7, 1.0) 5.03 (dd, 10.0, 1.0)
22	1.47, s	1.36, s
23	1.47, s	1.36, s

Calibration of $CDCl_3$ δ_H 7.26 ppm. [a]Huang et al., 1997.

4.2.9. Compound **115** (citrusarin A)

Compound **115** ($C_{14}H_{12}O_3$), yellow oil, was identified as citrusarin A based on spectroscopic data (**Table 9**) compared with these reported in literature (Chan et al., 2010). ^{1}H NMR spectrum of **115** in $CDCl_3$ was shown in **Figure A17**.

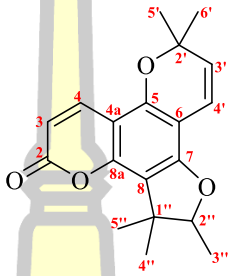

Table 9. ^{1}H (400 MHz) NMR spectroscopic data of **115** in $CDCl_3$

Position	**115**	**Citrusarin A**[a]
	δ_H, mult. (*J* in Hz)	δ_H, mult. (*J* in Hz)
1	-	-
2	-	-
3	6.07 (d, 9.6)	6.07 (d, 9.6)
4	7.93 (d, 9.6)	7.93 (d, 9.6)
4a	-	-
5	-	-
6	-	-
7	-	-
8	-	-
8a	-	-
1′	-	-
2′	-	-
3′	5.54 (d, 9.9)	5.54 (d, 9.9)
4′	6.45 (d, 9.9)	6.45 (d, 9.9)
5′	1.46, s	1.46, s
6′	1.46, s	1.46, s
1″	-	-
2″	4.48 (d, 6.6)	4.48 (d, 6.6)
3″	1.39 (d, 6.6)	1.39 (d, 6.6)
4″	1.25, s	1.25, s
5″	1.52, s	1.52, s

Calibration of $CDCl_3$ δ_H 7.26 ppm. [a]Chan et al., 2010.

4.3. Semi-synthetic compounds

Compounds **33** and **80** were obtained by methylation of **33a** and **80a** (**Figure 35**) with iodomethane (CH_3I). Compounds **33b** and **34b** were prepared by etherification of **33** and **34** with epichlorohydrin in alkali solution, whereas **33c** and **34c** were obtained by etherification of **33** and **34** with ethyl bromoacetate in alkali solution. Compounds **33d** and **34d were** obtained by basic hydrolysis of **33c** and **34c** (**Figure 25**), respectively.

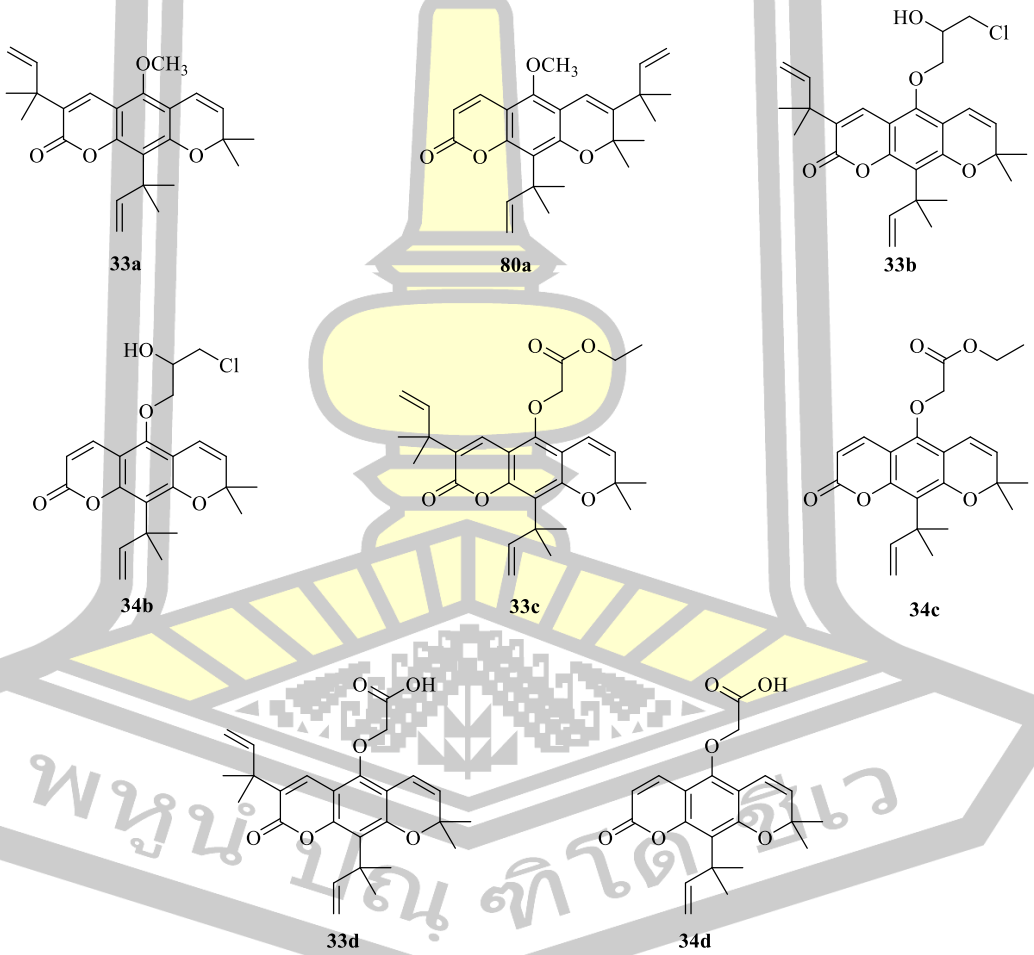

Figure 25. Structures of **33a**–**33d**, **80a**, and **34b**–**34d** (semi-synthetic analogs).

Table 10. Semi-synthetic analogs of compounds **33 34** and **80**.

Starting compound (weight)	Condition	Semi-synthetic product (weight)	% yield
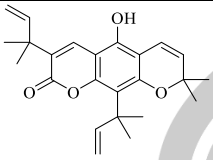 **33** **(20 mg)**	(1) Na_2CO_3 (excess) in CH_3CN, 15 min, rt. (2) CH_3I (excess) (3) Extraction	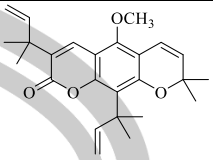 **33a** **(19.7 mg)**	98.5
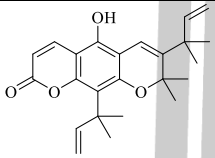 **80** **(3.6 mg)**	(1) Na_2CO_3 (excess) in CH_3CN, 15 min, rt. (2) CH_3I (excess) (3) Extraction	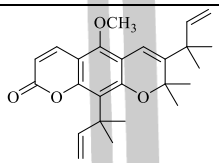 **80** **(1.1 mg)**	30.6
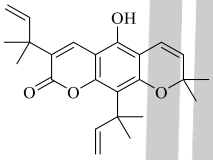 **33** **(20 mg)**	(1) Na_2CO_3 (excess) in CH_3CN, 15 min, rt. (2) Epichlorohydrin (1.0 mL), 4 h, 45–50 °C (3) Cooling to rt. (4) 10% H_2SO_4 (100 µL), 1h, 85–90 °C (5) Extraction	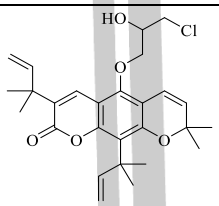 **33b** **(14.0 mg)**	70.0
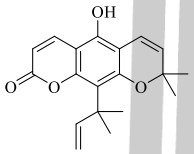 **34** **(20 mg)**	(1) Na_2CO_3 (excess) in CH_3CN, 15 min, rt. (2) Epichlorohydrin (1.0 mL), 4 h, 45–50 °C (3) Cooling to rt. (4) 10% H_2SO_4 (100 µL), 1h, 85–90 °C (5) Extraction	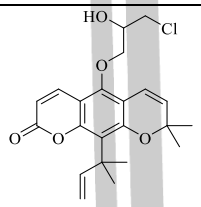 **34b** **(14.9 mg)**	74.5
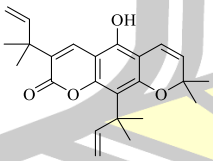 **33** **(20 mg)**	(1) Na_2CO_3 (excess) in CH_3CN, 15 min, rt. (2) Ethyl bromoacetate (1.0 mL), 2 h, 45–50 °C (3) Extraction	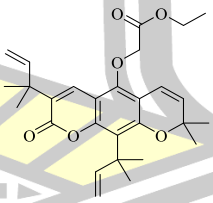 **33c** **(14.4 mg)**	72.0
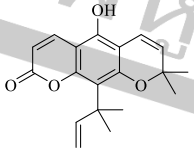 **34** **(20 mg)**	(1) Na_2CO_3 (excess) in CH_3CN, 15 min, rt. (2) Ethyl bromoacetate (1.0 mL), 2 h, 45–50 °C (3) Extraction	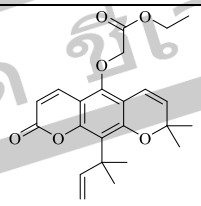 **34c** **(15.3 mg)**	76.5

Starting compound (weight)	Condition	Semi-synthetic product (weight)	% yield
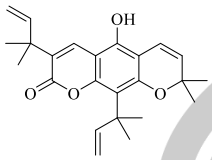 **33** **(20 mg)**	(1) 1 M NaOH (0.5 mL) in 1-propanol (0.5 mL), 1 h, 45–50 °C (2) Epichlorohydrin (1.0 mL), 4 h, 45–50 °C (3) Cooled in ice bath (4) Acidified to pH 5–6 by adding 10% H_2SO_4, 15 min. (5) Extraction	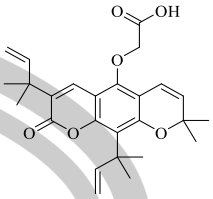 **33d** **(15.8 mg)**	79.0
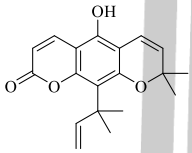 **34** **(20 mg)**	(1) 1 M NaOH (1.0 mL) in 1-propanol (1.0 mL), 1 h, 45–50 °C (2) Epichlorohydrin (2.0 mL), 4 h, 45–50 °C (3) Cooled in ice bath (4) Acidified to pH 5–6 by adding 10% H_2SO_4, 15 min. (5) Extraction	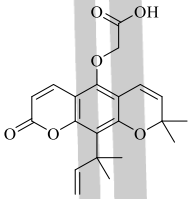 **34d** **(45.0 mg)**	90.0

4.3.1. Compounds **33a (***O*-methylclausarin) and **80a (***O*-methylkinocoumarin)

Compound **33a** ($C_{25}H_{30}O_4$), Colorless amorphous solid, was identified as *O*-methylclausarin based on ^1H, ^{13}C spectroscopic data (**Table 11**) and HRESIMS spectra (**Figure A20**). ^1H and ^{13}C NMR spectrum of **33a** in $CDCl_3$ was shown in **Figure A18–19**.

Compound **80a** ($C_{25}H_{30}O_4$), Colorless amorphous solid, was identified as *O*-methylkinocoumarin based on ^1H, ^{13}C spectroscopic data (**Table 11**) and HRESIMS spectra (**Figure A23**). ^1H and ^{13}C NMR spectrum of **80a** in $CDCl_3$ was shown in **Figure A21–22**.

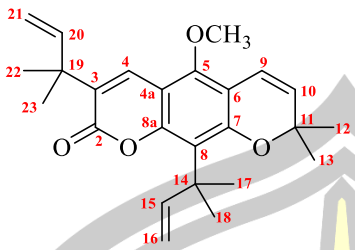

33a **80a**

Table 11. ^{1}H (400 MHz) NMR spectroscopic data of **33a** and **80a** in $CDCl_3$.

Position	**33a**	**80a**
	δ_H, mult. (*J* in Hz)	δ_H, mult. (*J* in Hz)
2	-	-
3	-	6.19 (d, 9.6)
4	7.73, s	7.90 (d, 9.6)
4a	-	-
5	-	-
6	-	-
7	-	-
8	-	-
8a	-	-
9	6.57 (d, 9.9)	6.57, s
10	5.67 (d, 9.9)	-
11	-	-
12	1.65, s	1.66, s
13	1.65, s	1.66, s
14	-	-
15	6.31 (dd, 17.4, 10.6)	6.31 (dd, 17.4, 10.6)
16	4.95 (dd, 17.4, 1.1)	4.94 (dd, 17.4, 1.1)
	4.82 (d, 10.6, 1.1)	4.89 (dd, 10.6, 1.1)
17	1.43, s	1.37, s
18	1.43, s	1.37, s
19	-	-
20	6.18 (dd, 17.4, 10.6)	5.94 (dd, 17.5, 10.6)
21	5.11 (d, 10.4)	5.11 (dd, 17.5, 0.9)
	5.07, s	5.07 (dd, 10.6, 0.9)
22	1.47, s	1.50, s
23	1.47, s	1.50, s
5-OCH_3	3.82, s	3.85, s

Calibration of $CDCl_3$ δ_H 7.26 ppm.

^{13}C NMR of **33a** ($CDCl_3$, 100 MHz) δ_C: 159.4, 154.9, 153.1, 151.0, 149.9, 145.6, 132.8, 130.4, 130.2, 118.5, 116.5, 112.0, 111.5, 108.5, 107.7, 77.2, 63.2, 41.1, 40.2, 29.3 (2C), 27.4 (2C), 26.1 (2C); HRESIMS *m/z*: 417.2037 $[M + Na]^+$ (calcd. for $C_{25}H_{30}O_4Na^+$, 417.2036).

^{13}C NMR of **88a** ($CDCl_3$, 100 MHz) δ_C: 160.9, 155.3, 153.6, 151.1, 149.6, 147.0, 146.6, 139.0, 118.8, 113.5, 113.1, 112.0, 111.6, 108.4, 107.6, 81.3, 63.3, 41.5, 41.1, 29.4 (2C), 28.0 (2C), 27.4 (2C); HRESIMS *m/z:* 417.2037 $[M + Na]^+$ (calcd. for $C_{25}H_{30}O_4Na^+$, 417.2036).

4.3.2. Compounds **33b** (clausarin 5-*O*-(3′-chloropropane-2′-ol)) and **34b** (nordentatin 5-*O*-(3′-chloropropane-2′-ol))

Compound **33b** ($C_{27}H_{33}ClO_5$), Colorless amorphous solid, was identified as (clausarin 5-*O*-(3′-chloropropane-2′-ol)) based on ^{1}H, ^{13}C spectroscopic data (**Table 12**) and HRESIMS spectra (**Figure A26**). ^{1}H and ^{13}C NMR spectrum of **33b** in $CDCl_3$ was shown in **Figure A24**–**25**.

Compound **34b** ($C_{22}H_{25}ClO_5$), Colorless amorphous solid, was identified as (nordentatin 5-*O*-(3′-chloropropane-2′-ol)) based on ^{1}H, ^{13}C spectroscopic data (**Table 12**) and HRESIMS spectra (**Figure A29**). ^{1}H and ^{13}C NMR spectrum of **80a** in acetone-d_6 was shown in **Figure A27**–**28**.

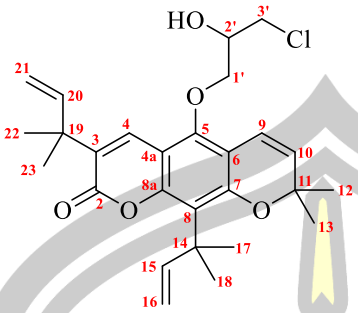

33b

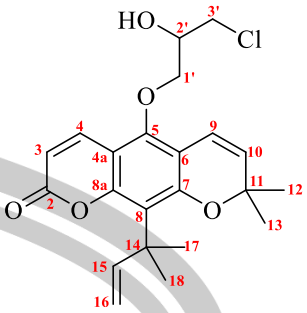

34b

Table 12. ^{1}H (400 MHz) NMR spectroscopic data of **33b** and **34b**.

Position	**33b** (in $CDCl_3$)	**34b** (in acetone-d_6)
	δ_H, mult. (*J* in Hz)	δ_H, mult. (*J* in Hz)
2	-	-
3	-	6.16 (d, 9.7)
4	7.80, s	8.15 (d, 9.7)
4a	-	-
5	-	-
6	-	-
7	-	-
8	-	-
8a	-	-
9	6.57 (d, 9.9)	6.75 (d, 9.9)
10	5.69 (d, 9.9)	5.85 (d, 9.9)
11	-	-
12	1.65, s	1.65, s
13	1.65, s	1.65, s
14	-	-
15	6.30 (dd, 17.4, 10.4)	6.31 (dd, 17.4, 10.6)
16	4.95 (dd, 17.4, 1.0)	4.92 (dd, 17.4, 1.1)
	4.88 (dd, 10.4, 1.0)	4.85 (dd, 10.6, 1.1)
17	1.43, s	1.47, s
18	1.43, s	1.47, s
19	-	-
20	6.18 (dd, 17.4, 10.4)	-
21	5.11 (dd, 17.4, 1.1)	-
	5.09 (dd, 10.5, 1.1)	
22	1.47, s	-
23	1.47, s	-
1′	3.83, m	3.87 (dd, 11.2, 5.8)
		3.78 (dd, 11.2, 5.8)
2′	4.23, m	4.26, m
3′	3.98, m	4.07, m

Calibration of $CDCl_3$ δ_H 7.26 ppm. Calibration of acetone-d_6 δ_H 2.05 ppm

^{13}C NMR of **33b** ($CDCl_3$, 100 MHz) δ_C: 159.3, 154.9, 153.1, 149.7, 148.9, 145.6, 132.7, 130.7 (2C), 119.0, 116.2, 112.1, 111.6, 108.1, 107.8, 75.5, 70.2, 45.5, 41.1, 40.5, 29.7, 29.2 (2C), 27.4 (2C), 26.0 (2C); HREIMS *m*/*z*: 495.1911 $[M + Na]^+$ (calcd. for $C_{27}H_{33}O_5ClNa^+$, 495.1909).

^{13}C NMR of **34b** (acetone-d_6, 100 MHz) δ_C: 160.2, 156.6, 154.9, 150.9, 150.7, 140.1, 131.4, 119.5, 117.1, 112.8, 112.3, 108.5, 78.3, 77.8, 70.9, 70.8, 46.4 (2C), 29.9 (2C), 27.6 (2C); HR-EIMS *m*/*z*: 427.1282 $[M + Na]^+$ (calcd. for $C_{22}H_{25}ClO_5Na^+$, 427.1283).

4.3.3. Compounds **33c** (clausarin 5-*O*-(ethyl acetate)) and **34c** (nordentatin 5-*O*-(ethyl acetate))

Compound **33c** ($C_{28}H_{34}O_6$), Colorless amorphous solid, was identified as (clausarin 5-*O*-(ethyl acetate)) based on ^{1}H, ^{13}C spectroscopic data (**Table 13**) and HRESIMS spectra (**Figure A32**). ^{1}H and ^{13}C NMR spectrum of **33c** in acetone-d_6 was shown in **Figure A30**–**31**.

Compound **34c** ($C_{22}H_{26}O_6$), Colorless amorphous solid, was identified as (nordentatin 5-*O*-(ethyl acetate)) based on ^{1}H, ^{13}C spectroscopic data (**Table 13**) and HRESIMS spectra (**Figure A35**). ^{1}H and ^{13}C NMR spectrum of **34c** in acetone-d_6 was shown in **Figure A33**–**34**.

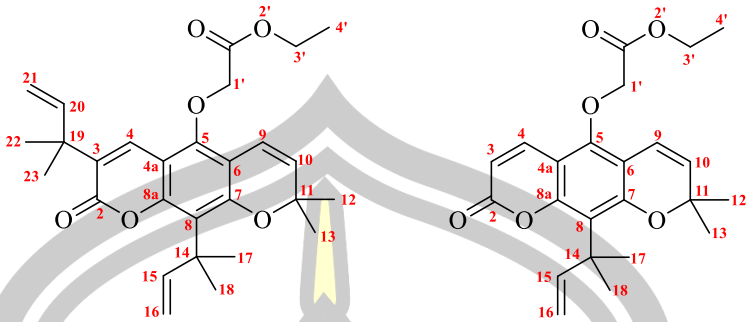

33c **34c**

Table 13. ^{1}H (400 MHz) NMR spectroscopic data of **33c** and **34c** in acetone-d_6.

Position	**33c**	**34c**
	δ_H, mult. (J in Hz)	δ_H, multri. (J in Hz)
2	-	-
3	-	6.18 (d, 9.7)
4	8.19, s	8.27 (d, 9.7)
4a	-	-
5	-	-
6	-	-
7	-	-
8	-	-
8a	-	-
9	6.70 (d, 9.9)	6.71 (d, 9.9)
10	5.87 (d, 9.9)	5.88 (d, 9.9)
11	-	-
12	1.65, s	1.65, s
13	1.65, s	1.65, s
14	-	-
15	6.30 (dd, 17.4, 10.6)	6.29 (dd, 17.4, 10.6)
16	4.92 (dd, 17.4, 1.0)	4.92 (dd, 17.4, 1.1)
	4.85 (dd, 10.6, 1.0)	4.85 (dd, 10.6, 1.1)
17	1.46, s	1.47, s
18	1.46, s	1.47, s
19	-	-
20	6.23 (dd, 17.5, 10.6)	-
21	5.08 (dd, 17.5, 1.0)	-
	5.04 (dd, 10.6, 1.0)	
22	1.47, s	-
23	1.47, s	-
1′	4.70, s	4.71, s
2′	-	-
3′	4.23 (q, 7.1)	4.22 (q, 7.1)
4′	1.26 (t, 7.1)	1.26 (t, 7.1)

Calibration of acetone-d_6 δ_H 2.05 ppm

^{13}C NMR of **33c** (acetone-d_6, 100 MHz) δ_C: 169.4, 159.3, 155.7, 153.9, 151.3, 150.7, 146.5, 134.6, 131.5, 130.7, 118.9, 117.4, 112.2, 108.7, 108.6, 78.0, 72.8, 61.7, 41.7, 40.9, 30.3, 29.9 (2C), 27.2 (2C), 26.4 (2C), 14.4; HREIMS *m*/*z*: 489.2257 [M + Na]$^+$ (calcd. for $C_{28}H_{34}O_6Na^+$, 489.2248).

^{13}C NMR of **34c** (acetone-d_6, 100 MHz) δ_C: 168.3, 159.2, 155.7, 153.9, 150.4, 149.8, 139.7, 130.7, 118.7, 116.3, 111.4, 111.3, 107.7, 107.6, 77.3, 71.9, 60.8, 40.9, 29.0 (2C) , 26.56 (2C) , 13.5; HREIMS *m*/*z*: 421.1621 [M + Na]$^+$ (calcd. for $C_{23}H_{26}O_6Na^+$, 421.1622).

4.3.4. Compounds **33d** (clausarin 5-*O*-(acetic acid)) and **34d** (nordentatin 5-*O*-(acetic acid))

Compound **33d** ($C_{26}H_{30}O_6$), Colorless amorphous solid, was identified as (clausarin 5-*O*-(acetic acid)) based on ^{1}H, ^{13}C spectroscopic data (**Table 14**) and HRESIMS spectra (**Figure A39**). ^{1}H and ^{13}C NMR spectrum of **33d** in CD_3OD and DMSO-d_6 were shown in **Figure A36**–**38**.

Compound **34d** ($C_{21}H_{22}O_6$), Colorless amorphous solid, was identified as (nordentatin 5-*O*-(acetic acid)) based on ^{1}H, ^{13}C spectroscopic data (**Table 15**) and HRESIMS spectra (**Figure A43**). ^{1}H and ^{13}C NMR spectrum of **34d** in CD_3OD and DMSO-d_6 were shown in **Figure A40**–**42**.

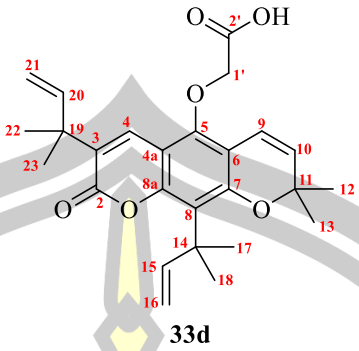

33d

Table 14. ^{1}H (400 MHz) NMR spectroscopic data of **33d**.

Position	**33d** (in CD_3OD)	**33d** (in DMSO-d_6)
	δ_H, mult. (J in Hz)	δ_H, mult. (J in Hz)
2	-	-
3	-	-
4	8.11, s	8.38, s
4a	-	-
5	-	-
6	-	-
7	-	-
8	-	-
8a	-	-
9	6.68 (d, 9.9)	6.68 (d, 9.9)
10	5.78 (d, 9.9)	5.79 (d, 9.9)
11	-	-
12	1.64, s	1.58, s
13	1.64, s	1.58, s
14	-	-
15	6.28 (dd, 17.4, 10.6)	6.24 (dd, 17.4, 10.6)
16	4.92 (d, 1.1) *overlap	4.87 (dd, 17.4, 1.1)
	4.84 (d, 1.1)	4.82 (dd, 10.6, 1.1)
17	1.42, s	1.38, s
18	1.42, s	1.38, s
19	-	-
20	6.17 (dd, 17.5, 10.6)	6.14 (dd, 17.4, 10.6)
21	5.06 (dd, 17.5, 1.1)	5.01 (dd, 17.4, 1.1)
	5.02 (dd, 10.6, 1.1)	4.97 (dd, 10.6, 1.1)
22	1.45, s	1.40, s
23	1.45, s	1.40, s
1′	4.29, s	4.13, s
2′	-	-

Calibration of CD_3OD δ_H 3.31 ppm. Calibration of DMSO-d_6 δ_H 2.50 ppm

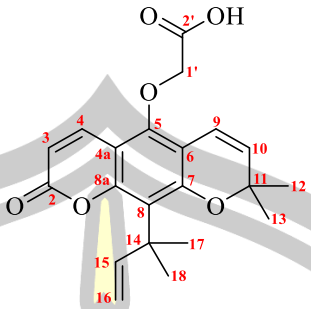

34d

Table 15. ^{1}H (400 MHz) NMR spectroscopic data of **34d**.

Position	**34d** (in CD_3OD)	**34d** (in DMSO-d_6)
	δ_H, mult. (*J* in Hz)	δ_H, mult. (*J* in Hz)
2	-	-
3	6.27 (d, 9.6)	6.24 (d, 9.7)
4	8.26 (d, 9.6)	8.51 (d, 9.7)
4a	-	-
5	-	-
6	-	-
7	-	-
8	-	-
8a	-	-
9	6.68 (d, 9.9)	6.68 (d, 9.9)
10	5.80 (d, 9.9)	5.80 (d, 9.9)
11	-	-
12	1.64, s	1.58, s
13	1.64, s	1.58, s
14	-	-
15	6.27 (dd, 17.4, 10.6)	6.24 (dd, 17.4, 10.6)
16	4.92 (d, 1.0) *overlap	4.87 (dd, 17.4, 1.1)
	4.84 (d, 1.0)	4.82 (dd, 10.6, 1.1)
17	1.47, s	1.39, s
18	1.47, s	1.39, s
1′	4.30, s	4.12, s
2′	-	-

Calibration of CD_3OD δ_H 3.31 ppm. Calibration of DMSO-d_6 δ_H 2.50 ppm

^{13}C NMR of **33d** (DMSO-d_6, 100 MHz) δ_C: 171.1 , 158.5, 154.4, 152.3, 151.6, 149.5, 145.5, 135.3, 129.9, 128.4, 117.0, 116.5, 111.7, 111.2, 108.1, 108.0, 76.8, 75.4, 40.5 (2C), 29.2 (2C), 26.8 (2C), 26.1 (2C); HREIMS *m/z:* 461.1932 $[M + Na]^+$ (calcd. for $C_{26}H_{30}O_6Na^+$, 461.1935).

^{13}C NMR of **34d** (DMSO-d_6, 100 MHz) δ_C 170.9, 159.7, 155.2, 153.2, 151.8, 149.6, 141.5, 130.0, 117.1, 116.9, 111.3, 110.3, 108.1, 107.9, 77.0, 75.6, 40.5, 29.2 (2C), 26.9 (2C); HREIMS *m/z:* 393.1307 $[M + Na]^+$ (calcd. for $C_{21}H_{22}O_6Na^+$, 393.1309).

4.4. Biological activities of the crude MeOH extract

The crude MeOH extract was tested for antimalarial activity against *P. falciparum* at the Drug Research Unit for Malaria (DRUM), Faculty of Tropical Medicine, Mahidol University, Bangkok, Thailand, at concentrations of 5 and 1 µg/mL. It showed antimalarial activities inhibition with 100% and 77.4% of at 5 and 1 µg/mL, respectively (**Table 16**).

NO inhibitory assay was conducted at the Faculty of Pharmacy, Mahasarakham University, Maha Sarakham, Thailand, at concentration 100 µg/mL. It showed NO inhibitory activity of 99.2% (**Table 16**).

Table 16. Biological activities of the crude methanol extract.

Activity	Concentration (µg/mL)	%Inhibition	%Cell Survival
Antimalaria	5	100	-
	1	77.4	-
Nitric oxide inhibition	100	99.2	9.0

The root extract was tested for its antimalaria activity against *P. falciparum*. It showed 100% inhibition of the proliferation of the malaria parasite at the tested concentrations of 5 or 1 µg/mL. The active root extract was fractionated by silica gel column chromatography (CC) using hexane-ethyl acetate with 5% acetic acid in ethyl acetate and then ethyl acetate-methanol with 5% acetic acid as eluents to obtain fourteen combined fractions, A–N, based on their similarity of TLC bands (**Figure 25**). Fractions A–L showed > 99 inhibition against the *P. falciparum* at 5 µg/mL (**Table 17**).

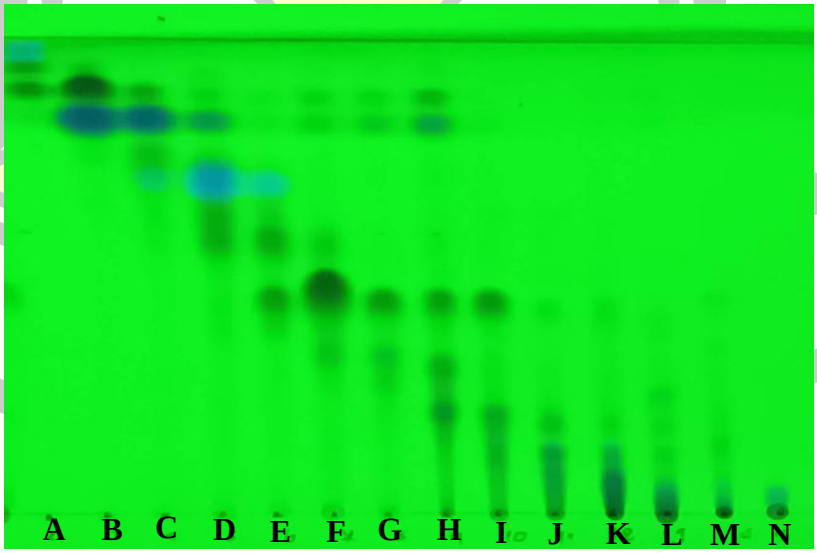

Figure 26. TLC chromatograms of the fractions from the methanol extract when observed under UV light 254 nm.

Table 17. Antimalaria activity of fractions from the crude methanol extract.

Fraction	%Inhibition	
	5 µg/mL	1 µg/mL
A	100	-
B	100	-
C	100	-
D	100	-
E	100	-
F	100	-
G	100	-
H	100	-
I	100	-
J	100	-
K	99.9	-
L	99.3	-
M	-	inactive
N	-	inactive

Inactive (%Inhibition less than 50).

4.5. Biological activity of pure compound and semi-synthetic

Compounds, **32**–**35**,**43**, **46**, **77**, **80**, **115**, **33a**–**33d**, **80a** and **34b**–**34d** were tested for biological activities, including antimalarial, α-glucosidase inhibitory activity, nitric oxide (NO) inhibitory activities and cytotoxicity assays against human lung cancer A549 cell lines.

4.5.1. Antimalarial activity

Compounds **32**–**35**,**43**, **46**, **77**, **80**, and **115** and the semi-synthetic derivatives, **33b**–**33d** and **34b**–**34d**, were preliminarily screened for their inhibitory activity against antimalarial at the concentration of 5 µM. Other compounds were not included in this assay due to their minute amount obtained. Compounds that showed more than 80% inhibition of antimalarial in the preliminary screening were further evaluated for their IC_{50} values. Among the isolated compounds tested, the pyranocoumarin **33** displayed the most potent antimalarial activity (IC_{50} = 0.58 µM), followed by **80** (IC_{50} = 1.10 µM), followed by **34** (IC_{50} = 5.62 µM) and **32** (IC_{50} = 7.66 µM) (Seephonkai et al., 2023). For the semi-synthetic analogs, **33a** displayed antimalaria activity (IC_{50} = 1.97 µM), and **80a** (IC_{50} = 3.25 µM), while **33b** and **33d** displayed weak activity (**Table 18**).

Table 18. Antimalarial activities of the isolated compounds of *C. excavata*.

Compound	IC_{50} (µM)
32	>7.66[ref]
33	0.58[ref]
34	5.62[ref]
35	ND
43	ND
46	ND
77	ND
80	1.10[ref]
115	ND
33a	1.97
80a	3.25
33b	Weakly active
34b	ND
33c	Weakly active
34c	ND
33d	ND
34d	ND
Artesunate	0.00234

At 95% confidence interval. ND = Not determined. [ref]Seephonkai et al., 2023.

4.5.2. α-Glucosidase inhibition activity

Compounds **43**, **46**, **80**, and, **115** and the semi-synthetic derivatives, **33b**–**33d** and **34b**–**34d**, were preliminarily screened for their inhibitory activity against α-glucosidase at a concentration of 50 µg/mL. Other compounds were not included in this assay due to their minute amount obtained. Compounds that showed more than 50% inhibition of α- glucosidase in the preliminary screening were further evaluated for their IC_{50} values. The α-glucosidase inhibitory activity of the tested compounds is

shown in **Table 19**. Compounds **46**, **80**, **33b**, **33c**, **34b** and **34c** displayed higher α-glucosidase inhibitory activity than the positive control, acarbose (IC_{50} 391.47 μM), with IC_{50} values ranging from 32.89 to 92.55 μM. Compound **80** and the semi-synthetic analogue, **33b**, exhibited the most potent 5 inhibitory effect, with IC_{50} values of 34.57 and 32.89 μM, respectively, which are more than 10 folds stronger than acarbose. When compared to the α-glucosidase inhibitory activity of **33**, **33a**, **34** and **34a**, recently reported by our group, 20 it was found that 2 showed an IC_{50} value slightly less than that of **34**, but ca. 4 folds higher than 3. These results suggested that the prenyl group at C-2 of the coumarin scaffold of linear pyranocoumarins plays a vital role in α-glucosidase inhibitory activity. The IC_{50} values of the semi-synthetic **33b** (IC_{50} = 32.89 μM) and **33c** (IC_{50} = 80.68 μM) are higher than those previously reported for **33a** (IC_{50} = 47.85 μM) and **33** (IC_{50} = 8.36 μM). Similarly, the IC_{50} values of the semi-synthetic analogs, **34b** (IC_{50} = 69.82 μM) and **34c** (IC_{50} = 92.55 μM), are higher than that of the previously reported for **34** (IC_{50} = 48.54 μM). 20 These results revealed that etherification of the phenolic hydroxyl group at C-5 of **33** and **34** dramatically decreases their α-glucosidase inhibitory activity. Interestingly, the semi-synthetic analogs with chlorine containing alkyl group (**33b** and **34b**) are more active than the analogs without chlorine (**33c** and **34c**). Despite the decreased activity of the 5-*O*-alkyl ether analogs (**33b**/**33c** and **34b**/**34c**) relative to the parent compounds (**33** and **34**) with a free 5-hydroxyl group, they showed stronger activity than the positive control, acarbose. Intriguingly, the analogs containing a carboxyl group (**33d** and **34d**), at 50 μg/mL, showed the enzyme inhibition less than 70% (**Table 19**).

Table 19. α-Glucosidase inhibition activity of the isolated compounds of *C. excavata*.

Compound	IC_{50} (μM)
32	147.46 ± 6.30[ref]
33	8.36 ± 0.43[ref]
34	48.54 ± 2.51[ref]
35	NT
43	ND
46	62.08[b] ± 2.10
77	NT
80	34.57[a] ± 5.55
115	ND
33a	47.85 ± 4.70[ref]
80a	NT
33b	32.89[a] ± 3.44
34b	69.82[b] ± 3.61
33c	80.68[b, c] ± 7.42
34c	92.55[c] ± 15.30
33d	ND
34d	ND
Acarbose	391.47[d] ± 2.05

Results are given at the lowest concentrations causing 50% of inhibition (IC_{50}), and are expressed as means ± SD of an experiment performed in triplicate for the compounds that showed the inhibition of >70% for the α-glucosidase at 50 μg/mL. NT = Not tested. ND = Not determined. Ref = Data reported by (Promden et al., 2024) with the IC_{50} of acarbose 430.35 ± 21.34 μM. Different small superscript letters (a, b, c, d) indicate significant differences between the IC_{50} values of the compounds (p <0.05, Tukey's HSD test).

4.5.3. Nitric oxide activity (NO) and cytotoxicity against A459 cell lines

Preliminary screening of **32**–**35**, **43**, **46**, **77**, **80**, and **115** as well as the semi-synthetic analogs, **33a**–**33d**, **80a**, and **34b**–**34d**, at a concentration of 20 µg/mL (except **33** which was tested at 15 µg/mL), for their capacity to reduce LPS-induced NO production in macrophage RAW 264.7 cells was performed and results are shown in **Table 20**. The compounds that showed more than 50% inhibition of NO production, and with at least 70% cell viability in the screening assay were further evaluated to determine their IC_{50} values. Among the isolated compounds tested, the pyranocoumarin **33** displayed the most potent NO inhibitory activity (IC_{50} = 27.95 µM), followed by **34** (IC_{50} = 35.41 µM) and **80** (IC_{50} = 38.25 µM), while the carbazole **43** displayed ca. 2 folds much weaker activity, (IC_{50} = 68.81 µM). For the semi-synthetic analogs, only **33d** displayed NO inhibitory activity with an IC_{50} = 33.62 µM. On the other hand, the semi-synthetic compounds **33b** and **34b** displayed cytotoxicity against RAW 264.7 cells the in α-glucosidase inhibitory activity assay with cell viability less than 70%. This might be due to the presence of chlorine atoms in the molecules of **33b** and **34b** that contributes the cytotoxicity. The chemical structure of the chlorinated compounds has a significantly higher influence on their toxicity.

Based on their cytotoxicity, the semi-synthetic analogs, **33b** and **34b**, were also assayed for their growth inhibitory activity against non-small cell lung cancer (A549) cells by the MTT method. Both **33b** and **34b**, which were toxic to RAW 264.7 cells, displayed potent growth inhibitory activity against the A549 cells, with IC_{50} values of 11.71 and 22.39 µM, respectively (**Table 20**). It is worth noting that **33b** is 2 folds more active than the positive control, cisplatin (IC_{50} = 21.56 µM).

Table 20. Nitric oxide inhibitory activities and cytotoxicity against A459 cell lines.

Compound	NO inhibitory activity IC_{50} (μM)	Cytotoxicity against A459 cell lines IC_{50} (μM)
32	ND	NT
33	$27.95^{a} \pm 1.74$	NT
34	$35.41^{a, b} \pm 0.63$	NT
35	ND	NT
43	$65.81^{c} \pm 4.31$	NT
46	ND	NT
77	NT	NT
80	$38.25^{b} \pm 1.64$	NT
115	ND	NT
33a	ND	NT
80a	NT	NT
33b	ND	$11.71^{a} \pm 0.53$
34b	ND	$23.39^{b} \pm 2.72$
33c	ND	NT
34c	ND	NT
33d	$33.62^{a, b} \pm 2.19$	NT
34d	ND	NT
Diclofenac	$222.42^{d} \pm 6.47$	
Cisplatin		$21.56^{b} \pm 1.98$

Results are given at the lowest concentrations causing 50% of inhibition (IC_{50}), and are expressed as means ± SD of an experiment performed in triplicate for the compounds that showed the inhibition of >60% without obvious cytotoxic effect on RAW 264.7 cells measured by the MTT assay (cell viability >70%) for the NO inhibitory activity. NT = Not tested. ND = Not determined. Different small superscript letters (a, b, c, d) indicate significant differences between the IC_{50} values of the compounds ($p < 0.05$, Tukey's HSD test).

CHAPTER 5

CONCLUSION

In summary, *C. excavata*, a medicinal plant with significant traditional use, has been investigated for its pyranocoumarins and carbazole alkaloids, which are valuable scaffolds for drug development. Re-examination of its root methanol extract led to the isolation of nine compounds and the generation of semisynthetic analogs via etherification. Bioactivity assays revealed that semisynthetic analogs generally had weaker α-glucosidase inhibitory and nitric oxide (NO) inhibitory activities compared to their parent compounds, with one analog (**33d**) showing mild NO inhibition and others (**33b** and **34b**) exhibiting cytotoxicity. Moreover, **33a** and **80a** displayed antimalarial activity with IC_{50} values of 1.97 and 3.25 μM, respectively.

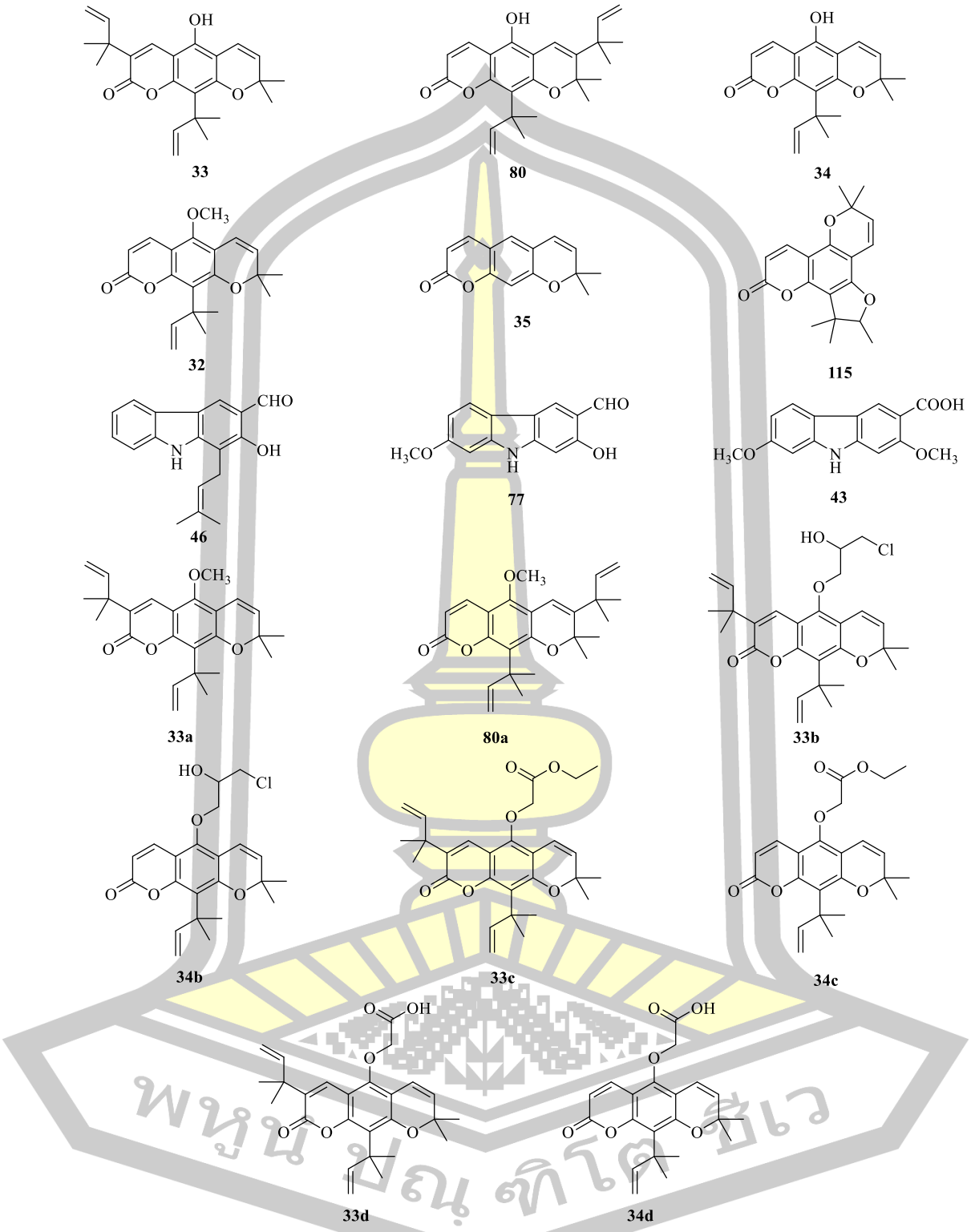

Figure 27. Structures of **32**–**35**, **80**, **115** (natural products), and **33a**–**33d**, **80a**, and **34b**–**34d** (semi-synthetic analogs).

REFERENCES

REFERENCES

Alley, M. C., Scudiero, D. A., Monks, A., Hursey, M., Czerwinski, M. J., Fine, D. L., Abbott, B. J., Mayo, J. G., Shoemaker, R., & Boyd, M. R. (1988). Feasibility of Drug Screening with Panels of Human Tumor Cell Lines Using a Microculture Tetrazolium Assay. *Cancer Research*, *48*(3), 584–588.

Alonso-Castro, A. J., Villarreal, M. L., Salazar-Olivo, L. A., Gomez-Sanchez, M., Dominguez, F., & Garcia-Carranca, A. (2011). Mexican medicinal plants used for cancer treatment: Pharmacological, phytochemical and ethnobotanical studies. *Journal of Ethnopharmacology*, *133*(3), 945–972.

Aminah, N. S., Thant, T. M., Kristanti, A. N., Ramadhan, R., Aung, H. T., & Takaya, Y. (2019). Carbazomarin: A new potential of α-glucosidase inhibitor from clausena excavata roots. *Natural Product Communications*, *14*(12), 1–5.

Bennett, T. N., Paguio, M., Gligorijevic, B., Seudieu, C., Kosar, A. D., Davidson, E., & Roepe, P. D. (2004). Novel, Rapid, and Inexpensive Cell-Based Quantification of Antimalarial Drug Efficacy. *Antimicrobial Agents and Chemotherapy*, *48*(5), 1807–1810.

Chakthong, S., Bindulem, N., Raknai, S., Yodwaree, S., Kaewsanee, S., & Kanjana-Opas, A. (2016). Carbazole-pyranocoumarin conjugate and two carbazole alkaloids from the stems of *Clausena excavata*. *Natural Product Research*, *30*(15), 1690–1697.

Chan, Y. Y., Li, C. H., Shen, Y. C., & Wu, T. S. (2010). Anti-inflammatory principles from the stem and root barks of *Citrus medica*. *Chemical and Pharmaceutical Bulletin*, *58*(1), 61–65.

Cristiane, d. M. C., Vanessa, d. C. D., Jaqueline, R. B., Odair C. B., Edson, R. F., Maria F. G. F. D. S., Paulo C. V., & João B. F. (2009). Isolation of xanthyletin, an inhibitor of ants' symbiotic fungus, by high-speed counter-current chromatography. *Journal of Chromatography A, 1216*(19), 4307–4312.

FlORa & FAUNA WEB. *Clausena excavata* Burm.f. https://www.nparks.gov.sg /florafaunaweb/flora/3/6/3675#. (January 20, 2025)

Pl@ntnet. *Clausena excavata* Burm.f. https://identify.plantnet.org/es/prosea/ observations/1016320338 (January 20, 2025).

He, H. P., Zhang, J. X., Shen, Y. M., He, Y. N., Chen, C. X., & Hao, X. J. (2002). Tetranortriterpenoids from *Clausena excavata*. *Helvetica Chimica Acta*, *85*(2), 671–677.

Heinrich, M., Ankli, A., Frei, B., Weimann, C., & Sticher, O. (1998). Medicinal plants in Mexico: Healers' consensus and cultural importance. *Social Science and Medicine*, *47*(11), 1859–1871.

Huang, S. C., Wu, P. L., & Wu, T. S. (1997). Two coumarins from the root bark of *Clausena excavata*. *Phytochemistry*, *44*(1), 179–181.

Ito, C., Itoigawa, M., Katsuno, S., Omura, M., Tokuda, H., Nishino, H., & Furukawa, H. (2000). Chemical constituents of *Clausena excavata*: Isolation and structure elucidation of novel furanone-coumarins with inhibitory effects for tumor-promotion. *Journal of Natural Products*, *63*(9), 1218–1224.

Kongkathip, B.; Kongkathip, N.; Sunthitikawinsakul, A.; Napaswat, C.; & Yoosook, C. (2005). Anti-HIV-1 constituents from *Clausena excavata*: Part II. Carbazoles and a pyranocoumarin. *Phytotherapy Research*, *19*(8), 728–731.

Kongkathip, N., & Kongkathip, B. (2009). Constituents and bioactivities of *Clausena excavata*. *Heterocycles*, *79*, 121–144.

Kumar, R., Saha, A., & Saha, D. (2012). A new antifungal coumarin from *Clausena excavata*. *Fitoterapia*, *83*(1), 230–233.

Lim, P. C., Ramli, H., Kassim, N. K., Ali, Z., Khan, I. A., Shaari, K., & Ismail, A. (2019). Chemical constituents from the stem bark of *Clausena excavata* Burm. f. *Biochemical Systematics and Ecology*, *82*(August 2018), 52–55.

Liu, Y. P.; Li, Y. J.; Zhao, Y. Y.; Guo, J. M.; Liu, Y. Y.; Wang, X. P.; Shen, Z. Y.; Qiang, L.; Fu, Y. H. (2021). Carbazole alkaloids from the fruits of Clausena anisum-olens with potential PTP1B and α-glucosidase inhibitory activities. *Bioorganic Chemistry*, *110*, 104775.

Makchuchit, S., & Ruchilak Rattarom, A. I. c. (2017). The anti-allergic and anti-inflammatory effects of Benjakul extract (a Thai traditional medicine), its constituent plants and its some pure constituents using in vitro experiments. *Biomedicine & Pharmacotherapy*, *89*, 1018–1026.

Peng, W. W., Zeng, G. Z., Song, W. W., & Tan, N. H. (2013). A new cytotoxic carbazole alkaloid and two new other alkaloids from *Clausena excavata*. *Chemistry and Biodiversity*, *10*(7), 1317–1321.

Peng, W. W., Zheng, Y. Q., Chen, Y. S., Zhao, S. M., Ji, C. J., & Tan, N. H. (2013). Coumarins from roots of *Clausena excavata*. *Journal of Asian Natural Products Research*, *15*(3), 215–220.

Phumthum, M., Srithi, K., Inta, A., Junsongduang, A., Tangjitman, K., Pongamornkul, W., Trisonthi, C., & Balslev, H. (2018). Ethnomedicinal plant diversity in Thailand. *Journal of Ethnopharmacology*, *214*(May 2017), 90–98.

Promden, W., Chanvorachote, P., Viriyabancha, W., Sintupachee, S., & De-Eknamkul, W. (2024). Maclura cochinchinensis (Lour.) Corner Heartwood Extracts Containing Resveratrol and Oxyresveratrol Inhibit Melanogenesis in B16F10 Melanoma Cells. *Molecules*, *29*(11), 2473.

Promden,W., Lophaet, A., Sripadung, P., Sungthong, B., Samsee, T., Ploylearmsang, C., Kijjoa, A., & Seephonkai, P. (2024). α-Glucosidase Inhibitory Activity of Prenylated Pyranocoumarins from *Clausena excavata*: Mechanism of Action, ADMET and Molecular Docking. *Chemistry and Biodiversity*, *21*(9), e202401141.

Ruangrungsi, N., Ariyaprayoon, J., Lange, G. L., Organ, M. G., & Organ, G. (1990). Studies on Thai medicinal plants. Part XI. Three new carbazole alkaloids isolated from *Murraya siamensis*. *Journal of Natural Products*, *53*(4), 946–952.

Seephonkai, P., Kaewtong, C., Wangchuk, P., Jearawuttanakul, K., Borwornpinyo, S., & Khulmanee, T. (2023). Bioassay-Guided Isolation and Identification of Antiplasmodial Compounds from the Stem Bark of *Clausena excavata*. *Planta Medica*, *89*(12), 1165−1169.

Smilkstein, M., Sriwilaijaroen, N., Kelly, J. X., Wilairat, P., & Riscoe, M. (2004). Simple and Inexpensive Fluorescence-Based Technique for High-Throughput Antimalarial Drug Screening. *Antimicrobial Agents and Chemotherapy*, *48*(5), 1803–1806.

Songsiang, U., Thongthoom, T., Zeekpudsa, P., Kukongviriyapan, V., Boonyarat, C., Wangboonskul, J., & Yenjai, C. (2012). Antioxidant activity and cytotoxicity against cholangiocarcinoma of carbazoles and coumarins from *Clausena harmandiana*. *ScienceAsia*, *38*(1), 75–81.

Sripisut, T., & Laphookhieo, S. (2010). Carbazole alkaloids from the stems of Clausena excavata. *Journal of Asian Natural Products Research*, *12*(7), 614–617.

Sripisut, T., Cheenpracha, S., Ritthiwigrom, T., Prawat, U., & Laphookhieo, S. (2012). *Chemical Constituents from the Roots of Clausena excavata and Their Cytotoxicity*. *4*(June 2010), 386–389.

Su, C. R., Yeh, S. F., Liu, C. M., Damu, A. G., Kuo, T. H., Chiang, P. C., Bastow, K. F., Lee, K. H., & Wu, T. S. (2009). Anti-HBV and cytotoxic activities of pyranocoumarin derivatives. *Bioorganic and Medicinal Chemistry*, *17*(16), 6137–6143.

Sunthitikawinsakul, A., Kongkathip, N., Kongkathip, B., Phonnakhu, S., Daly, J. W., Spande, T. F., Nimit, Y., Napaswat, C., Kasisit, J., & Yoosook, C. (2003). Anti-HIV-1 Limonoid: First Isolation from *Clausena excavata*. *Phytotherapy Research*, *17*(9), 1101–1103.

Tan, M. A., Sharma, N., & An, S. S. A. (2022). Phyto-Carbazole Alkaloids from the Rutaceae Family as Potential Protective Agents against Neurodegenerative Diseases. *Antioxidants*, *11*(3), 493.

Takemura, Y., Keiko, N., Tomiko, H., Ju-ichi, M., Ito, C., & Furukawa, H. (2002). Four New Furanone-Coumarins from *Clausena excavata*. *Chemical Pharmaceutical Bulletin*, *48*(4), 582–584.

Taufiq-Yap, Y. H., Peh, T. H., Ee, G. C. L., Rahmani, M., Sukari, M. A., Ali, A. M., & Muse, R. (2007). A new cytotoxic carbazole alkaloid from *Clausena excavata*. *Natural Product Research*, *21*(9), 810–813.

Thaithong, S. G. H. B., & M. Chutmongkonkul. (1983). Susceptibility of *Plasmodium*

falciparum to five drugs: An in vitro study of isolates mainly from Thailand. *Transactions of the Royal Society of Tropical Medicine and Hygiene*, *77*(2), 228–231.

Thant, T. M., Aminah, N. S., Kristanti, A. N., Ramadhan, R., Aung, H. T., & Takaya, Y. (2019). Antidiabetes and Antioxidant agents from *Clausena excavata* root as medicinal plant of Myanmar. *Open Chemistry*, *17*(1), 1339–1344.

Thant, T. M., Aminah, N. S., Kristanti, A. N., Ramadhan, R., Aung, H. T., & Takaya, Y. (2020). *Cytotoxic Carbazole Alkaloid from the Root of Clausena cxcavata on Hela Cell Line*. *Icocsti 2019*, 141–144.

Thant, T. M., Aminah, N. S., Kristanti, A. N., Ramadhan, R., Phuwapraisirisan, P., & Takaya, Y. (2021). A new pyrano coumarin from *Clausena excavata* roots displaying dual inhibition against α-glucosidase and free radical. *Natural Product Research*, *35*(4), 556–561.

Thongthoom, T., Songsiang, U., Phaosiri, C., & Yenjai, C. (2010). Biological activity of chemical constituents from *Clausena harmandiana*. *Archives of Pharmacal Research*, *33*(5), 675–680.

Trager, W., & Jensen, J. B. (2005). Human malaria parasites in continuous culture. *Journal of Parasitology*, *91*(3), 484–486.

Wiart, C., (2006). *Medicinal Plants of the Asia-Pacific Drugs for the Future?* World Scientific Connect.

Wu, T. S., & Furukawa, H. (1982). Biological and phytochemical investigation of *Clausena excavata*. *Journal of Natural Products, 45(6)*, 718–720.

Wu, T. S., Huang, S. C., Wu, P., & Lee, K. H. (1994). Structure and synthesis of clausenaquinone-a. A novel carbazolequinone alkaloid and bioactive principle

from *clausena excavata*. *Bioorganic and Medicinal Chemistry Letters*, *20*(4), 2395–2398.

Wu, T. S., Huang, S. C., Wu, P. L., & Teng, C. M. (1996). Carbazole alkaloids from *Clausena excavata* and their biological activity. *Phytochemistry*, *43*(1), 133–140.

Xin, Z. Q., Lu, J. J., Ke, C. Q., Hu, C. X., Lin, L. P., & Ye, Y. (2008). Constituents from *Clausena excavata*. *Chemical and Pharmaceutical Bulletin*, *56*(6), 827–830.

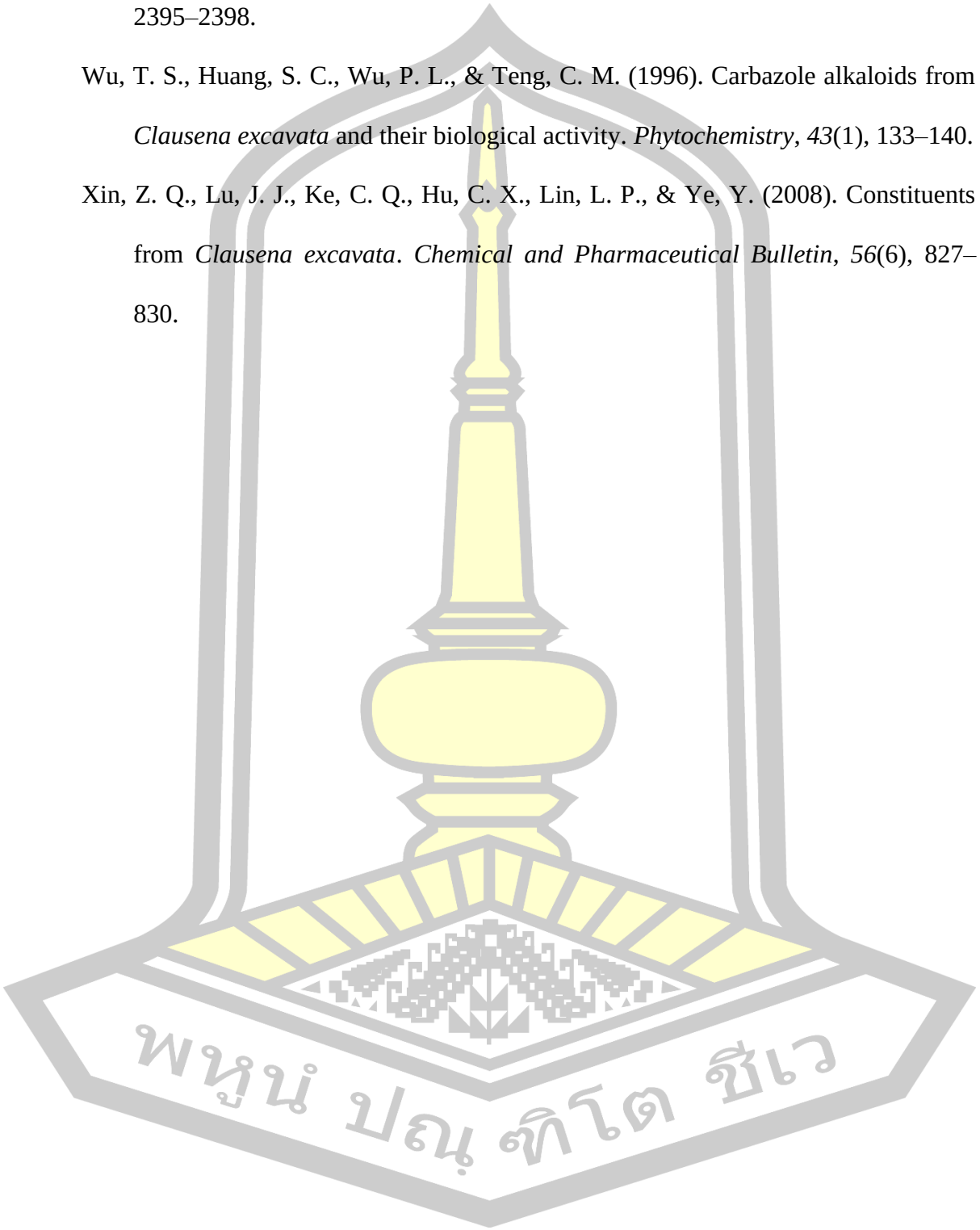

APPANDIX

LIST OF FIGURES

Figure **Page**

Figure **Page**

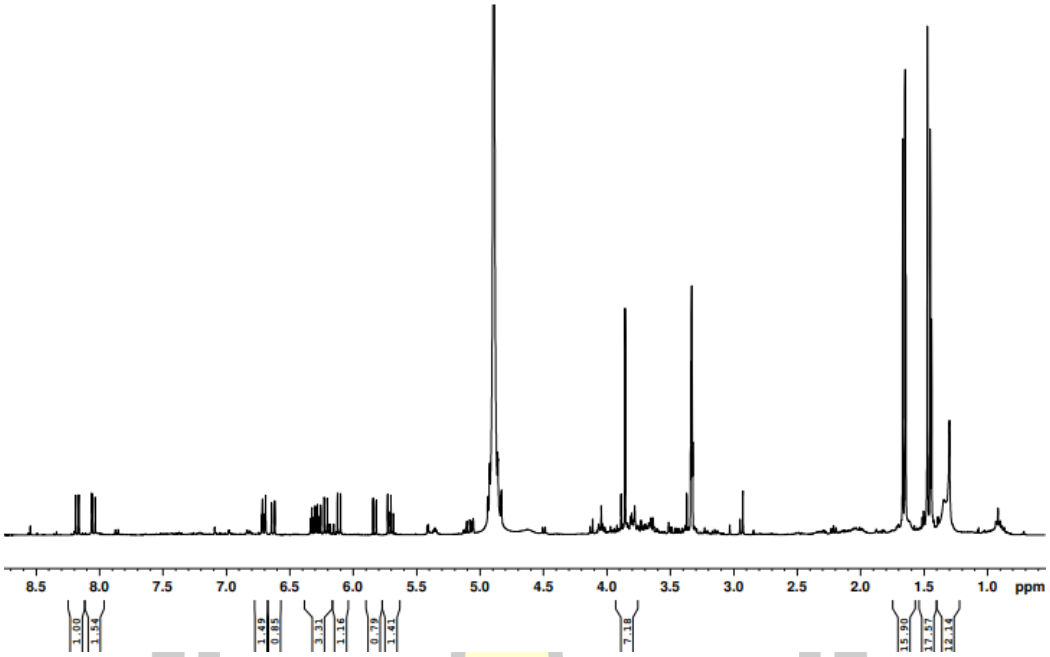

Figure A1. ^{1}H NMR spectrum of crude methanol in $CDCl_3$ (400 MHz).

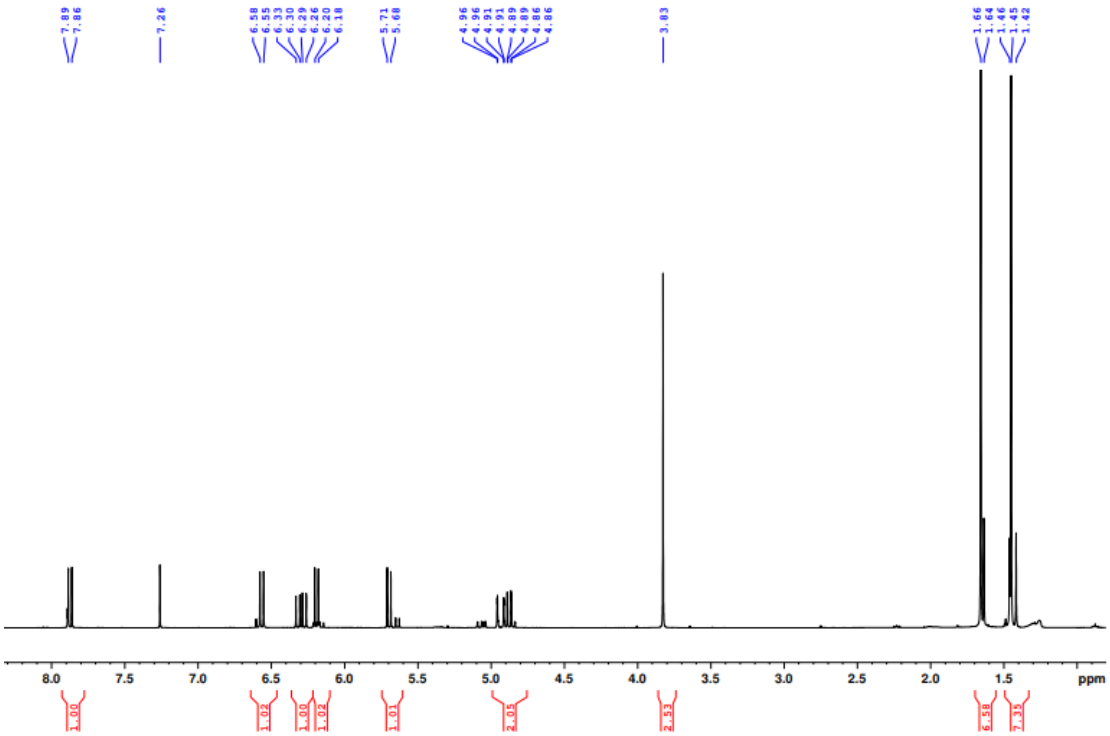

Figure A2. ^{1}H NMR spectrum of **32** in $CDCl_3$ (400 MHz).

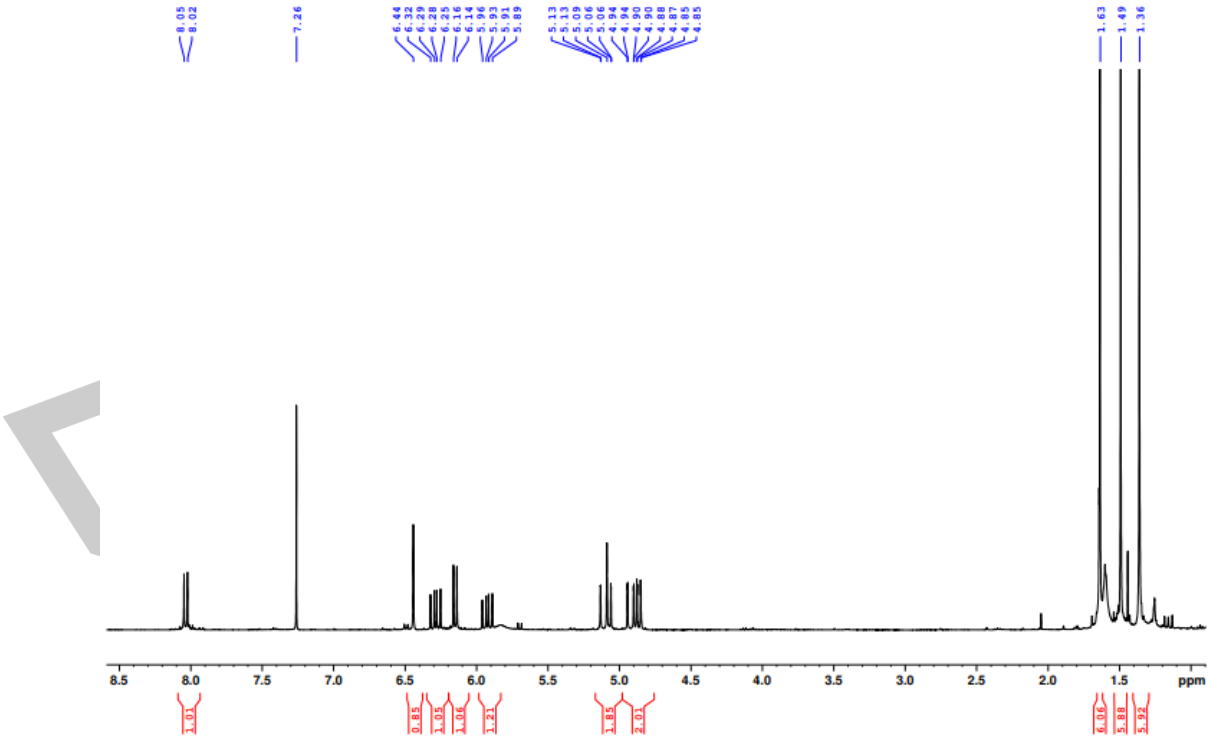

Figure A3. ^{1}H NMR spectrum of **33** in $CDCl_3$ (400 MHz).

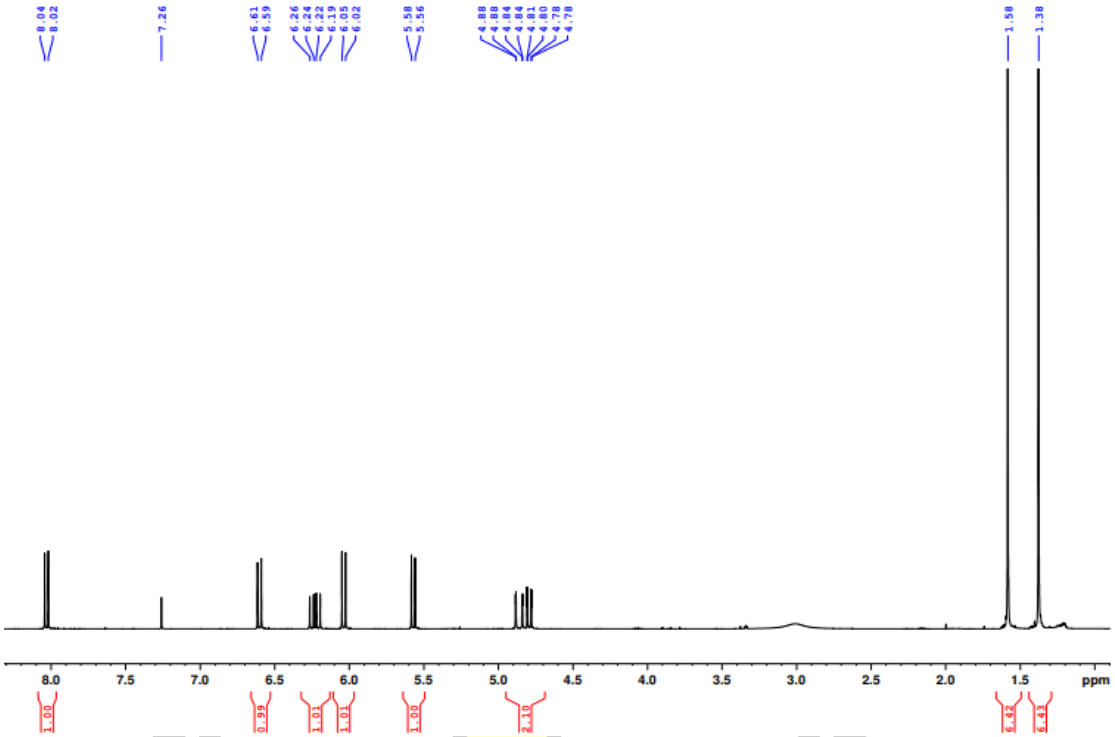

Figure A4. ^{1}H NMR spectrum of **34** in $CDCl_3$ (400 MHz).

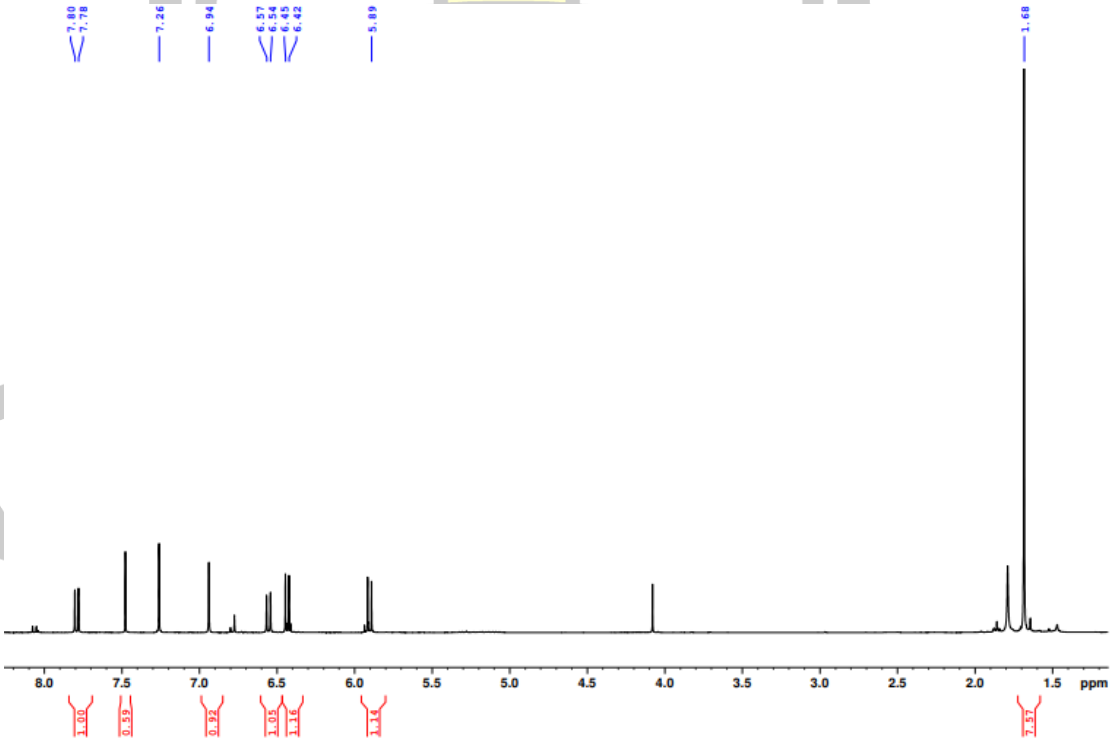

Figure A5. ^{1}H NMR spectrum of **35** in $CDCl_3$ (400 MHz).

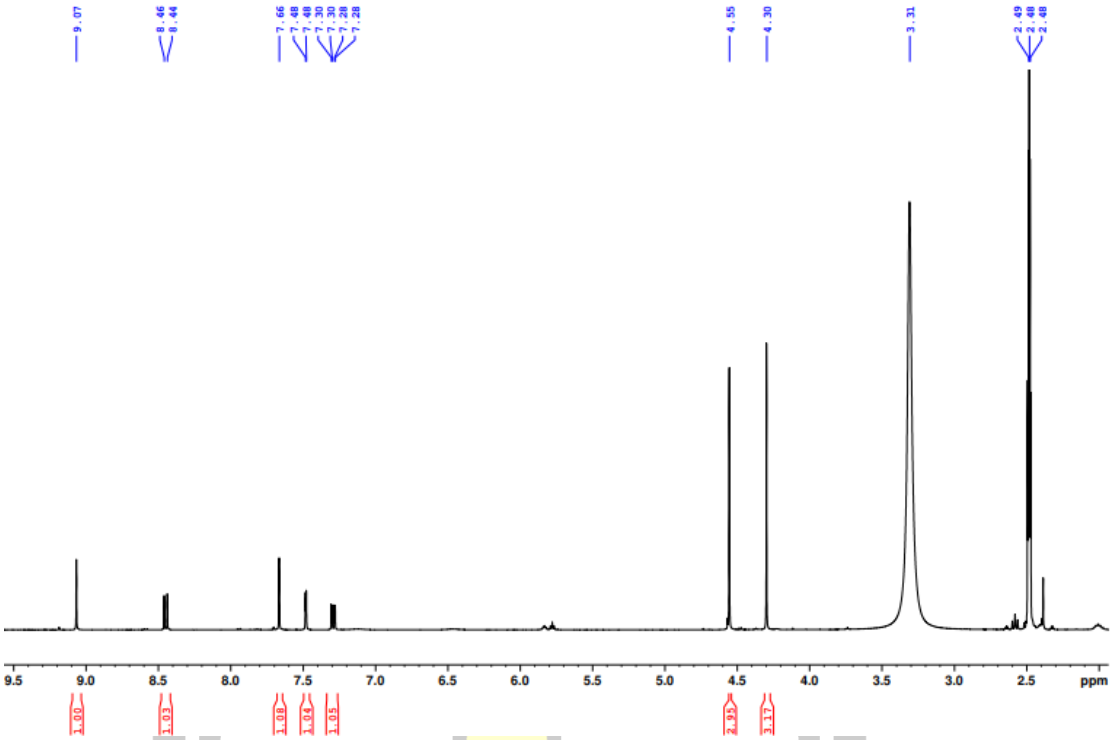

Figure A6. ^{1}H NMR spectrum of **43** in CD_3OD (400 MHz).

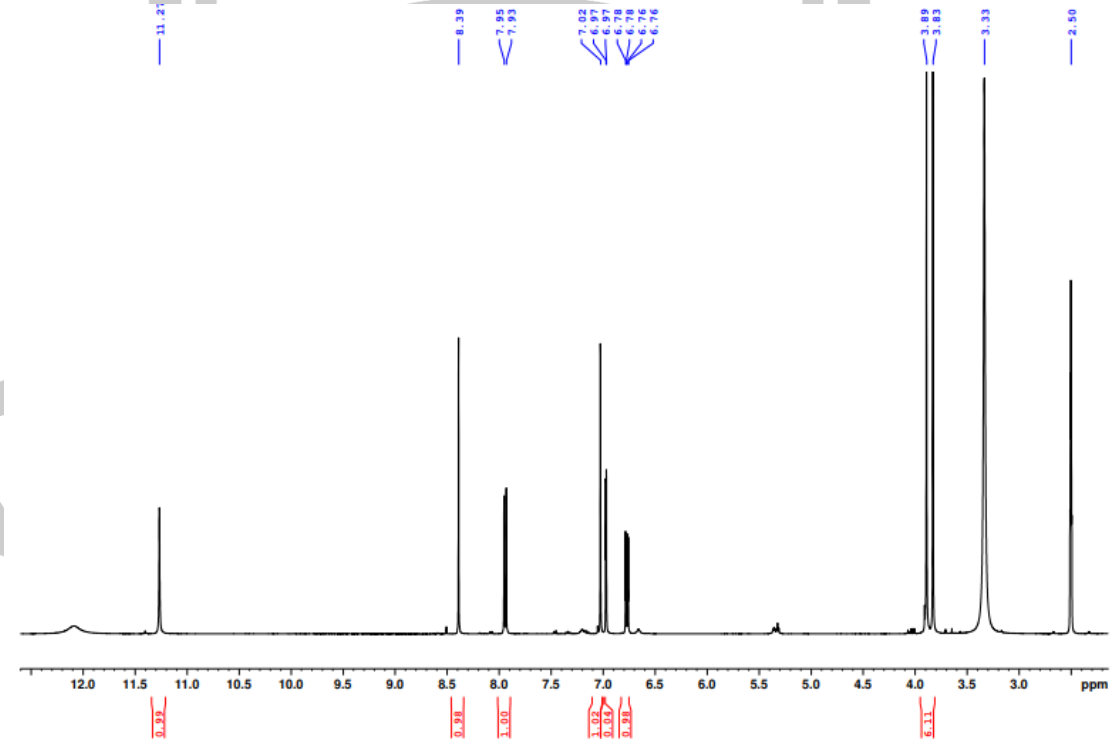

Figure A7. ^{1}H NMR spectrum of **43** in DMSO-d_6 (400 MHz).

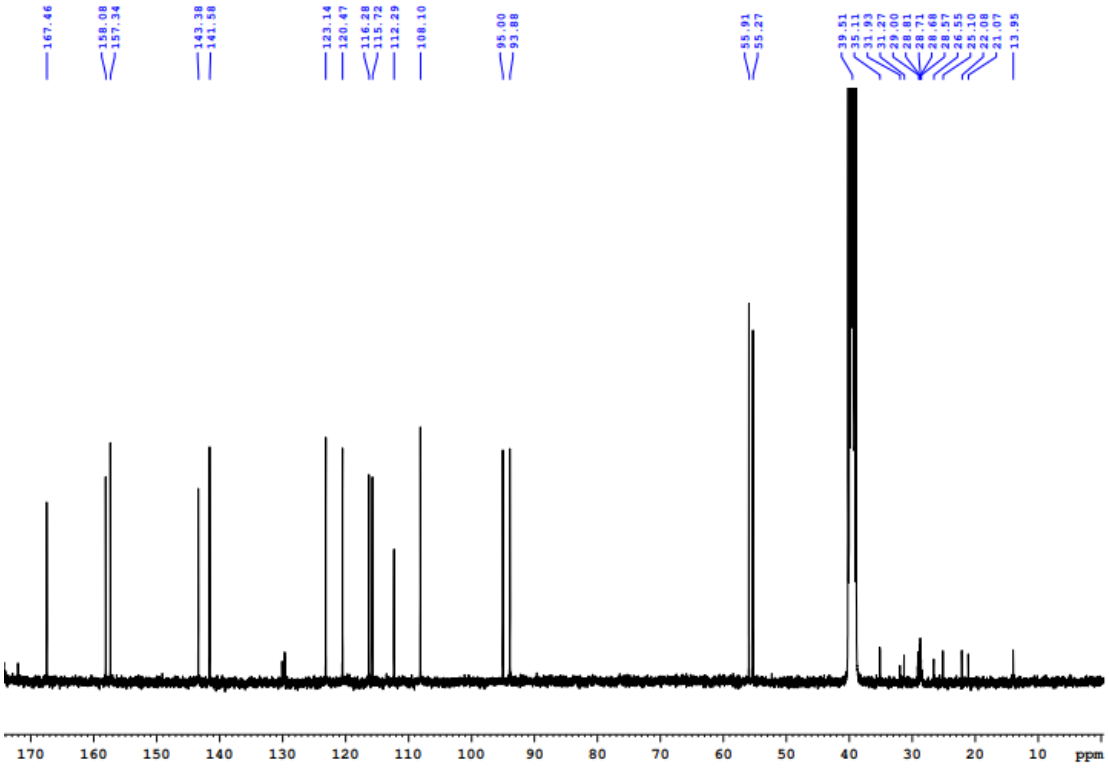

Figure A8. ^{13}C NMR spectrum of **43** in DMSO-d_6 (100 MHz).

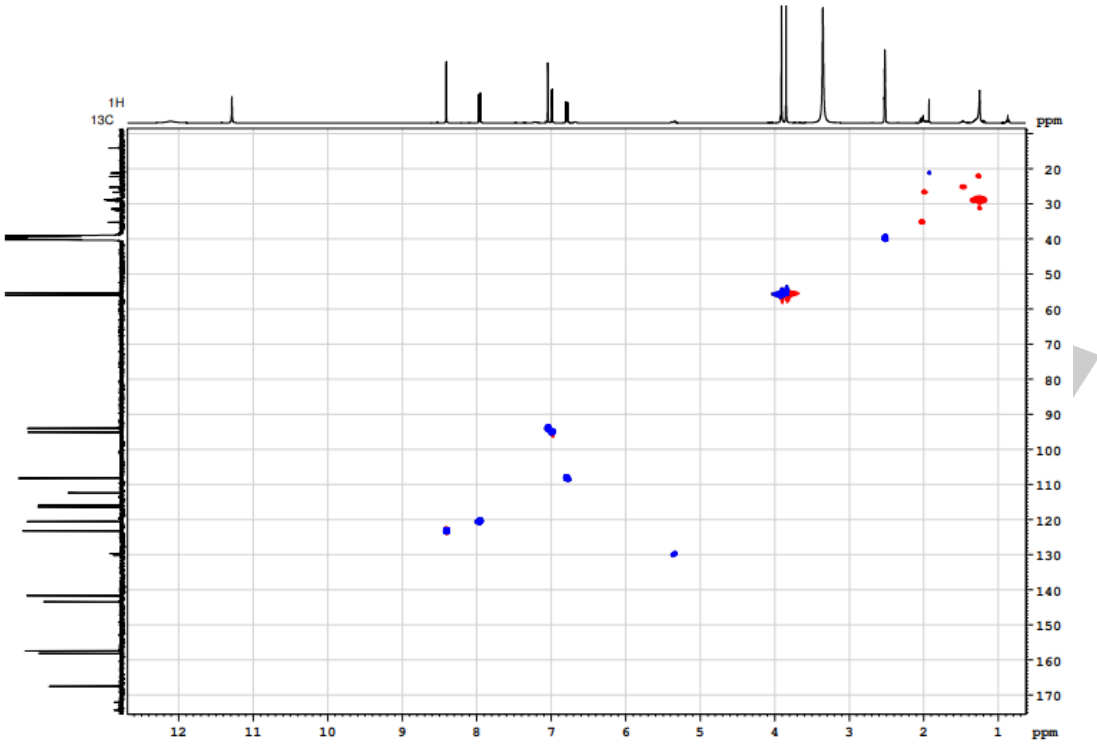

Figure A9. HSQC spectrum of **43** in DMSO-d_6 (100 MHz).

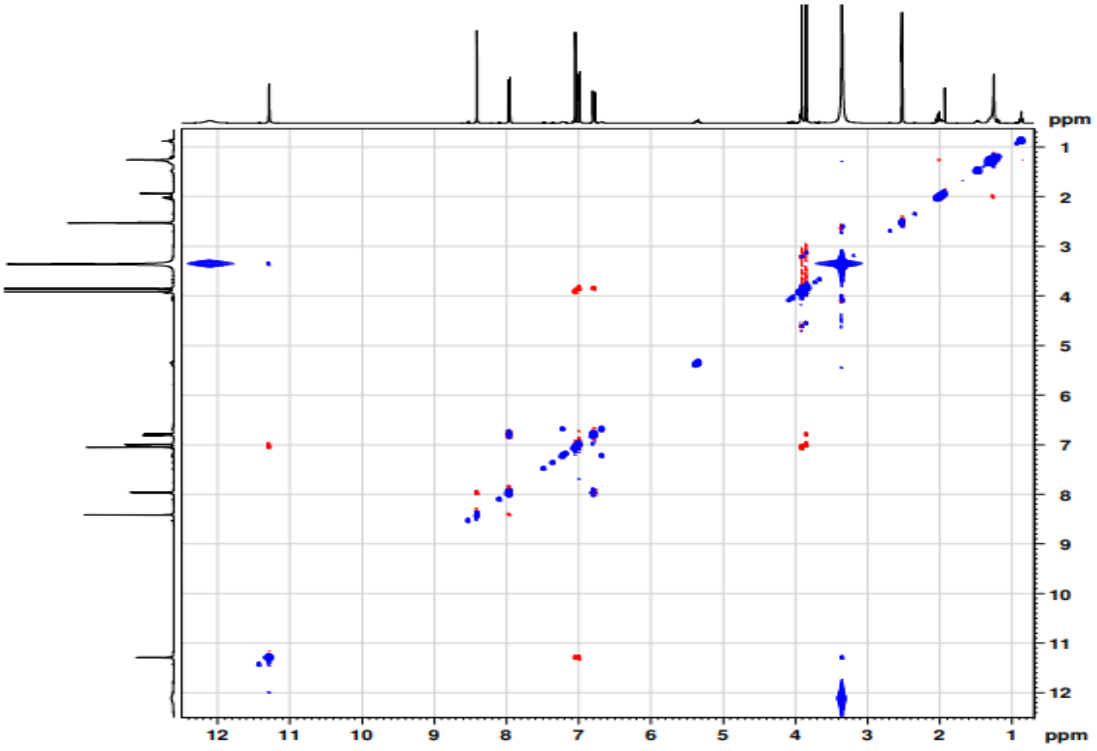

Figure A10. NOSEY spectrum of **43** in DMSO-d_6 (100 MHz).

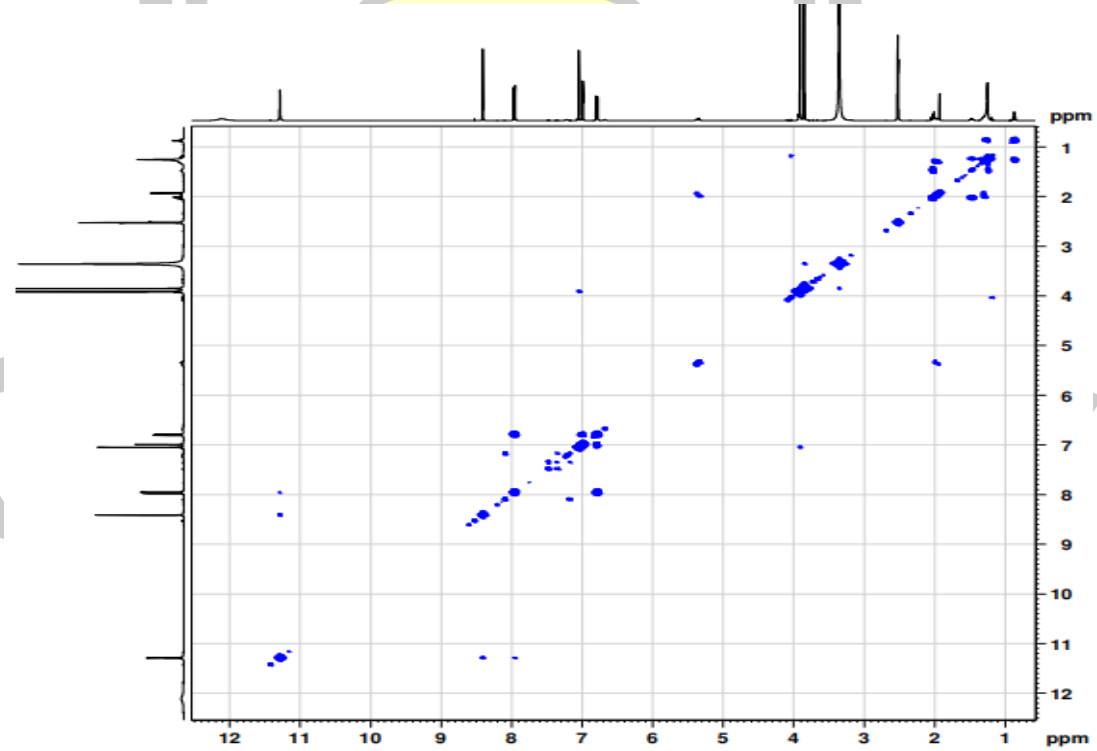

Figure A11. COSY of **43** in DMSO-d_6 (100 MHz).

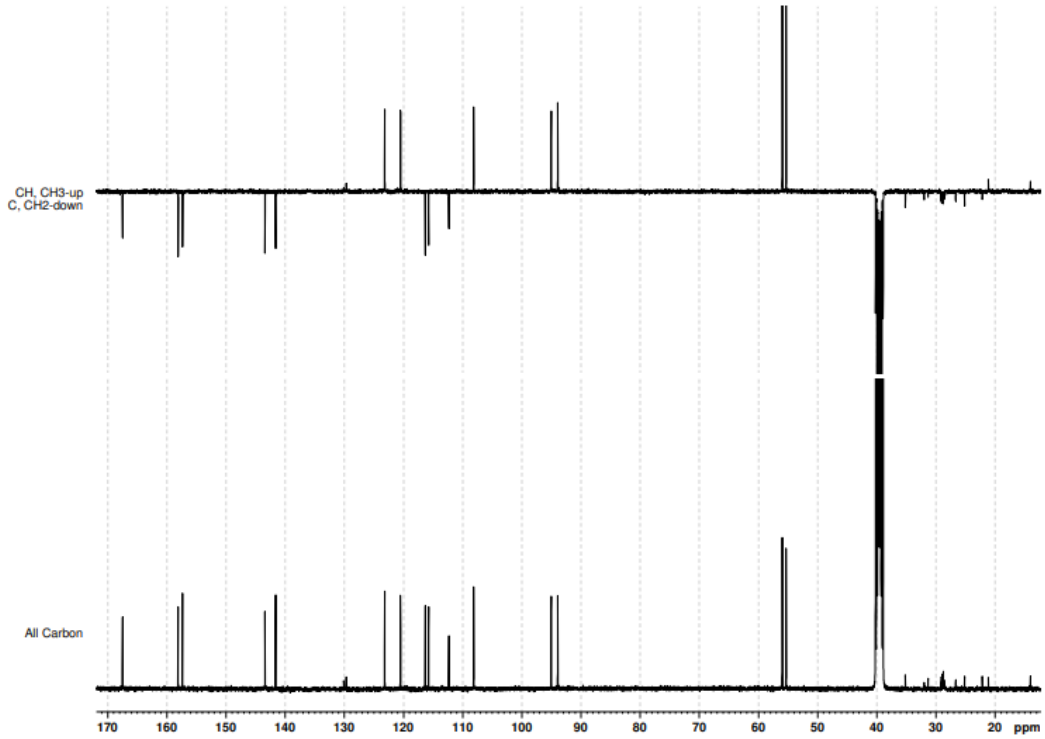

Figure A12. Dept of **43** in DMSO-d_6 (100 MHz).

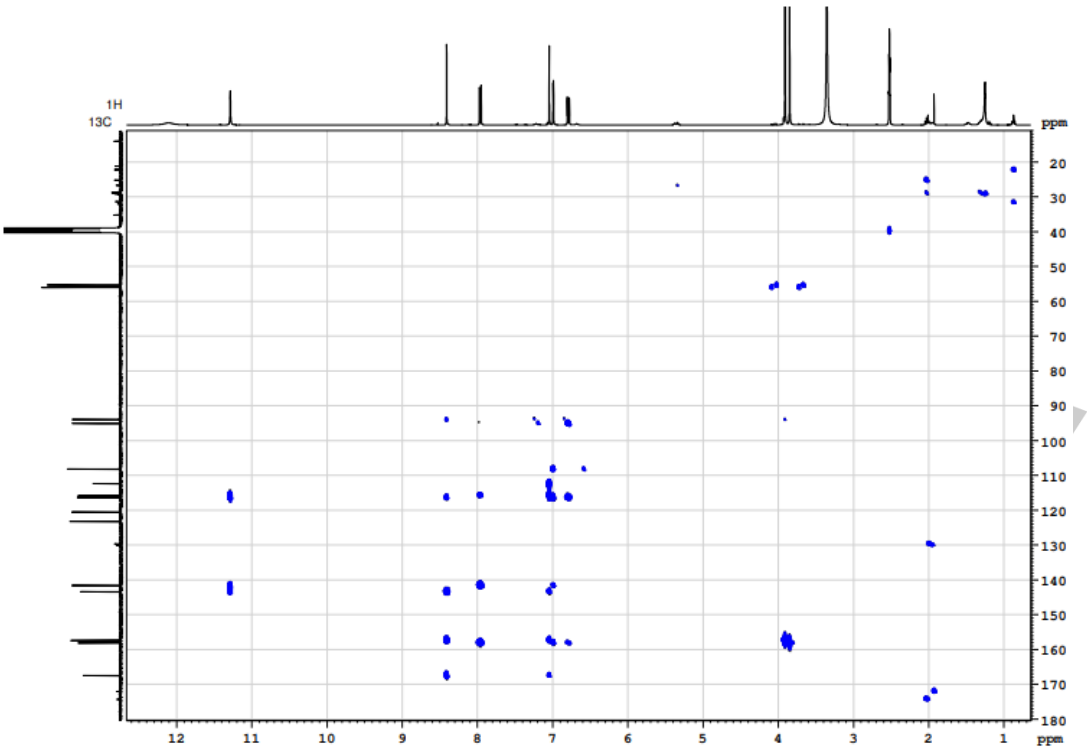

Figure A13. HMBC of **43** in DMSO-d_6 (100 MHz).

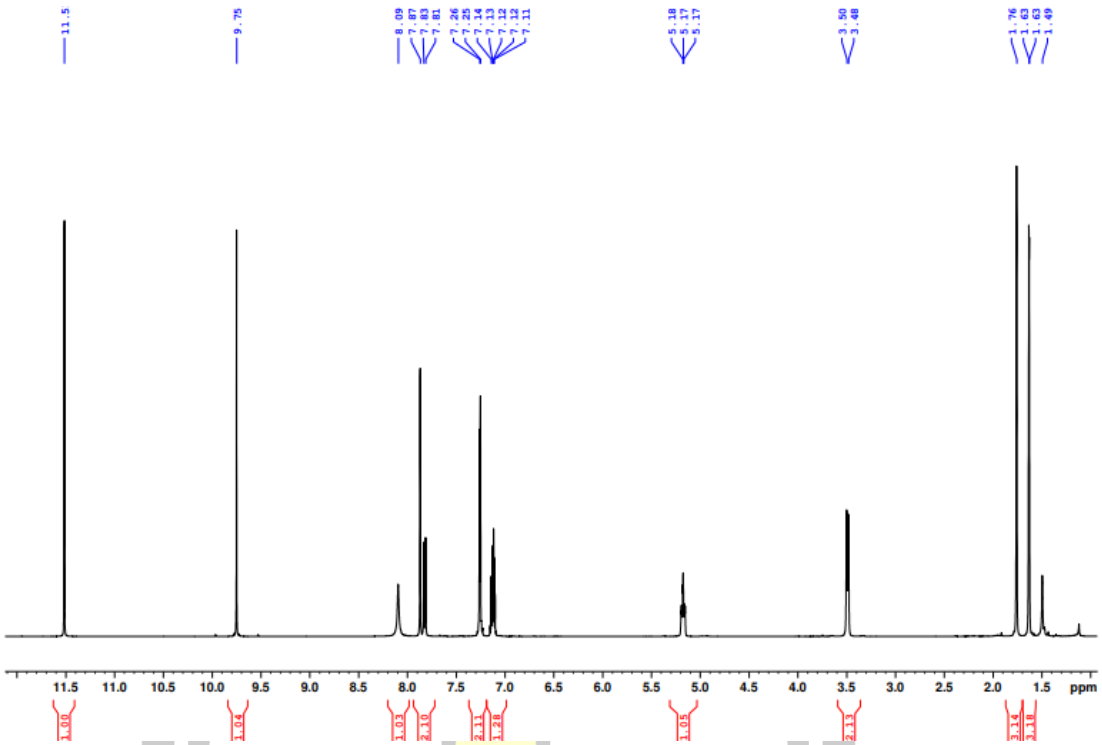

Figure A14. ^{1}H NMR spectrum of **46** in $CDCl_3$ (400 MHz).

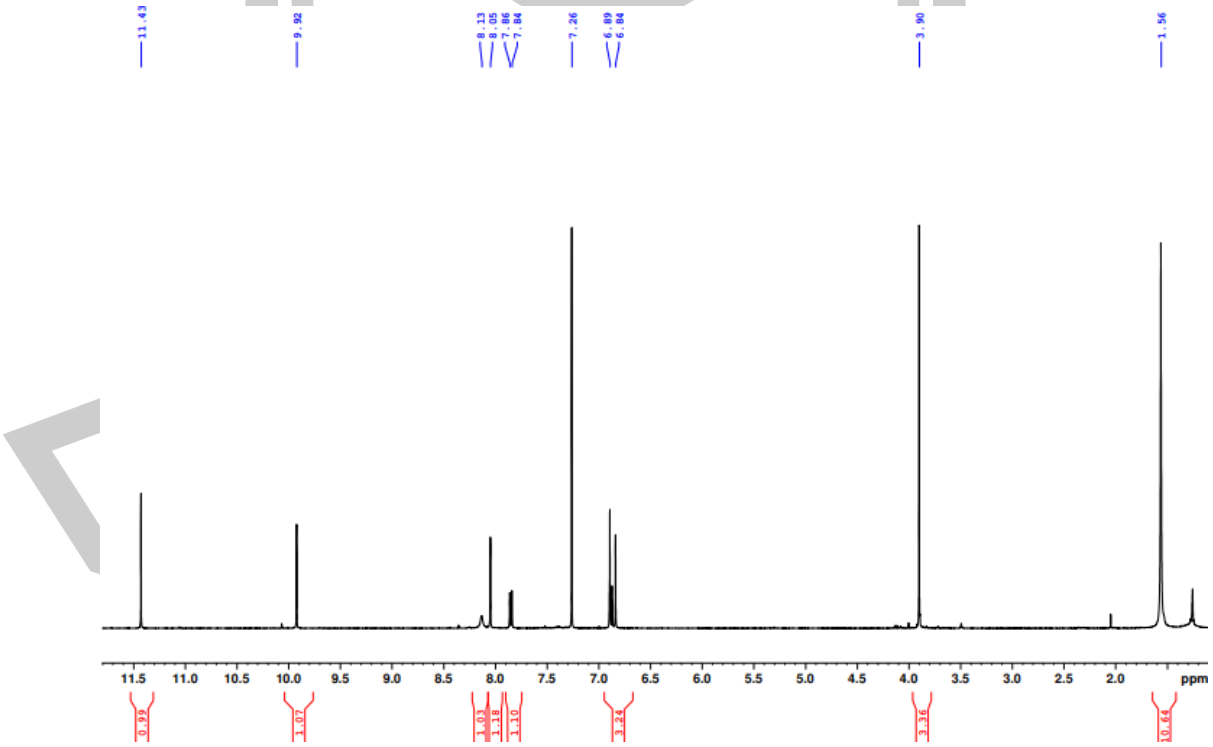

Figure A15. ^{1}H NMR spectrum of **77** in $CDCl_3$ (400 MHz).

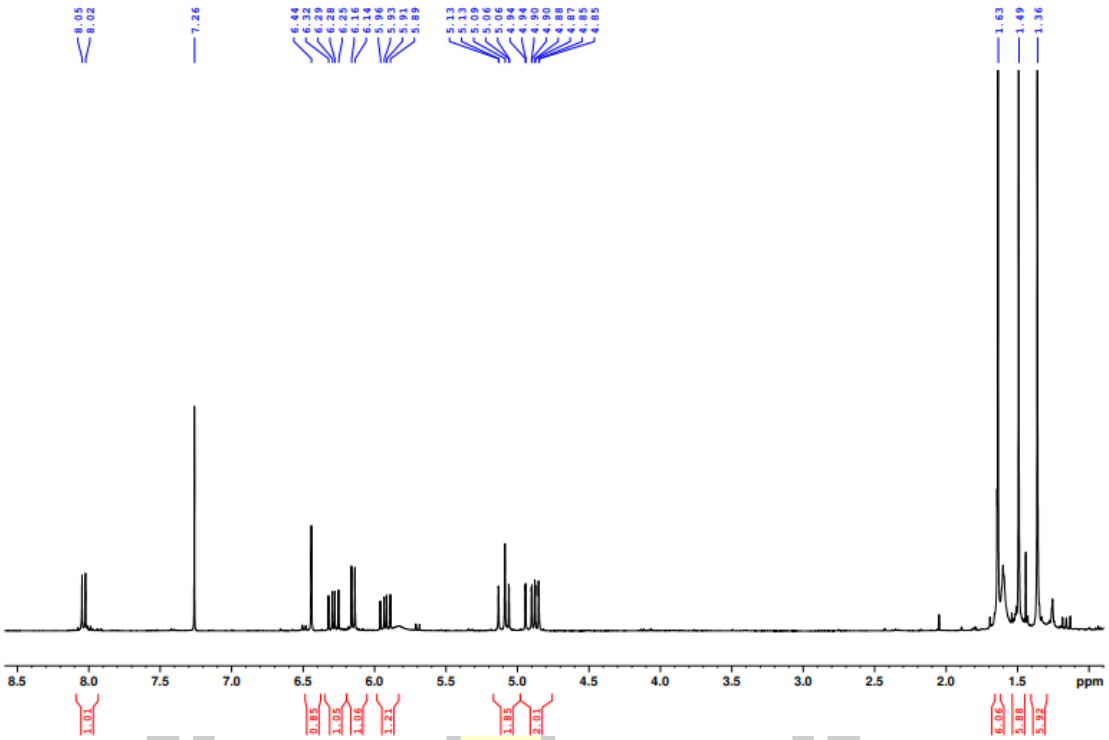

Figure A16. ^{1}H NMR spectrum of **80** in $CDCl_3$ (400 MHz).

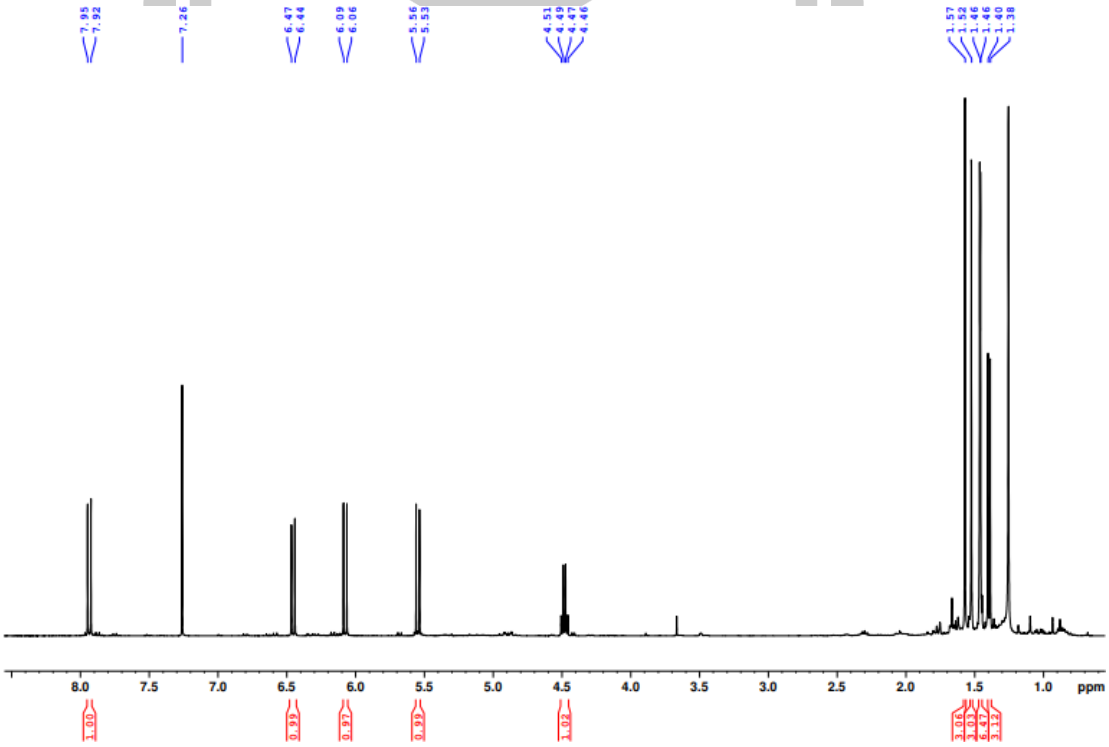

Figure A17. ^{1}H NMR spectrum of **115** in $CDCl_3$ (400 MHz).

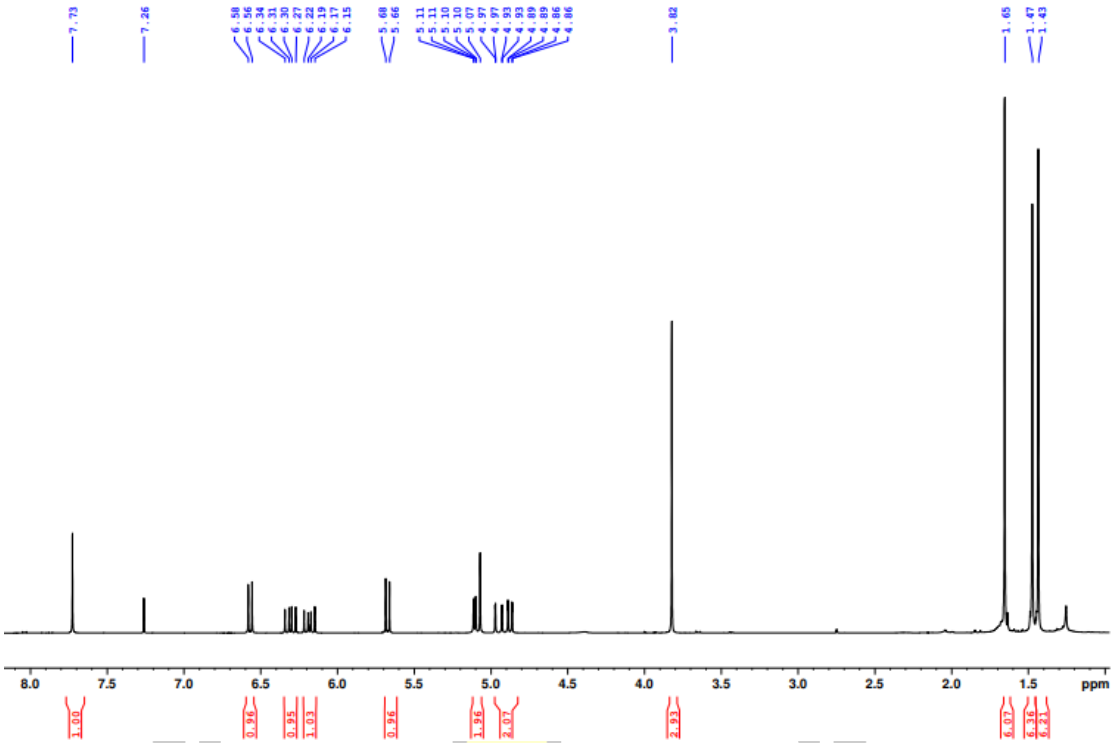

Figure A18. ^{1}H NMR spectrum of **33a** in $CDCl_3$ (400 MHz).

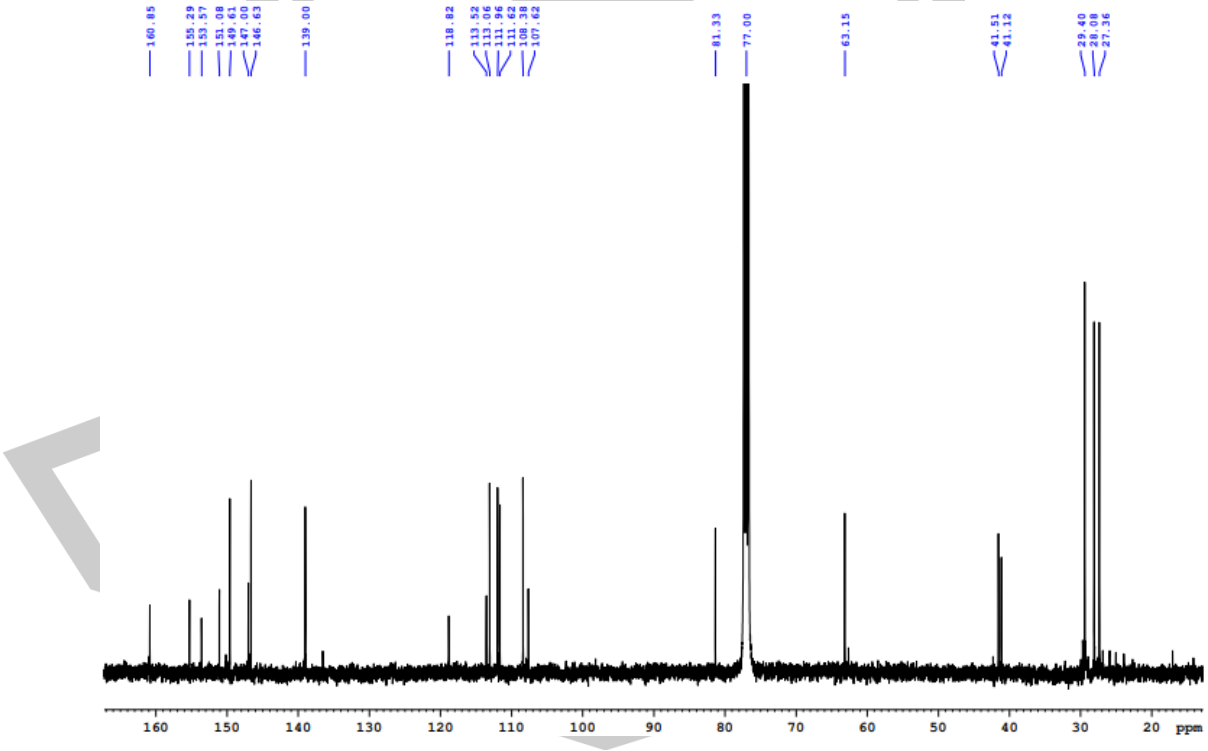

Figure A19. ^{13}C NMR spectrum of **33a** in $CDCl_3$ (100 MHz)

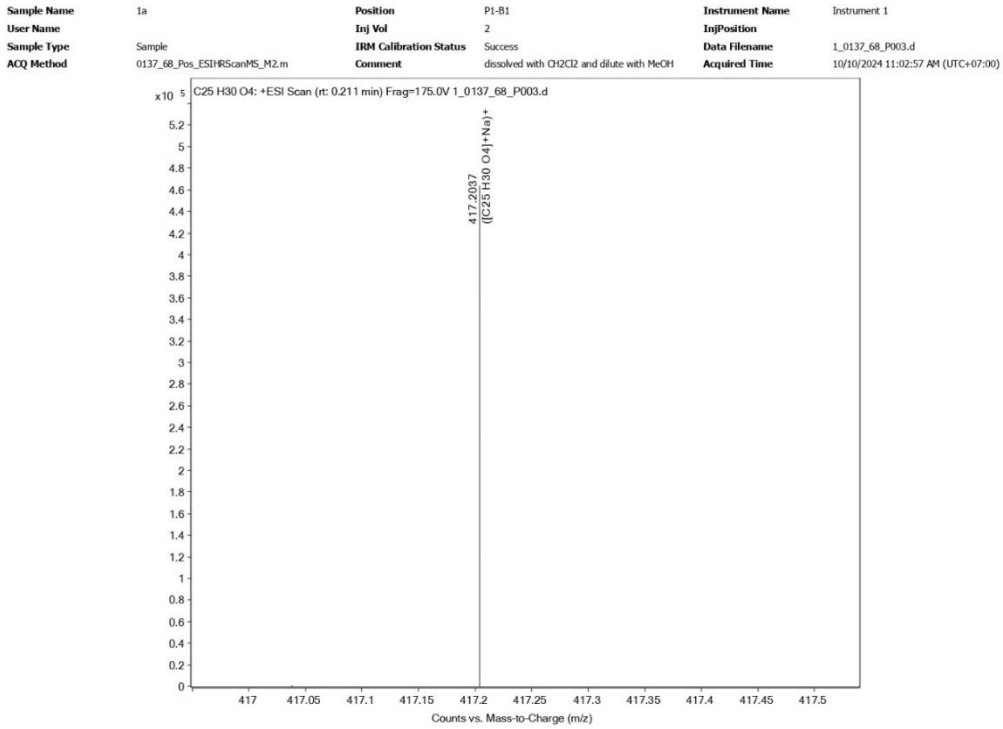

Figure A20. HRESIMS of **33a** (positive ion mode).

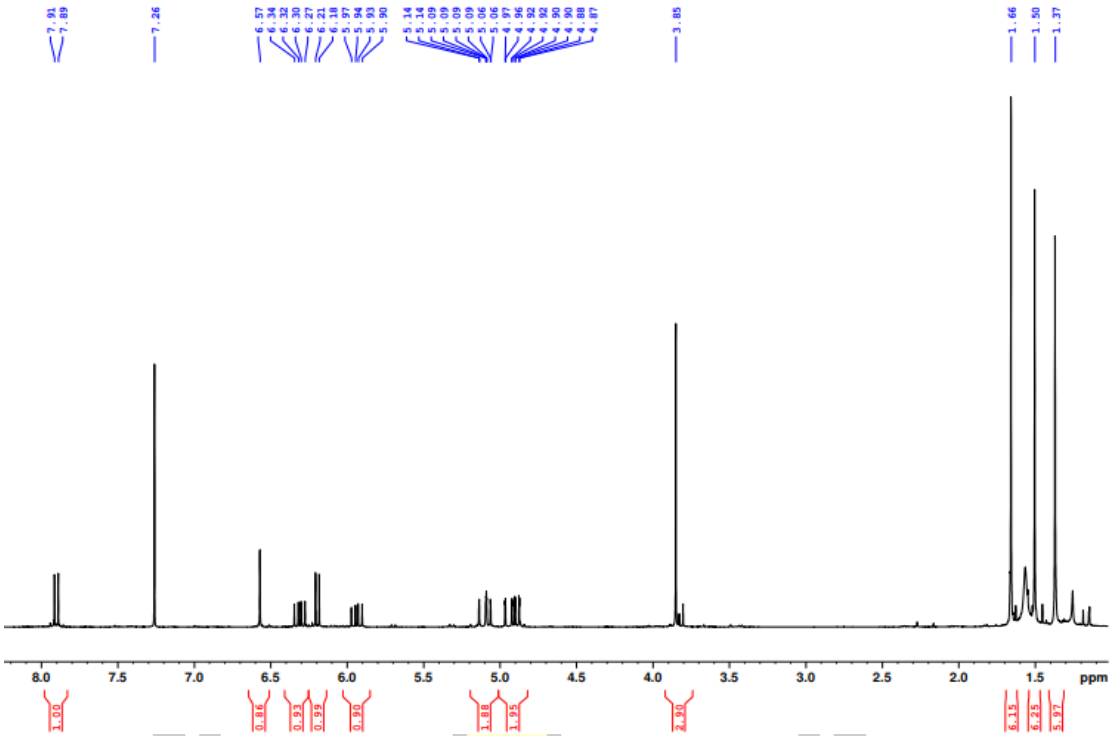

Figure A21. ^{1}H NMR spectrum of **80a** in $CDCl_3$ (400 MHz).

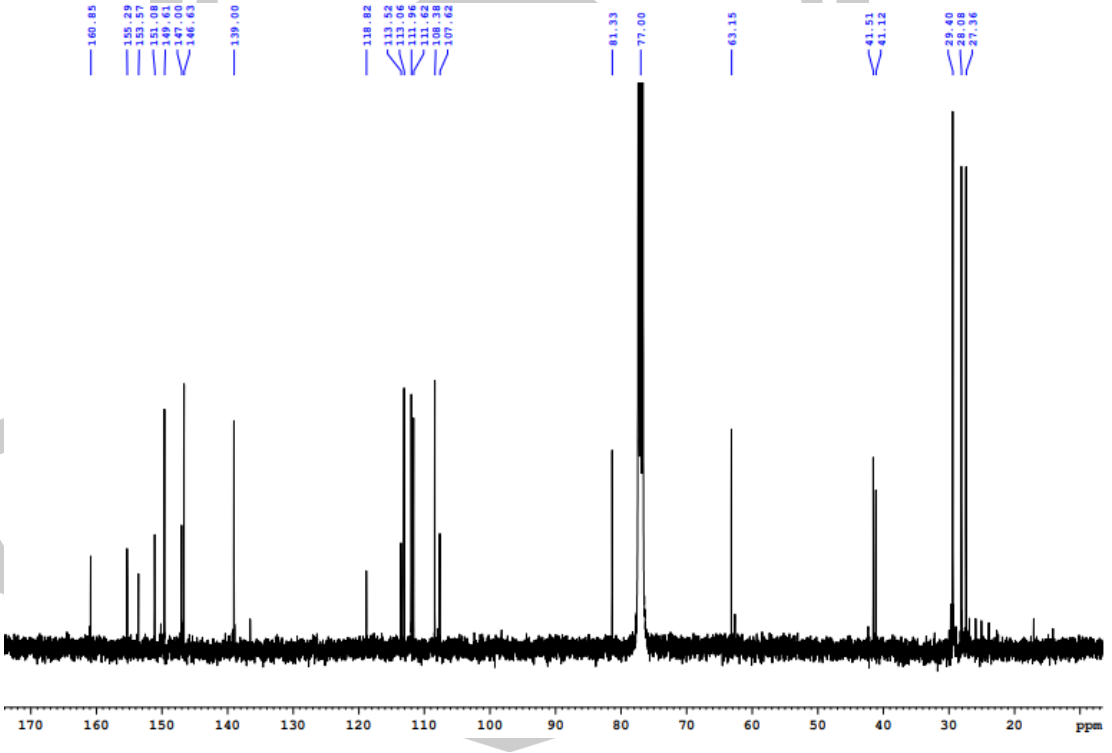

Figure A22. ^{13}C NMR spectrum of **80a** in $CDCl_3$ (100 MHz).

Sample Name	2a	**Position**	P1-C1	**Instrument Name**	Instrument 1
User Name		**Inj Vol**	2	**InjPosition**	
Sample Type	Sample	**IRM Calibration Status**	Success	**Data Filename**	2_0137_68_P003.d
ACQ Method	0137_68_Pos_ESIHRScanMS_M2.m	**Comment**	dissolved with CH2Cl2 and dilute with MeOH	**Acquired Time**	10/10/2024 11:13:21 AM (UTC+07:00)

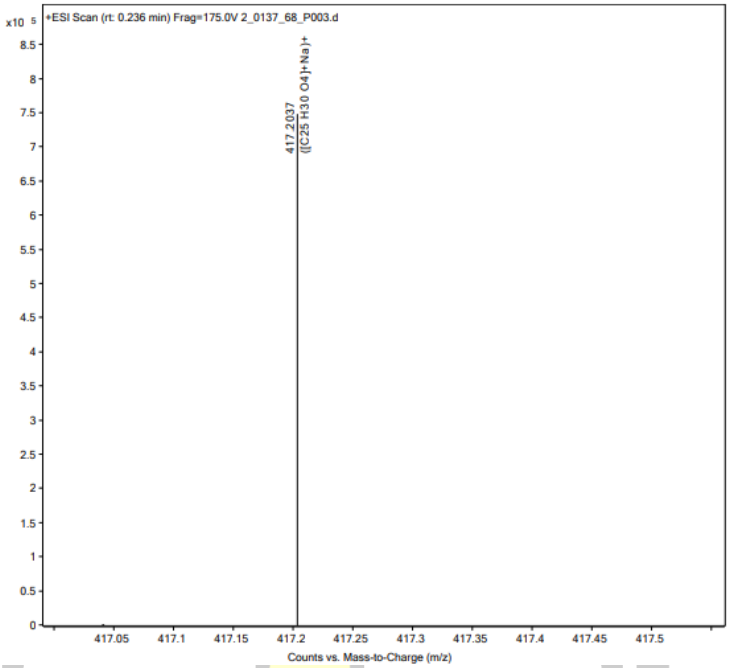

Figure A23. HRESIMS of **80a** (positive ion mode).

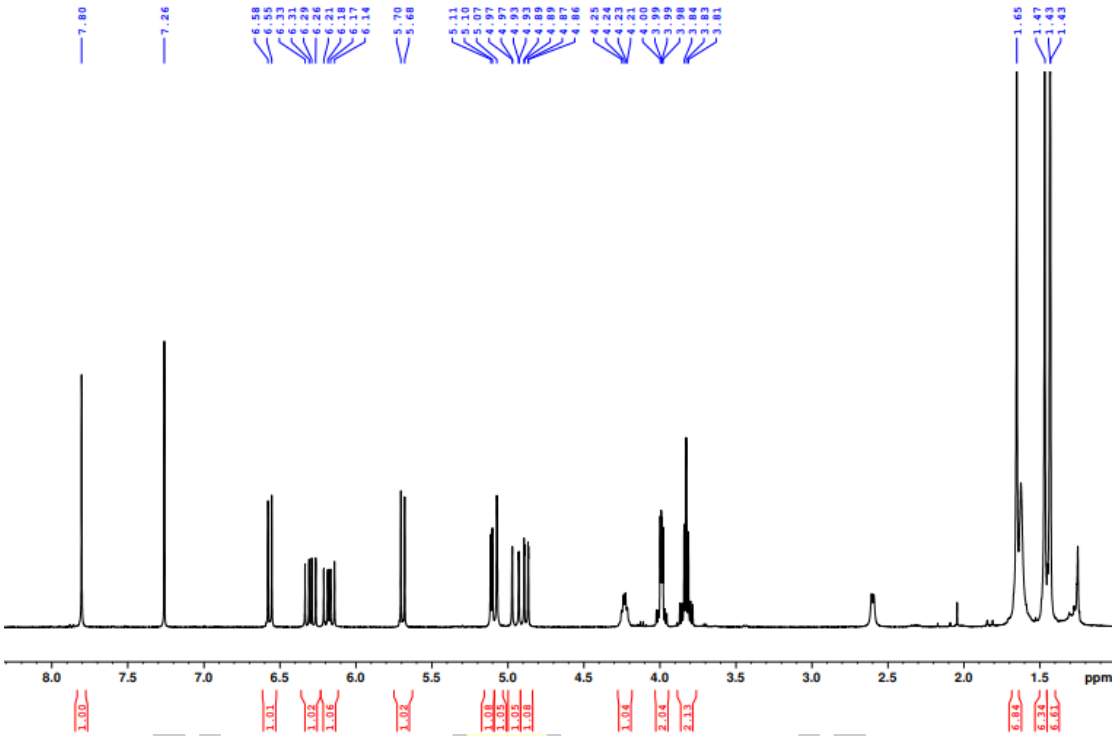

Figure A24. ^{1}H NMR spectrum of **33b** in $CDCl_3$ (400 MHz).

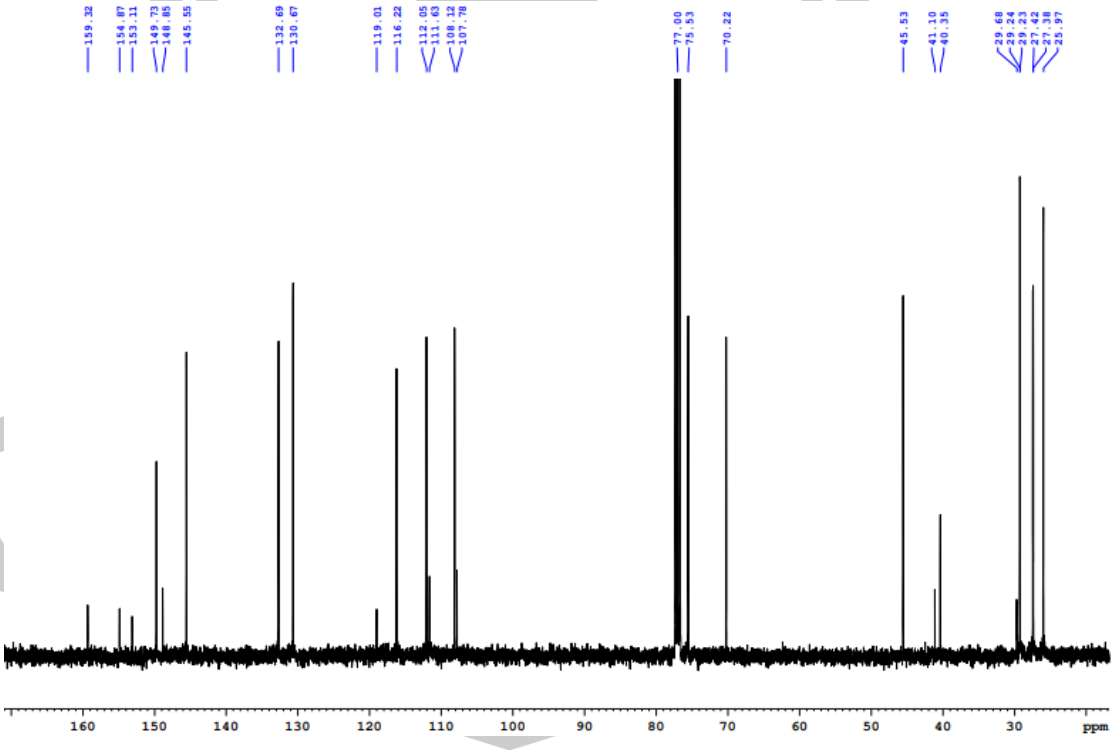

Figure A25. ^{13}C NMR spectrum of **33b** in $CDCl_3$ (100 MHz).

BIORESOURCES RESEARCH UNIT

High resolution report

		Acquisition Date	7/16/2024 8:59:35 AM
Analysis Name	D:\Data\masahiko\33b.dd		
Method	NaFormate_pos low.m	Operator	Sutichai Ext: 3560
Sample Name	33	Instrument	micrOTOF Bruker
		Calibrate by	Sodium Formate

Acquisition Parameter

Source Type	ESI	Ion Polarity	Positive	Set Nebulizer	1.0 Bar
Focus	Not active			Set Dry Heater	180 ?C
Scan Begin	100 m/z	Set Capillary	4500 V	Set Dry Gas	5.0 l/min
Scan End	3000 m/z	Set End Plate Offset	-500 V	Set Divert Valve	Source

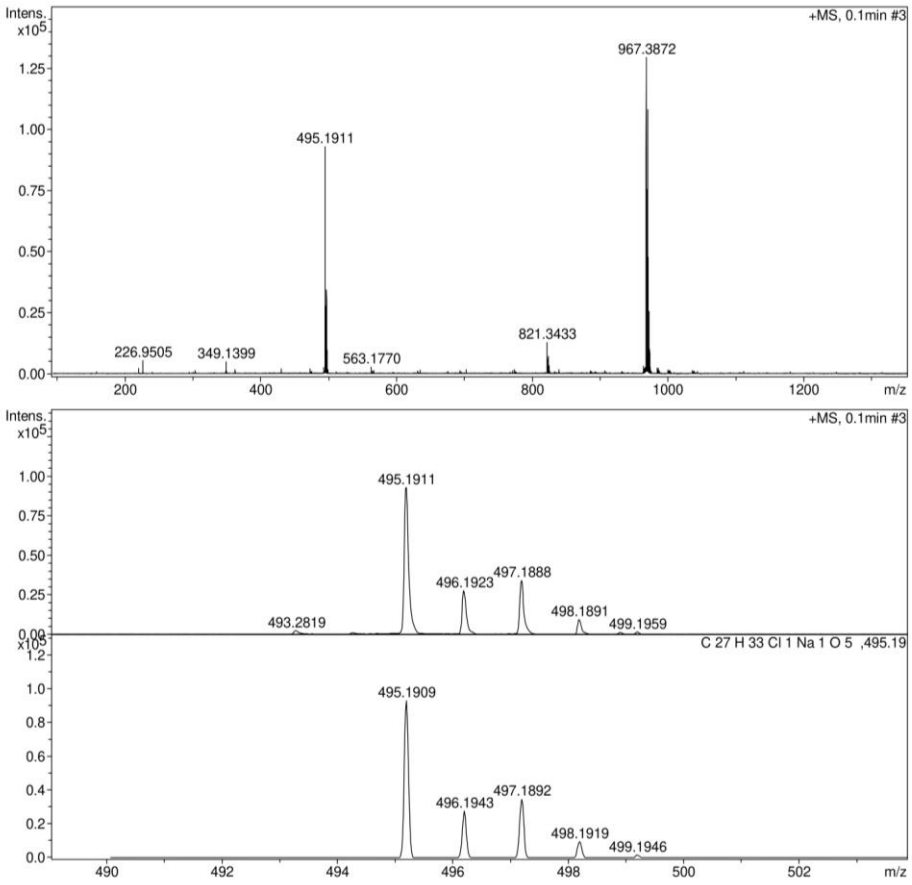

Figure A26. HRESIMS of **33b** (positive ion mode).

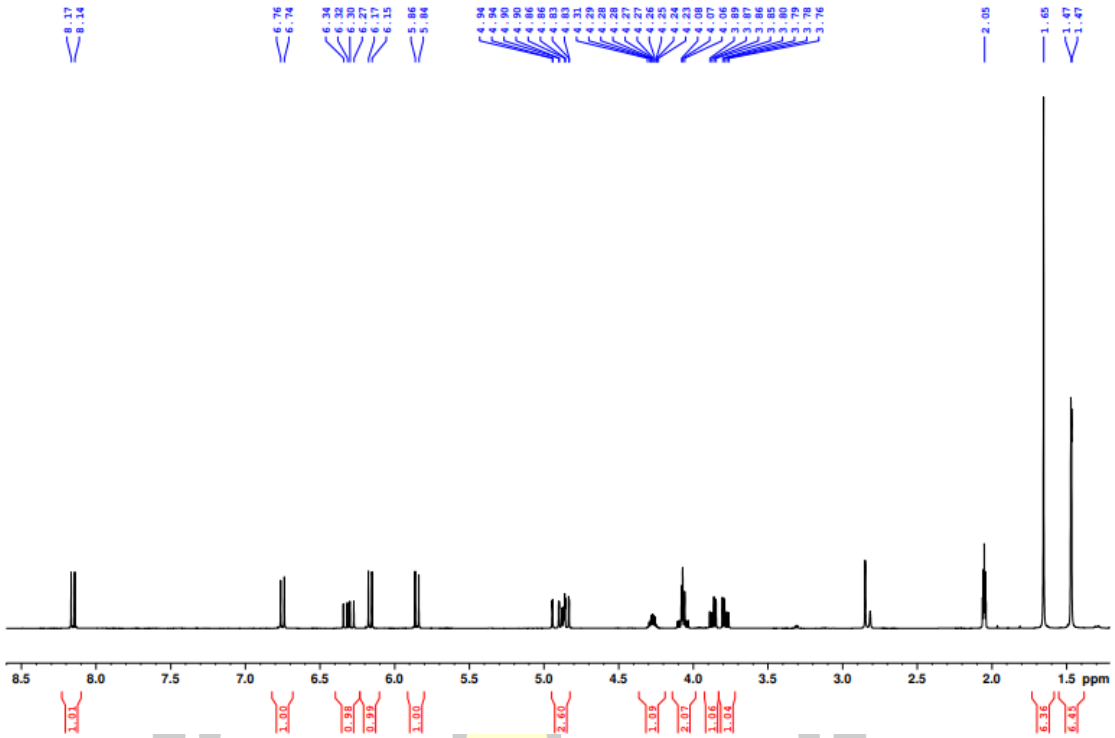

Figure A27. ^{1}H NMR spectrum of **34b** in acetone-d_6 (400 MHz).

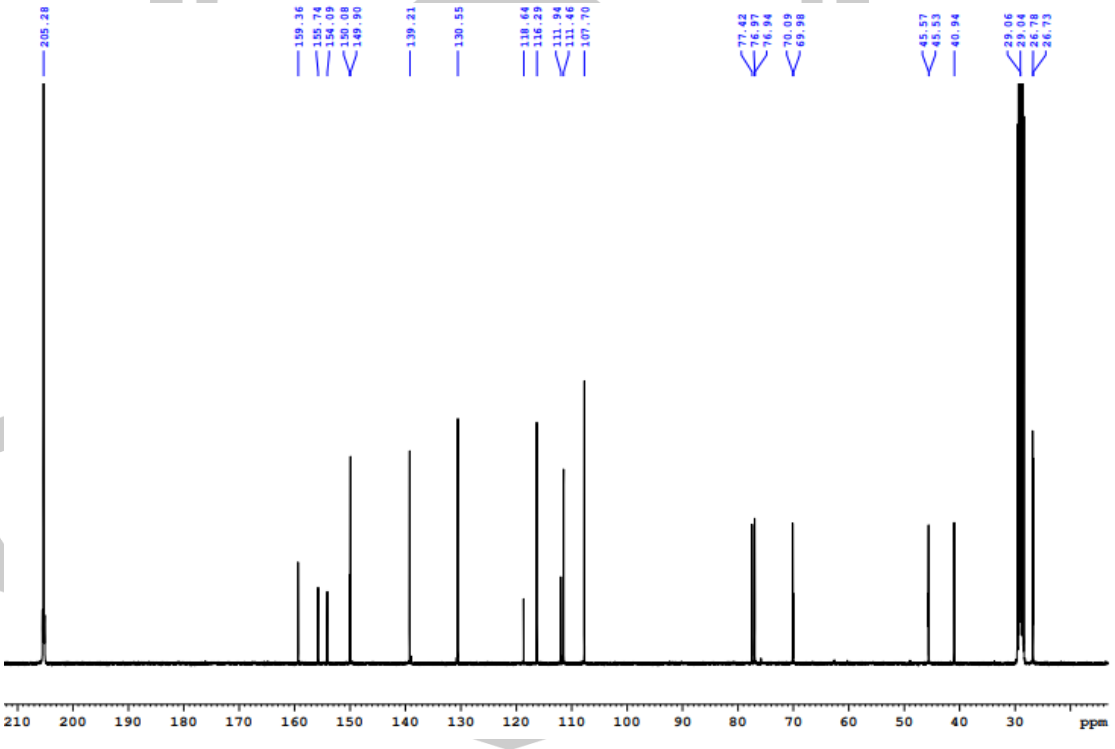

Figure A28. ^{13}C NMR spectrum of **34b** in acetone-d_6 (100 MHz).

Sample Name	3b	**Position**	P1-D1	**Instrument Name**	Instrument 1
User Name		**Inj Vol**	2	**InjPosition**	
Sample Type	Sample	**IRM Calibration Status**	Success	**Data Filename**	3_0137_68_P005.d
ACQ Method	0137_68_Pos_ESIHRScanMS_M2.m	**Comment**	dissolved with Acetone and dilute with MeOH	**Acquired Time**	10/10/2024 11:23:43 AM (UTC+07:00)

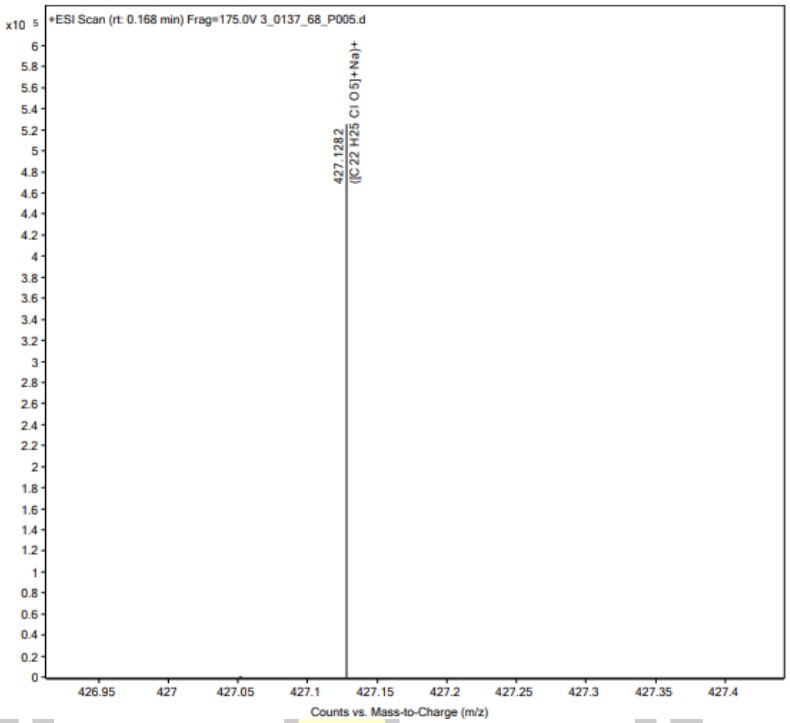

Figure A29. HRESIMS of **34b** (positive ion mode).

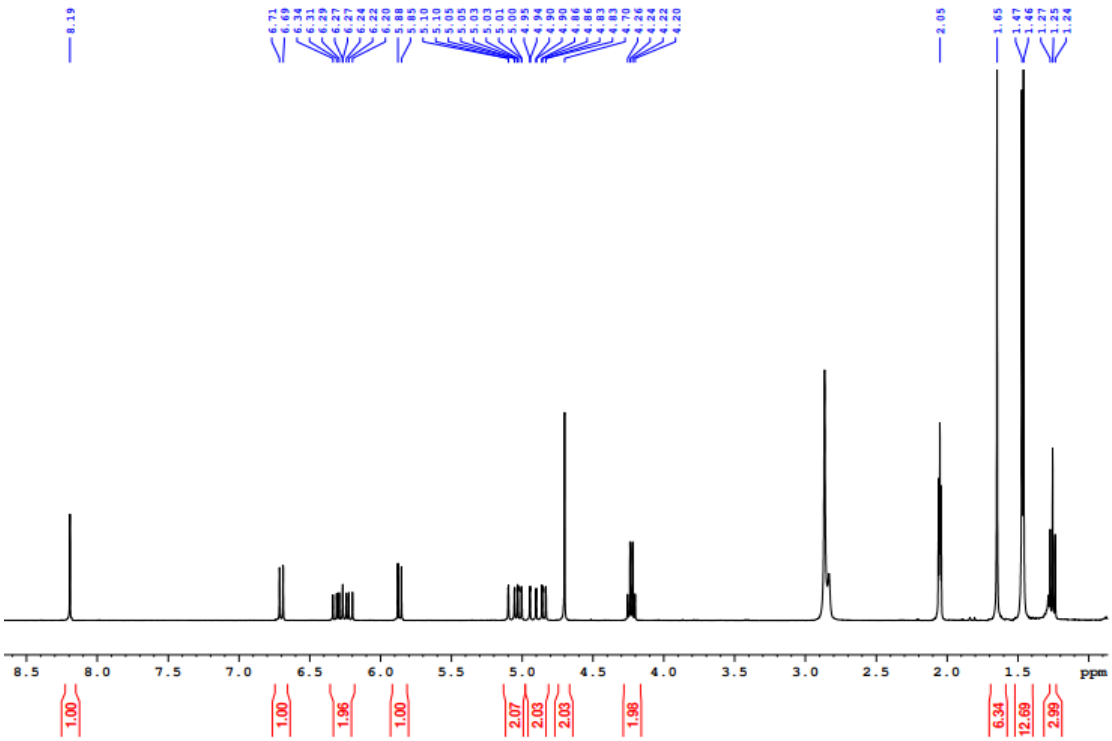

Figure A30. ^{1}H NMR spectrum of **33c** in acetone-d_6 (400 MHz).

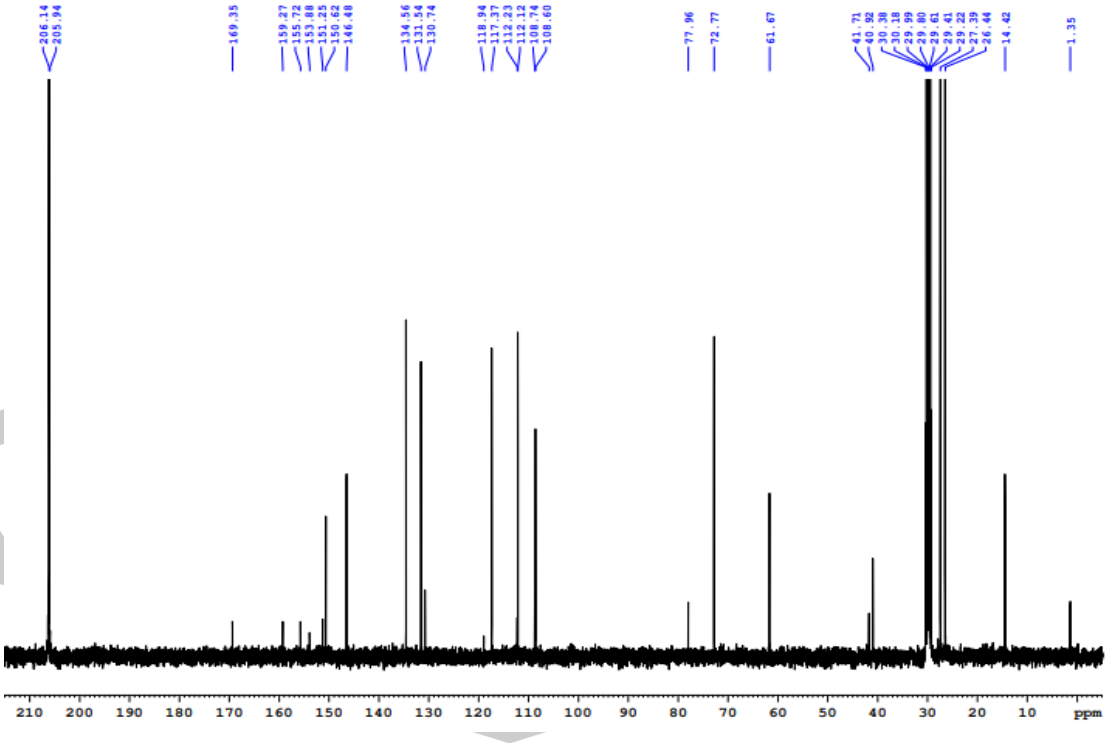

Figure A31. ^{13}C NMR spectrum of **33c** in acetone-d_6 (100 MHz).

BIORESOURCES RESEARCH UNIT

High resolution report

Analysis Name	D:\Data\masahiko\33c.d	Acquisition Date	7/15/2024 12:20:26 PM
Method	NaFormate_pos low.m		
Sample Name	1c	Operator	Sutichai Ext: 3560
		Instrument	micrOTOF Bruker
		Calibrate by	Sodium Formate

Acquisition Parameter

Source Type	ESI	Ion Polarity	Positive	Set Nebulizer	1.0 Bar
Focus	Not active			Set Dry Heater	180 ?C
Scan Begin	100 m/z	Set Capillary	4500 V	Set Dry Gas	5.0 l/min
Scan End	3000 m/z	Set End Plate Offset	-500 V	Set Divert Valve	Source

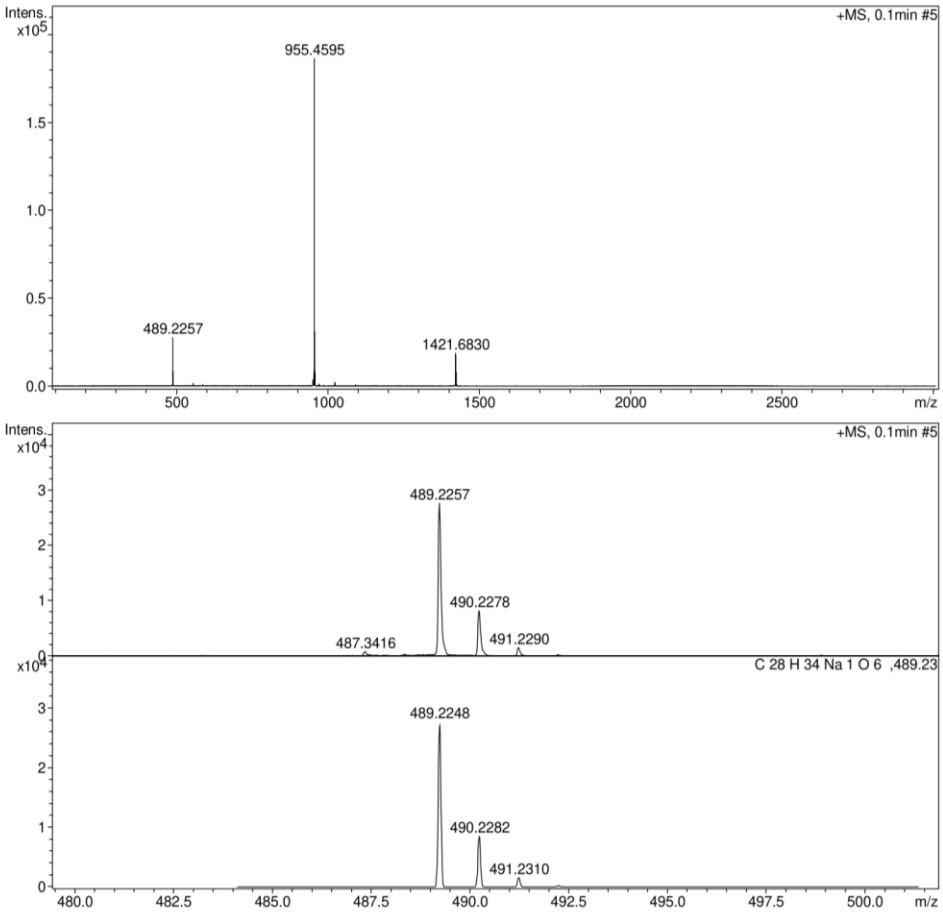

Figure A32. HRESIMS of **33c** (positive ion mode).

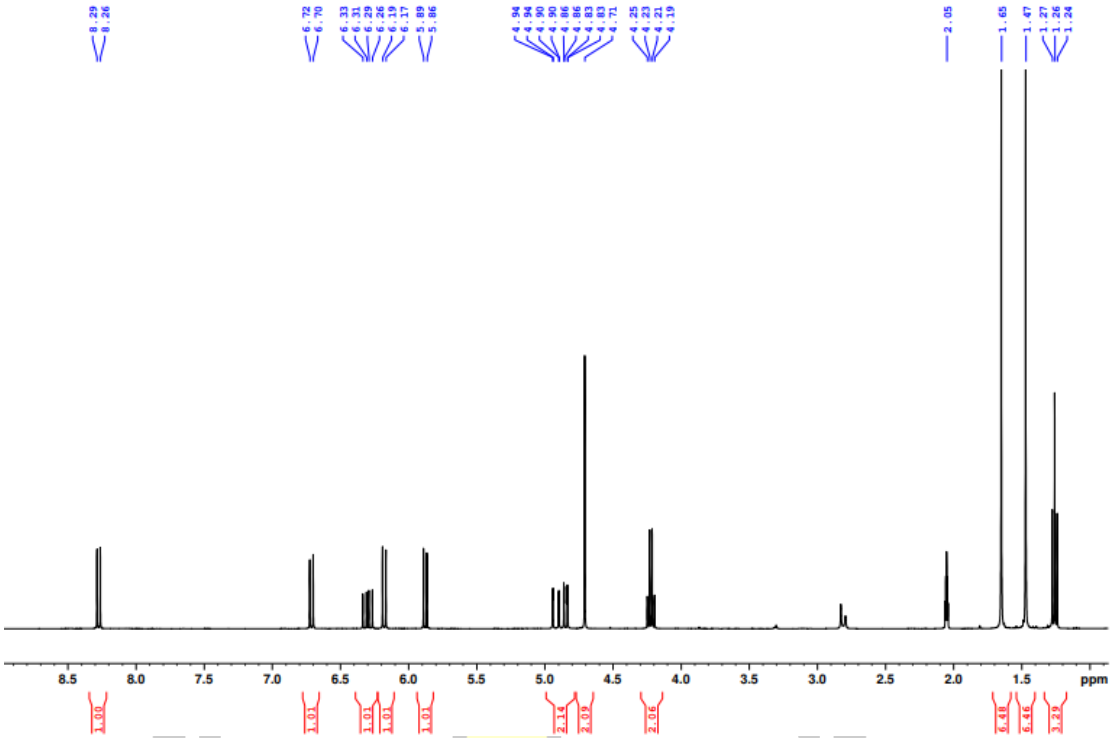

Figure A33. ^{1}H NMR spectrum of **34c** in acetone-d_6 (400 MHz).

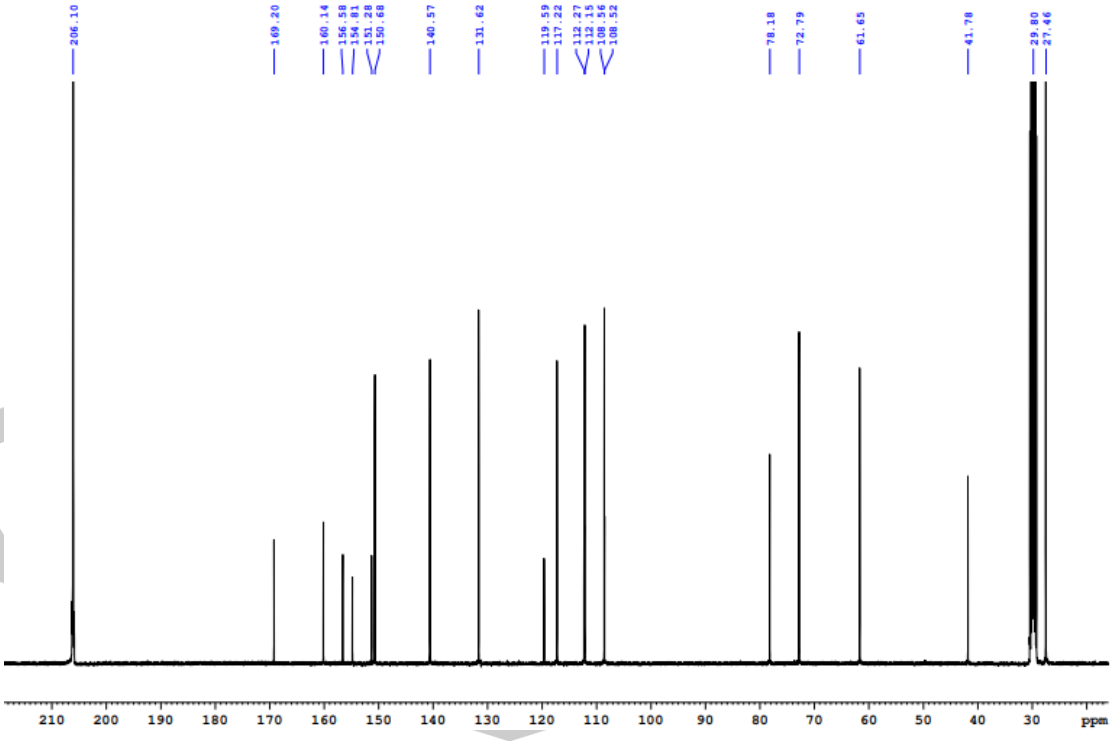

Figure A34. ^{13}C NMR spectrum of **34c** in acetone-d_6 (100 MHz).

Sample Name	3c	**Position**	P1-E1	**Instrument Name**	Instrument 1
User Name		**Inj Vol**	2	**InjPosition**	
Sample Type	Sample	**IRM Calibration Status**	Success	**Data Filename**	4_0137_68_P003.d
ACQ Method	0137_68_Pos_ESIHRScanMS_M2.m	**Comment**	dissolved with Acetone and dilute with MeOH	**Acquired Time**	10/10/2024 11:34:01 AM (UTC+07:00)

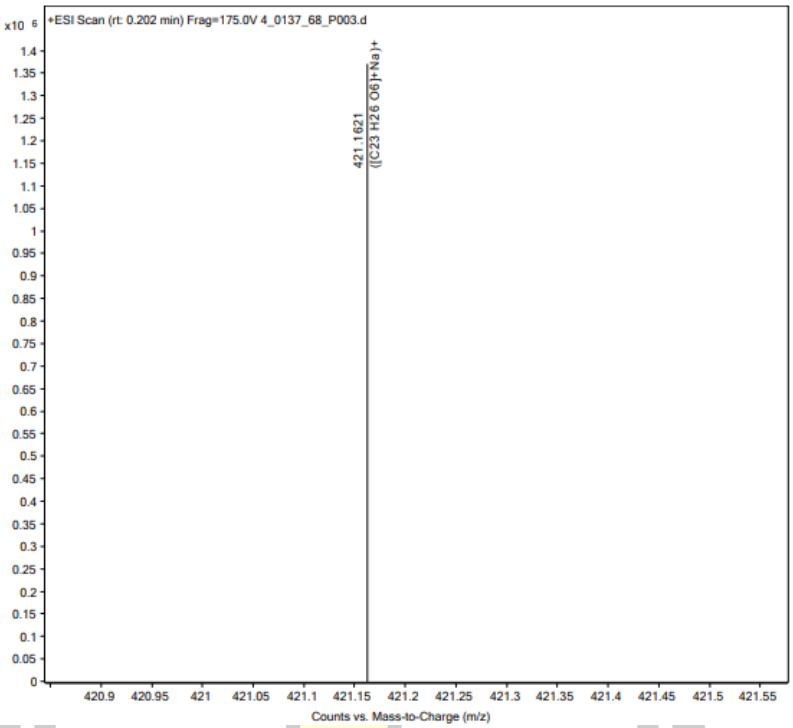

Figure A35. HRESIMS of **34c** (positive ion mode).

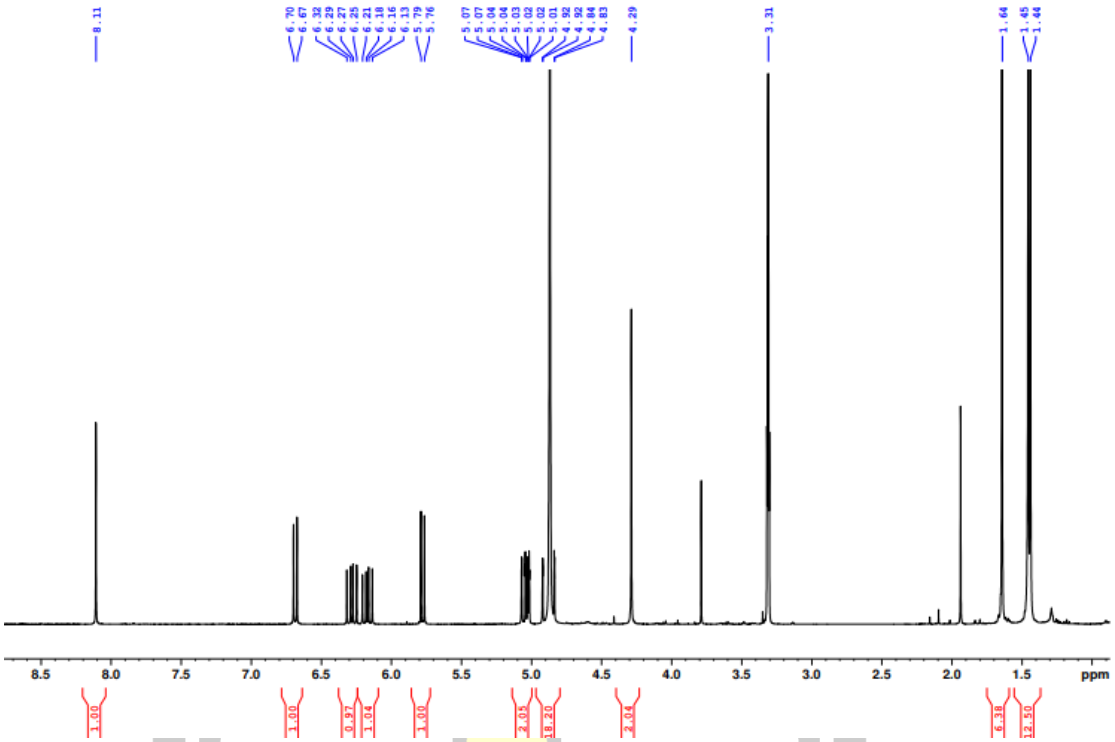

Figure A36. ^{1}H NMR spectrum of **33d** in CD_3OD (400 MHz).

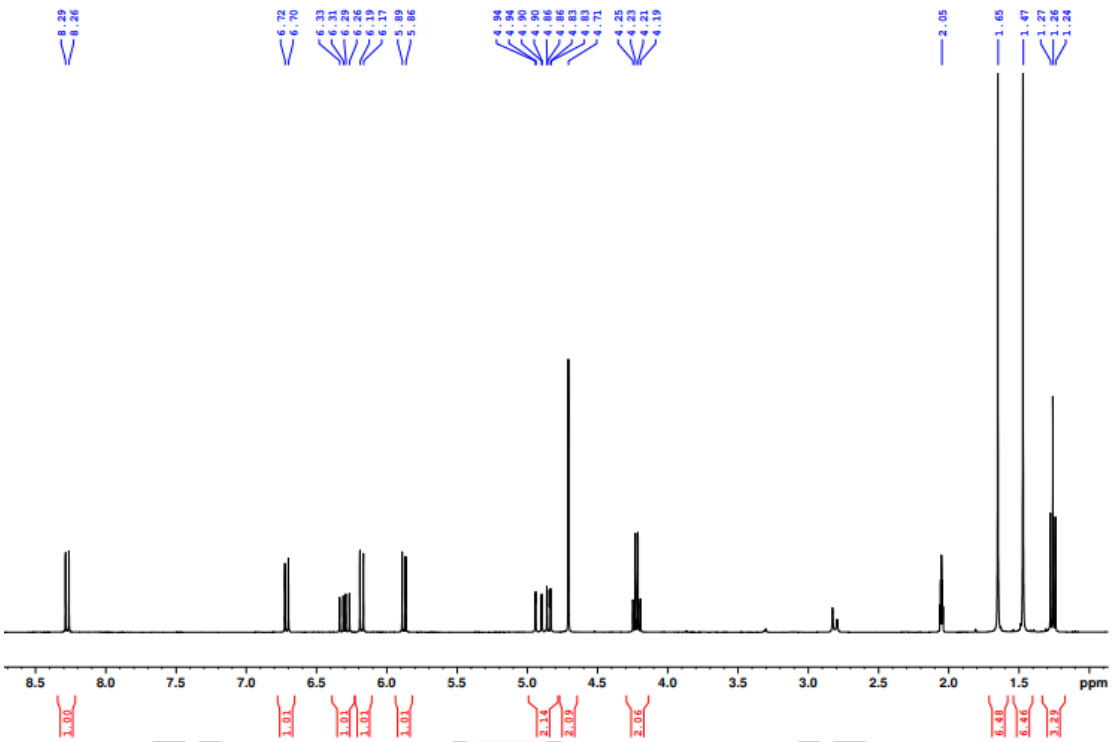

Figure A37. ^{1}H NMR spectrum of **33d** in DMSO-d_6 (400 MHz).

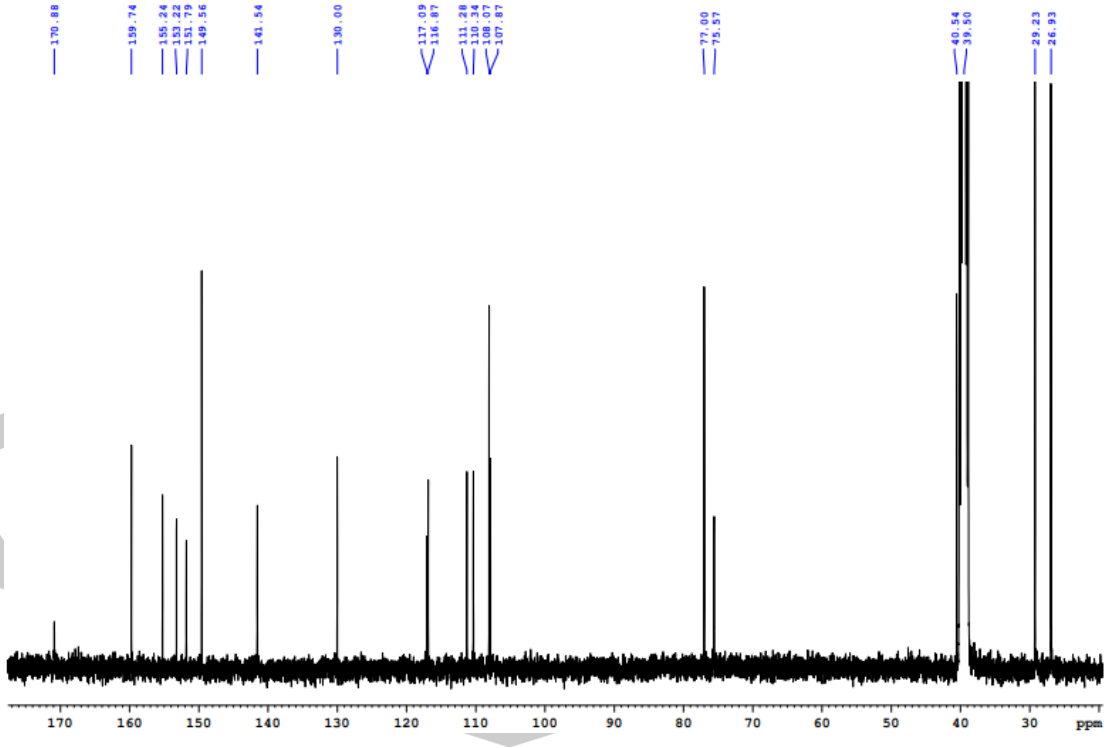

Figure A38. ^{13}C NMR spectrum of **33d** in DMSO-d_6 (100 MHz).

Sample Name	2. 1d	**Position**	P1-F2	**Instrument Name**	Instrument 1
User Name		**Inj Vol**	2	**InjPosition**	
Sample Type	Sample	**IRM Calibration Status**	Success	**Data Filename**	2_0420_68_P005.d
ACQ Method	0420_68_Pos_ESIHRScanMS_M1.m	**Comment**	dissolved with MeOH	**Acquired Time**	10/24/2024 10:25:54 AM (UTC+07:00)

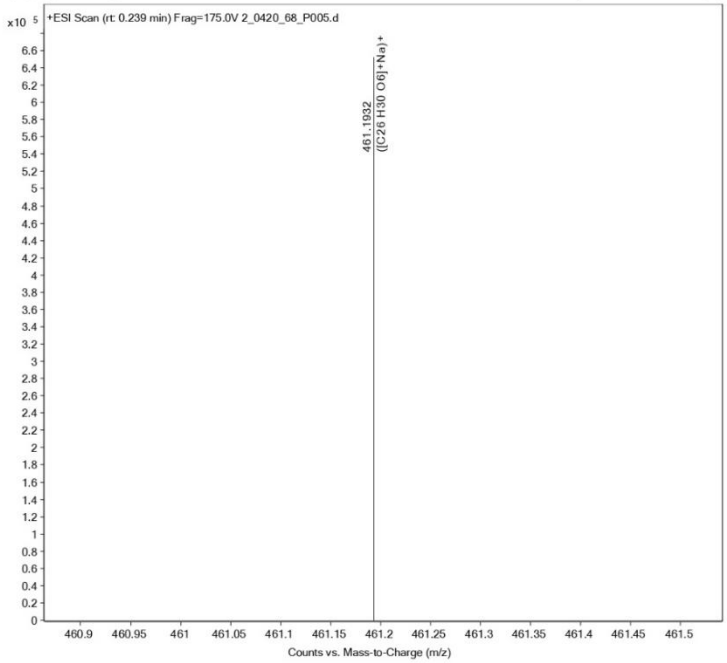

Figure A39. HRESIMS of **33d** (positive ion mode).

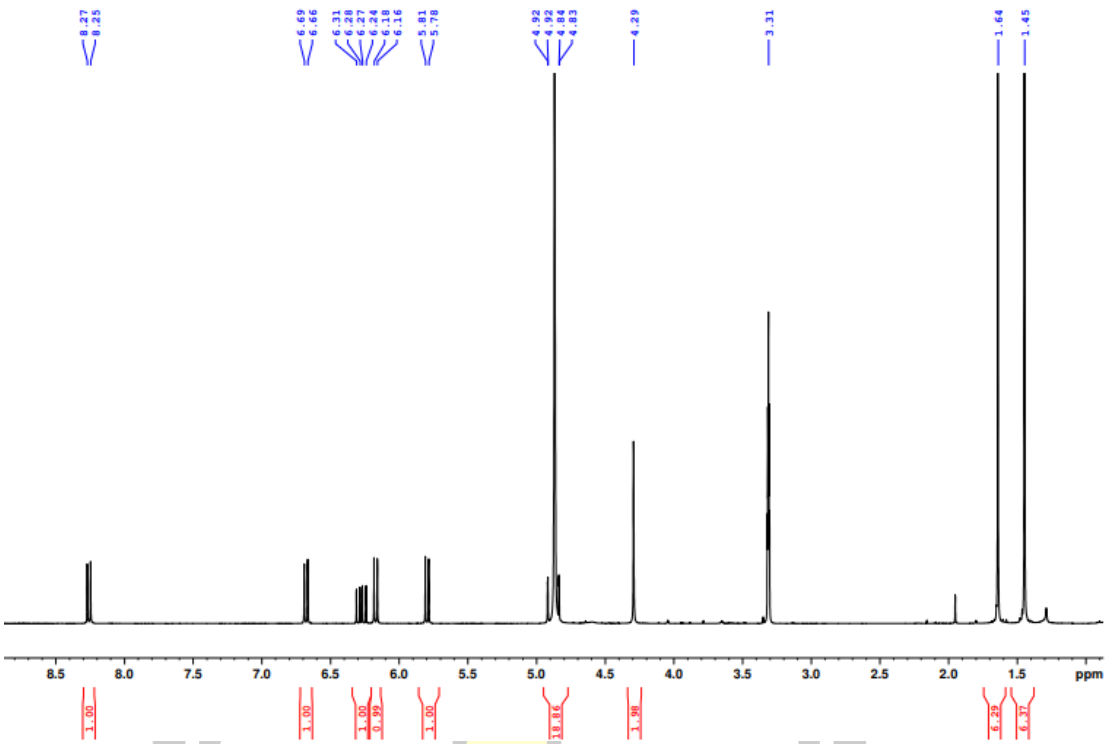

Figure A40. ^{1}H NMR spectrum of **34d** in CD_3OD (400 MHz).

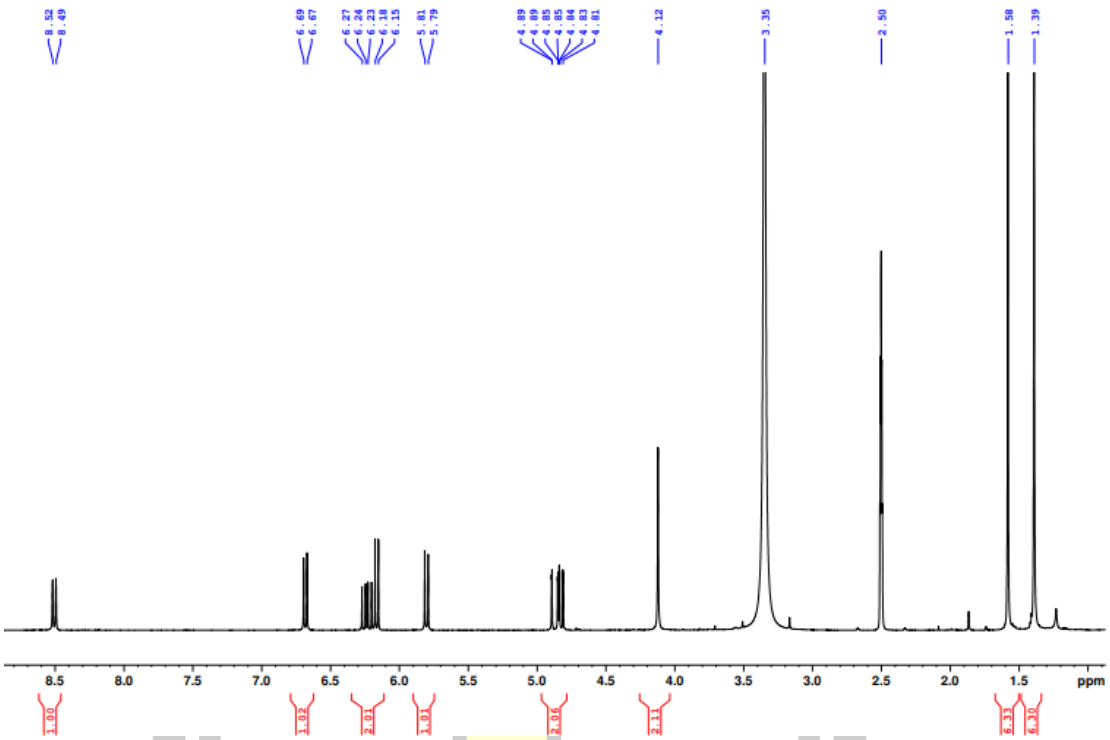

Figure A41. ^{1}H NMR spectrum of **34d** in DMSO-d_6 (400 MHz).

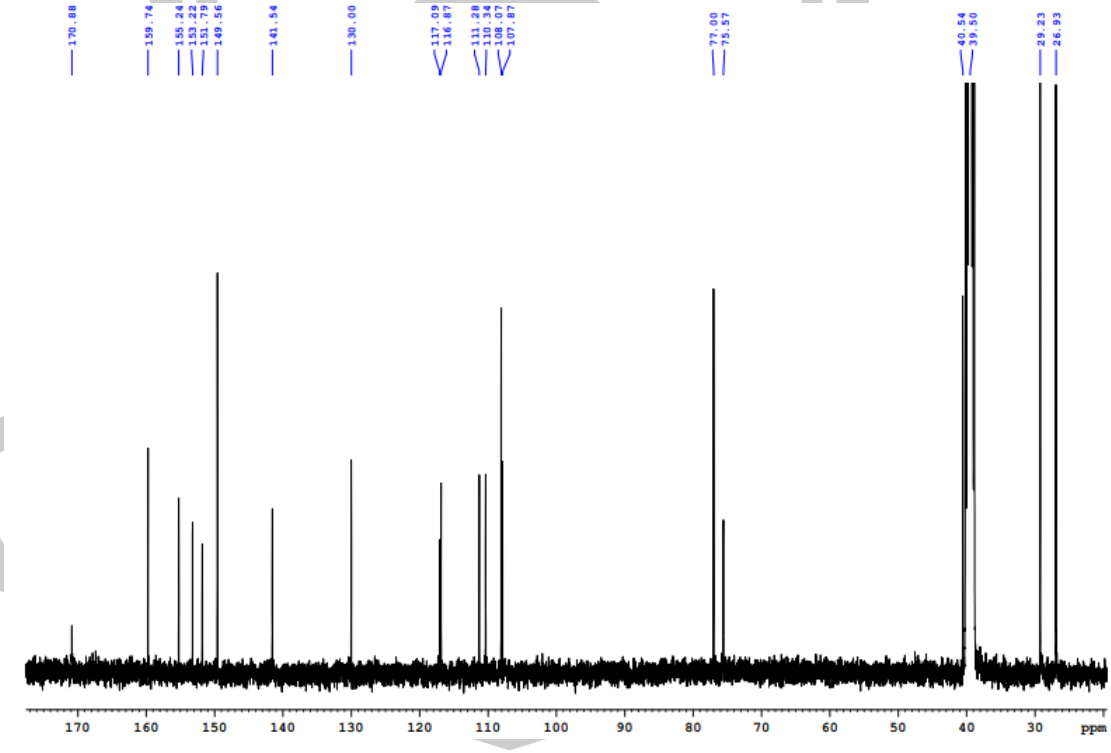

Figure A42. ^{13}C NMR spectrum of **3d** in DMSO-d_6 (100 MHz).

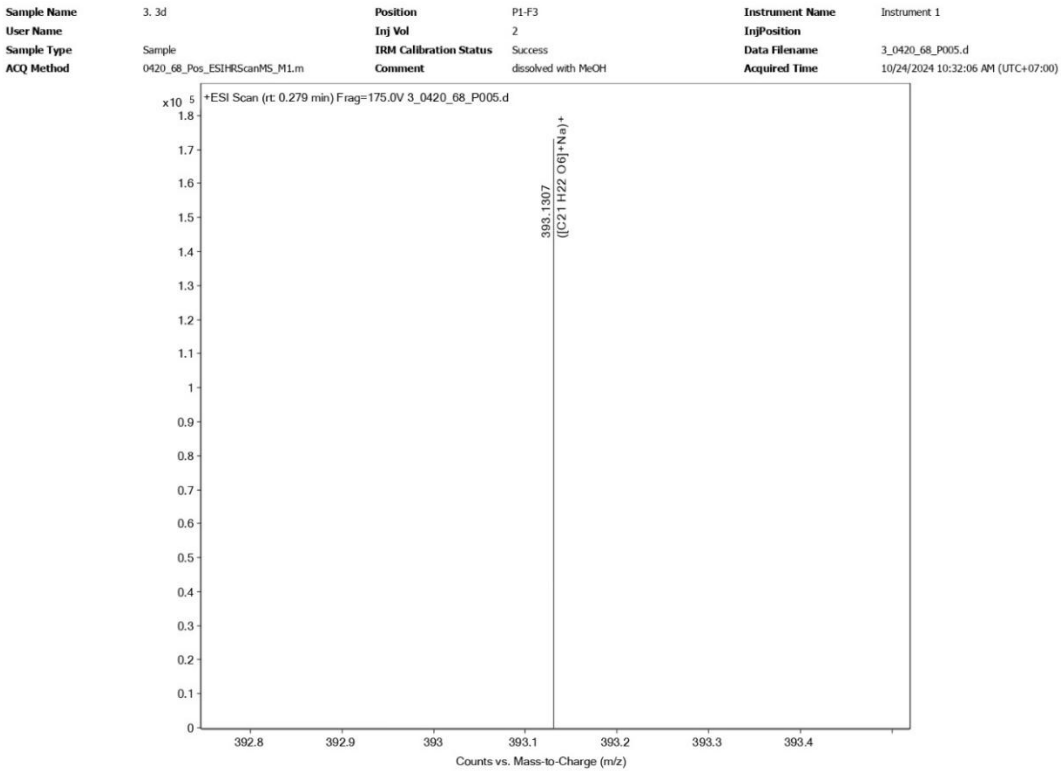

Figure A43. HRESIMS of **34d** (positive ion mode).

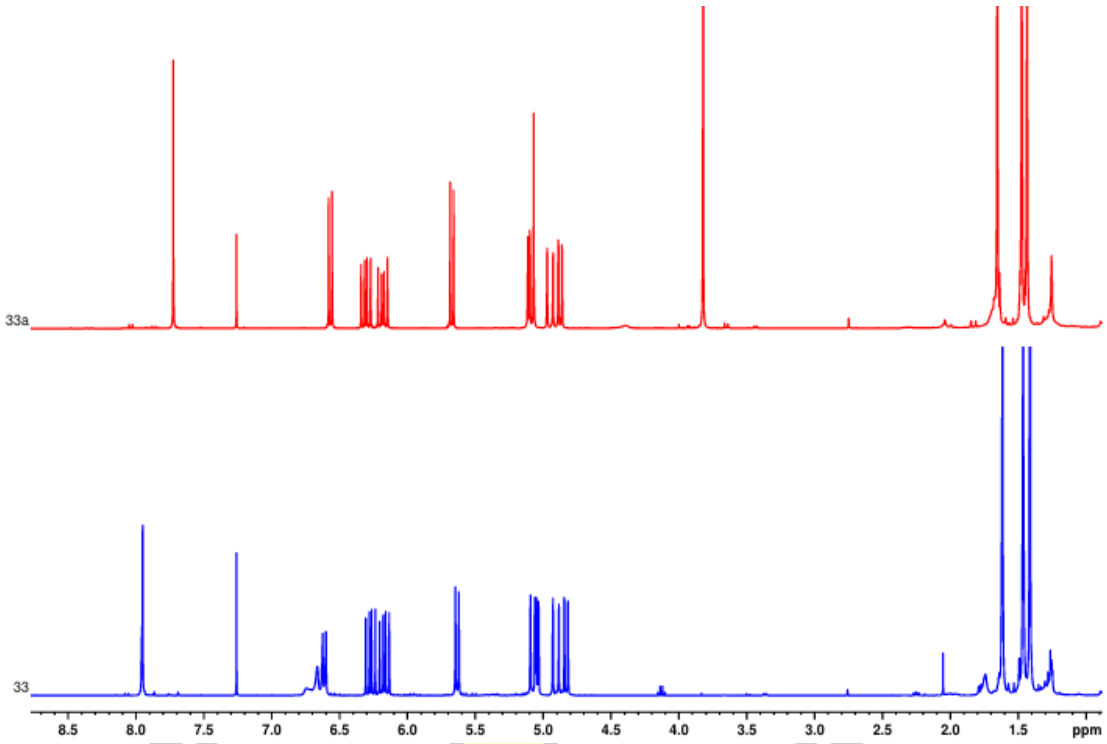

Figure A44. ^{1}H NMR spectrum of **33** and **33a** in $CDCl_3$.

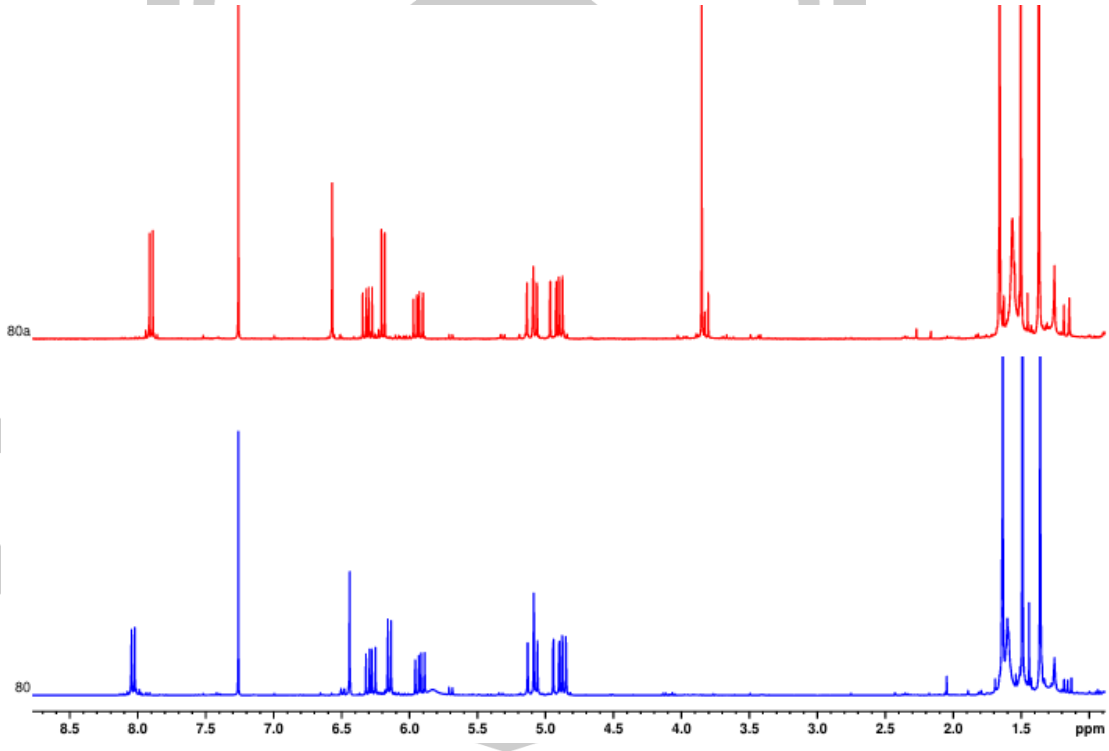

Figure A45. ^{1}H NMR spectrum of **80** and **80a** in $CDCl_3$.

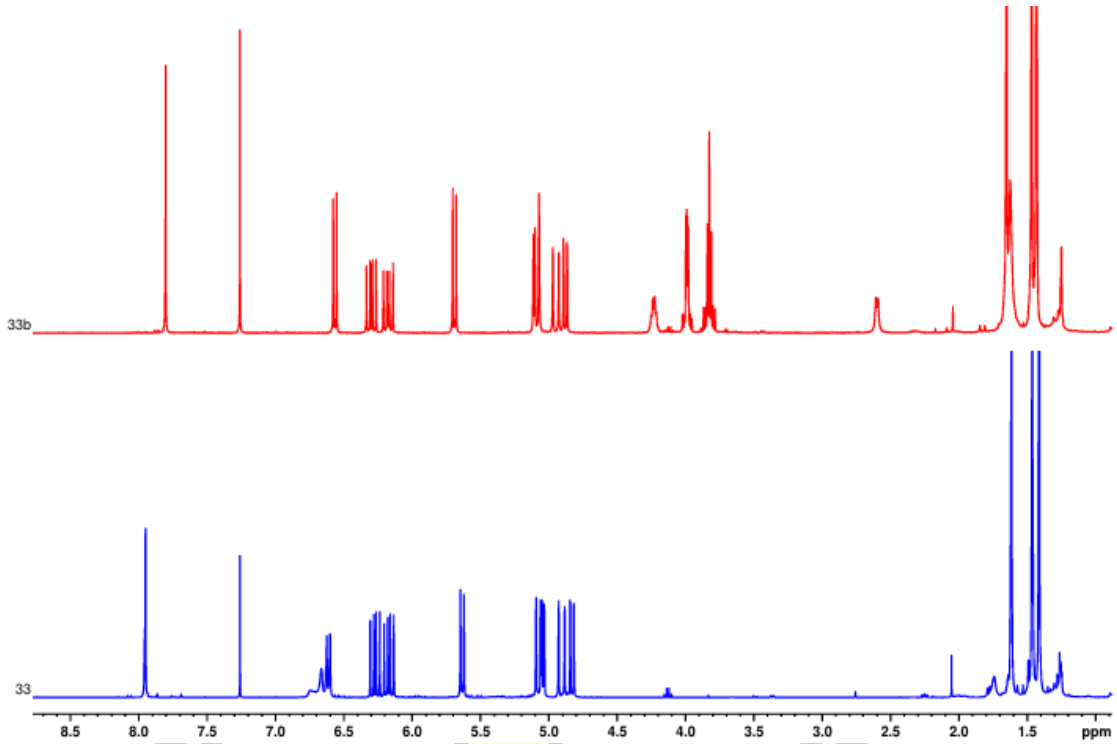

Figure A46. ^{1}H NMR spectrum of **33** and **33b** in $CDCl_3$.

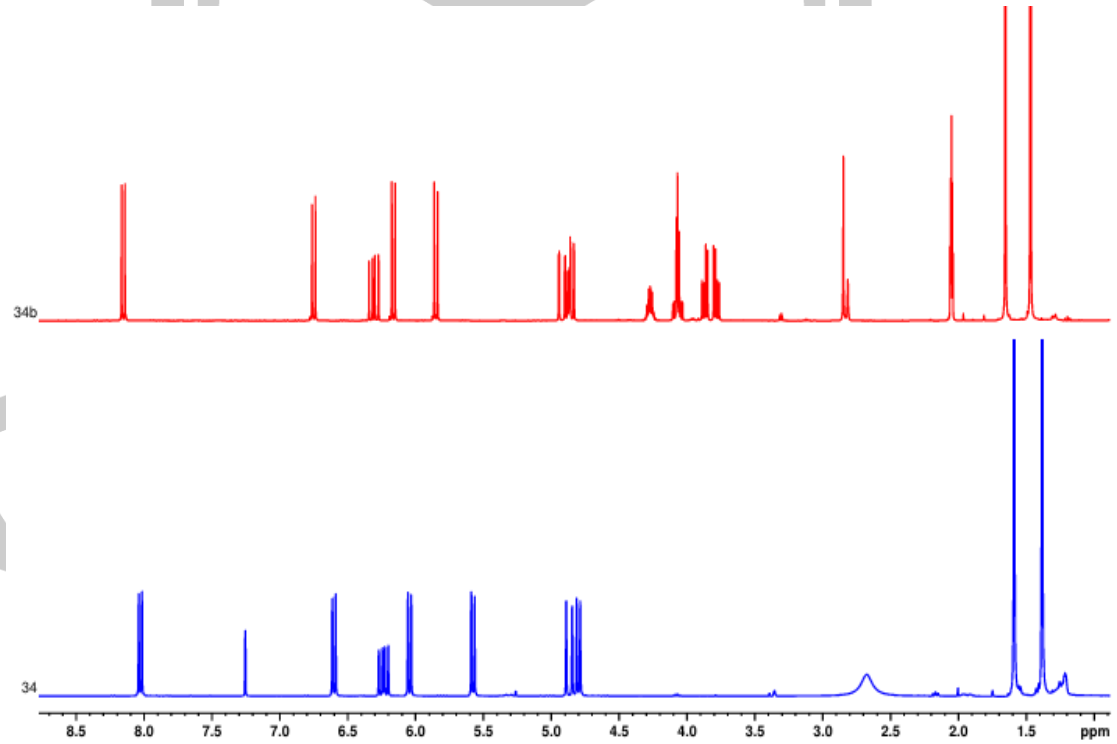

Figure A47. ^{1}H NMR spectrum of **34** ($CDCl_3$) and **34b** (acetone-d_6).

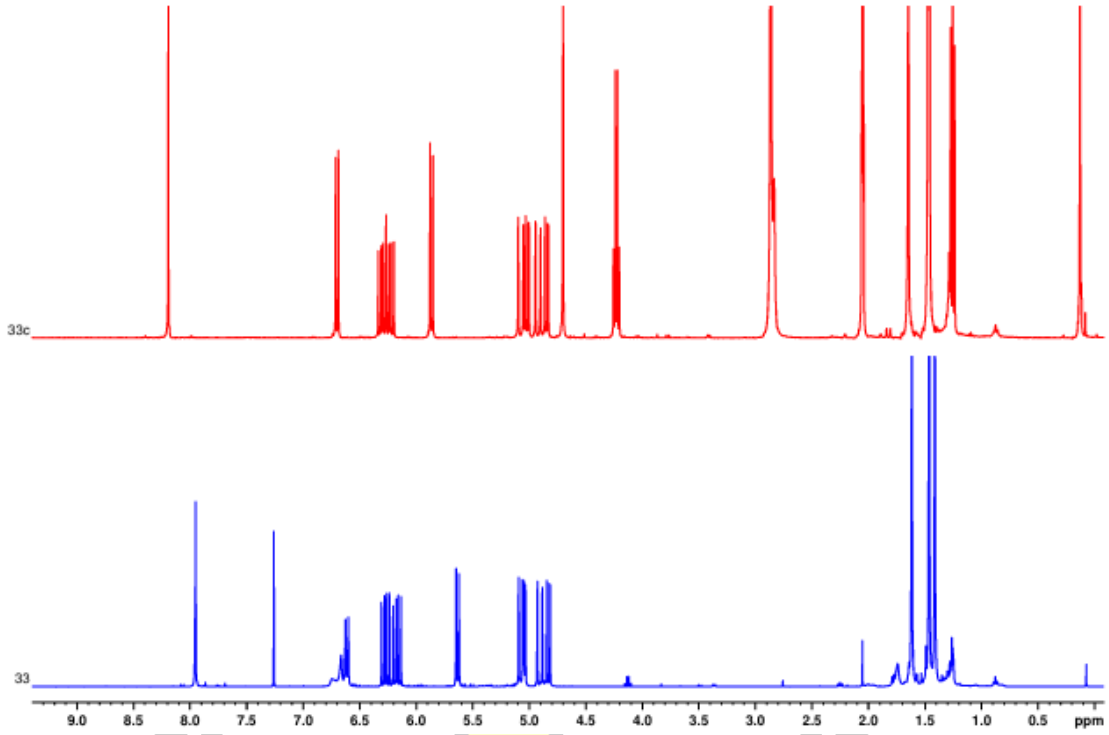

Figure A48. ^{1}H NMR spectrum of **33** ($CDCl_3$) and **33c** (acetone-d_6).

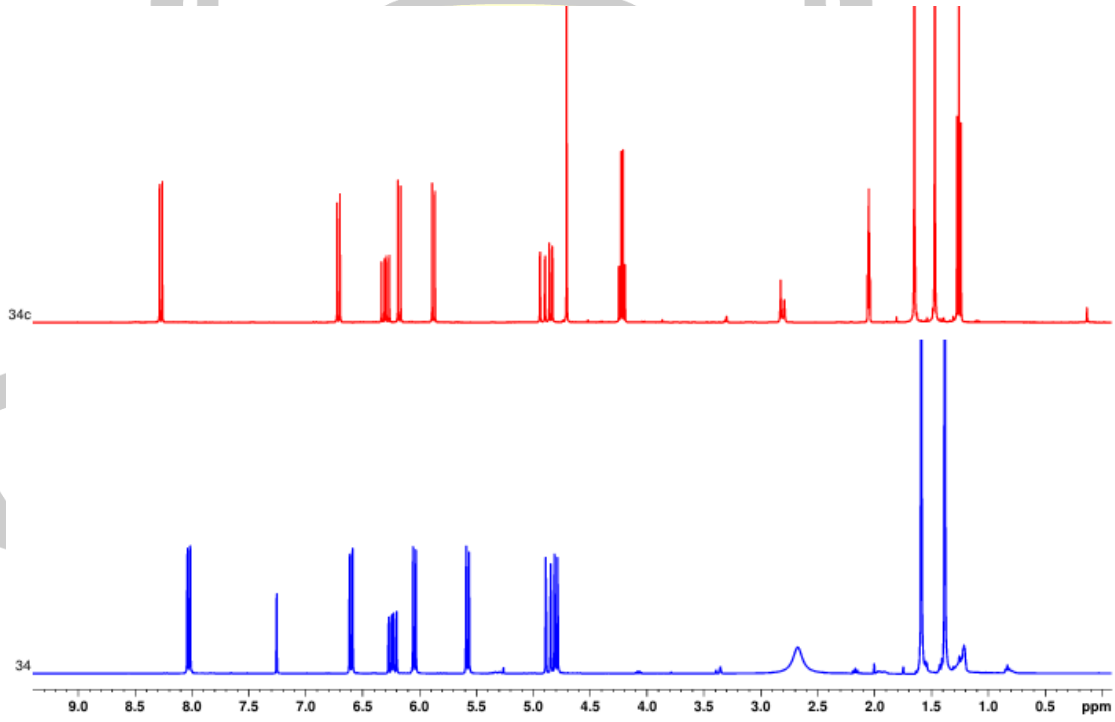

Figure A49. ^{1}H NMR spectrum of **34** ($CDCl_3$) and **34c** (acetone-d_6).

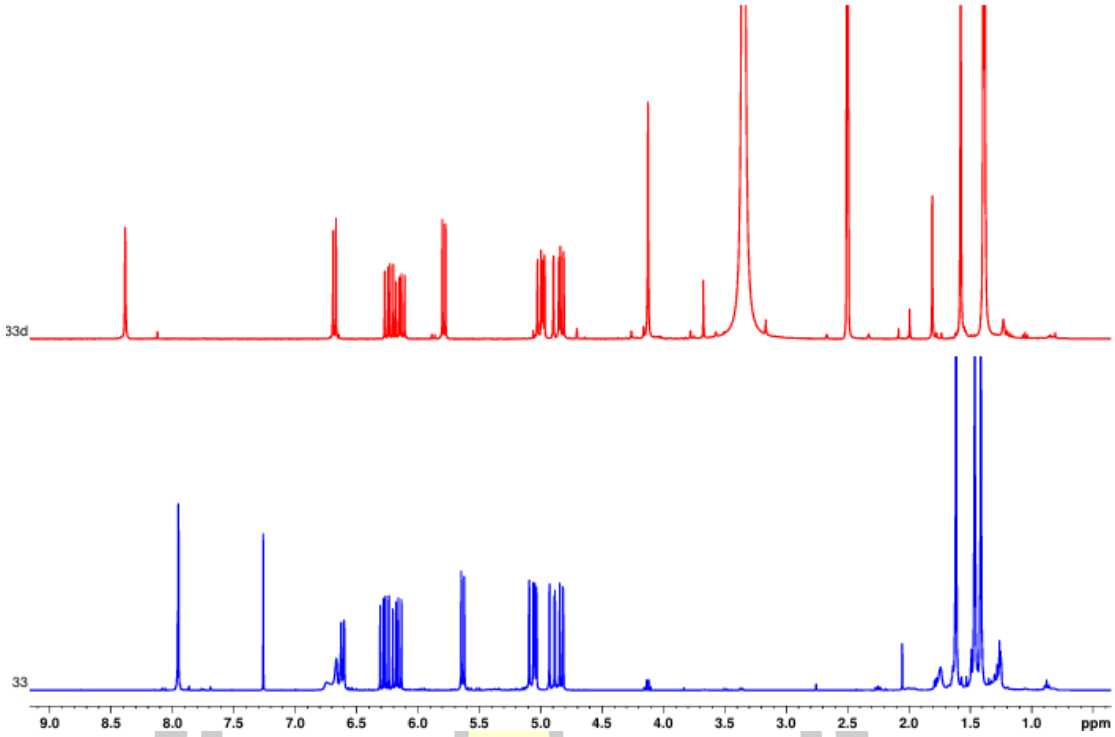

Figure A50. ^{1}H NMR spectrum of **33** ($CDCl_3$) and **33d** (DMSO-d_6).

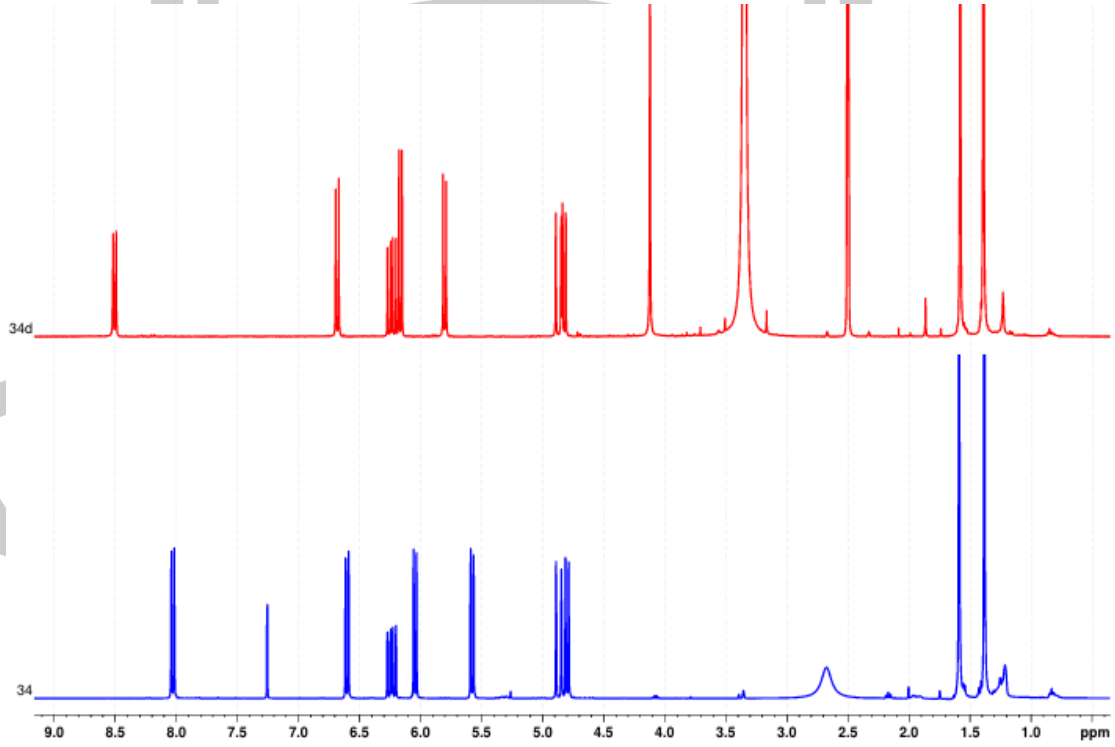

Figure A51. ^{1}H NMR spectrum of **34** ($CDCl_3$) and **34d** (DMSO-d_6).

BIOGRAPHY

NAME	Thanatcha Samsee
DATE OF BIRTH	10 October 1999
PLACE OF BIRTH	Maha Sarakham hospital
ADDRESS	Number 65 village No.9 khokphra Sub-district, kantarawichai district, Maha Sarakham 44150
PLACE OF WORK	Mahasarakham university
EDUCATION	2015-2017 High School Certificate equivalent, Sarakhampittayakhom, Mahasarakham, Thailang 2018-2021 Bachelor of Science, Mahasarakham University, Mahasarakham, Thailand 2022-Present Masters of Science, Mahasarakham University, Mahasarakham, Thailand